

Properties of foam/sand mixtures for tunnelling applications

A thesis submitted for the degree of Master of Science to the Department of
Engineering Science

Sotiris Psomas



St Hugh's College

Michaelmas 2001

“Properties of foam/sand mixtures for tunnelling applications”

Sotirios Psomas

St Hugh's College

A thesis submitted for the degree of Master of Science to the University of Oxford.

Michaelmas 2001

ABSTRACT

This thesis presents experimental work on foam/sand mixtures carried out in the Civil Engineering Laboratory at Oxford University, as well as the findings associated with it. This research represents the preliminary stage of a research project on Soil Conditioning Agents in Pipe Jacking and Mechanised Tunnelling, sponsored by the Pipe Jacking Association (PJA) and three water companies. The experimental work was carried out in order to evaluate the fundamental soil properties of foamed sand, in particular its compressibility, permeability and shear strength.

The first chapter deals with basic aspects of soil conditioning agents and their application to tunnelling, and provides an understanding of the fundamentals of foam behaviour. An introduction to the problems encountered in tunnelling is given. A brief study of foams and their properties is presented and the role of foams as soil conditioning agents is described.

In the second chapter, a description of the foam generator used is provided. Two types of sand (fine and coarse), four types of foaming agents and a specific polymer mixture were employed for the testing. In some cases, sodium bentonite was used alone or in combination with foam and polymer. The sample preparation method, together with the results from measuring the reduction of the power input required to mix sand with foam, are presented.

The third chapter presents the compression tests performed in a 75 mm Rowe cell. Results are presented as volume changes variation with the applied vertical stress. Quality control was carried out on the test results in order to evaluate the likely inconsistencies during the preparation and measurements. The most notable outcome was that for fine sand even at high pressure the final voids ratio of foam/sand mixtures after the compression remained higher than the maximum voids ratio of dry sand. Some measurements of the foam/sand mixtures permeability were also performed in the Rowe cell. Tests were carried out using the constant head principle with a "Marriotte bottle". Permeability values determined from testing are compared with indirect evaluation from the compression tests.

In the fourth chapter direct shear strength tests in a standard shear-box are presented. Fine and coarse sand mixed with foam were tested in shear under seven different vertical loads. Results are presented as plots of shear strength against horizontal deformation. Very low values of shear strength for foamed sand tests are recorded. The shear strength is plotted against the relative density index along with the experimental results from Bolton's correlation. Foamed sand shear strength values are scattered within a range below that of Bolton's correlation. Finally, the conclusions from the test results are discussed.

ACKNOWLEDGEMENTS

I am grateful to my supervisor Professor G.T. Houlsby for his support, advice and crucial guidance throughout the duration of my research.

To Dr. G.W.E. Milligan, who was the industrial liaison officer of the research project, I would like to express my sincere gratitude for providing me with valuable feedback and encouragement.

From the Civil Engineering Group, I would like to express my appreciation to Dr. G.C. Sills who was helpful and supportive and to Mr. R. Sawala, who willingly offered his technical expertise by fixing and fabricating various pieces of the experimental equipment.

I would like also to thank my family, friends and colleagues for their moral support. I am indebted to Ms G. Kalkanis who provided immense help and editorial assistance.

I was honoured to be an MCR member of St Hugh's college. I would like to thank the MCR and the college staff for making my stay so enjoyable and memorable.

Finally, I would like to acknowledge the Pipe Jacking Association (PJA), the water companies (Thames Water, Severn Trent and North West Water) and the State Scholarships Foundation of Greece (IKY) for their financial support, without which I would not have been able to carry out this research.

ABSTRACT	1
ACKNOWLEDGEMENTS	2
CHAPTER 1. FOAMS AS SOIL CONDITIONING AGENTS	5
1.1 INTRODUCTION.....	5
1.1.1 General	5
1.1.2 Mechanised tunnelling and pipe jacking.....	5
1.1.3 Soil conditioning in tunnelling and pipe jacking.....	7
1.1.4 Soil conditioning agents for EPB machines	11
1.2 FOAMS	12
1.2.1 General	12
1.2.2 Foam properties.....	15
1.2.3 Testing foamed soil.....	16
1.3 CURRENT PRACTICE IN THE USE OF FOAMS IN TUNNELLING.....	19
1.3.1 Main issues using foam with EPBs	19
1.3.2 Case studies.....	22
1.4 SUMMARY OF THE EFFECTS OF THE CONDITIONED SOIL PROPERTIES ON EPB PERFORMANCE	23
1.4.1 Compressibility.....	24
1.4.2 Permeability.....	24
1.4.3 Shear strength.....	24
1.5 RESEARCH OBJECTIVES.....	25
CHAPTER 2. SAMPLE PREPARATION AND PROPERTIES	27
2.1 EQUIPMENT SET-UP	27
2.1.1 Small scale testing.....	27
2.1.2 Soil mixer.....	28
2.1.3 Foam generator.....	28
2.1.4 Foam testing.....	30
2.2 MATERIALS USED	31
2.2.1 Sands.....	31
2.2.2 Foaming agents.....	31
2.2.3 Bentonite and polymer	32
2.3 FOAM/SAND MIXING.....	35
2.3.1 Foamed soil samples	35
2.3.2 Foam/sand mixing test.....	36
CHAPTER 3. COMPRESSION TESTS	39
3.1 COMPRESSIBILITY OF FOAMED SOIL.....	39
3.1.1 Introduction.....	39
3.1.2 Volume changes and pore fluids.....	40
3.1.3 Scope and objectives.....	43
3.2 COMPRESSIBILITY TESTS IN ROWE CELL	44
3.2.1 Description and calibration of the apparatus.....	44
3.2.2 Test procedure.....	46
3.3 TESTS RESULTS.....	47
3.3.1 Calculation procedure.....	47
3.3.2 Quality control.....	51
3.3.2 Compression variation with time.....	55
3.3.3 Void ratio variation with vertical stress.....	56
3.3.4 Void ratio variation	59
3.4 PERMEABILITY EVALUATION.....	61
3.4.1 Indirect evaluation.....	61
3.4.2 Permeability tests in Rowe cell.....	64
3.5 DISCUSSION OF TEST RESULTS.....	65
3.5.1 Foaming agents	65

3.5.2 Volume change behaviour.....	66
3.5.3 Foamed soil structure.....	69
CHAPTER 4. DIRECT SHEAR-BOX TESTS.....	71
4.1 SHEAR STRENGTH PARAMETERS.....	71
4.1.1 Shear strength and dilatancy.....	71
4.1.2 Objectives of the study.....	74
4.2 APPARATUS AND EXPERIMENTAL PROCEDURE.....	75
4.2.1 Description of the apparatus.....	75
4.2.2 Test procedure.....	75
4.3 SHEAR-BOX TEST RESULTS.....	77
4.3.1 Shear stress variation with displacement.....	78
4.3.2 Shear strength parameters against vertical pressure.....	79
4.4 DISCUSSION ON THE RESULTS.....	80
4.4.1 Test procedure and measurements.....	80
4.4.2 Shear strength and relative density.....	80
CHAPTER 5. CONCLUDING REMARKS	84
5.1 SUMMARY OF FINDINGS	84
5.1.1 Main Findings.....	84
5.1.2 Other observations.....	85
5.2 RECOMMENDATIONS FOR FUTURE WORK.....	86
REFERENCES	88
TABLES	92
FIGURES & PHOTOS	107

Chapter 1. Foams as Soil Conditioning Agents

1.1 Introduction

1.1.1 General

The past decades have been marked by a rapid growth in underground construction. Worldwide, there is a growing need for new infrastructure such as pipelines and communication cables as well as roads and railways. Additionally, public authorities and private companies have recognised the benefits offered by underground construction as an alternative to open excavation for transportation and services networks (sewers, pipelines, cables), especially in urban environments. The utilisation of underground space offers a new approach to urban planning and infrastructure.

Tunnelling and trenchless technology are considered to be more suitable than open excavation in cases where ground conditions are unfavourable or where the surface disruption is expected to be high. The term tunnelling encompasses many different methods and techniques from conventional methods (drill and blast) to more advanced methods utilising sophisticated Tunnel Boring Machines (TBM). Trenchless technology is a broad term used to describe a range of methods, materials and equipment that can be used for construction, installation or rehabilitation of underground infrastructure (ISST, 1998).

1.1.2 Mechanised tunnelling and pipe jacking

Tunnelling and pipe jacking are methods of underground (or trenchless) construction. Some of the techniques developed more recently include mechanised tunnelling and microtunnelling whereas others (conventional tunnelling and pipe jacking) have been employed for decades. The term mechanised tunnelling has become synonymous with tunnelling by TBM. The performance of these machines can be enhanced significantly by using suitable additives during the excavation process. By utilising mechanised techniques, benefits in reduction of construction time and consequently construction cost can be achieved.

Pipe jacking is a specific trenchless technology method as well as an underground construction process. It can be described as the process in which pipes are directly installed behind a shield machine by hydraulic jacking from a shaft, such that the pipes form a continuous pipeline in the ground (ISTT, 1998). The pipe jacking technique can be defined as the installation of pipes over 900 mm internal diameter whereas the microtunnelling technique involves installation of pipes of less than 900 mm internal diameter. As a result, the distinction between pipe jacking and microtunnelling is “a matter of size” (ISTT, 1998).

Pipe jacking and microtunnelling differ from the other methods of tunnelling in the way the lining is installed. Thus, shields for pipe jacking and tunnelling are similar in principle and operation. The advent of closed face TBMs brought about significant progress by extending the operational limits of TBMs in unfavourable ground conditions (Biggart, 1999). In soft ground conditions, there are two principal types of shield machines usually employed: slurry shield machines and earth pressure balance machines (EPB). Both of them use artificial means to support the face during excavation in an attempt to control the rate of advance and keep the ground deformation within some limits (Anagnostou & Kovari, 1996). In slurry shields, face support is provided by slurry that is formed behind the cutting head by mixing water with a well ‘designed’ fluid (usually bentonite-based). A further development of slurry shield is the ‘Hydro-shield’ (Herrenknecht, 1999), which uses an air bubble within the machine head in order to control efficiently face pressure variations or changes in advance rate.

EPB machines (*Figure 1.1*) are specific kinds of tunnel boring machines (TBM), which are increasingly being seen as the answer to many tunnelling problems where adverse geological conditions are encountered. In EPB machines, mechanical pressure is applied to the excavated soil in order to provide counterbalance to the earth pressure at the face and prevent heave or subsidence. EPB offers many of the advantages of slurry shields. In EPB shields, support is provided by the excavated soil behind the cutting head in the excavation chamber. In contrast to other methods, the EPB can do without a secondary support medium such as compressed air because the excavated material itself serves as a support medium. Between the earth slurry in the excavation chamber and the ground at the face the pressure balance is reached. The excavated ground is pressed through the openings of the cutting wheel into the excavation chamber where it is mixed with the earth slurry. The bulkhead presses the earth slurry mixture and the pressure of the earth slurry in the

excavation chamber is controlled by the rate of spoil removal. The torque should be kept low to achieve successful performance and to keep the construction cost below that of other conventional tunnelling methods (Melis, 1999).

Slurry shields machines work successfully in every type of soft ground (Maidl, 1996) but are widely used in non-cohesive ground. In discussing the use of the two types of machines, Herrenknecht (1994) noted that in the case of slurry shields, consideration must be given to the particle size distribution of the soil. The main concern is that the excavated material must be separated from the bentonite slurry and the presence of fine material makes the separation process expensive and onerous. For an EPB shield machine, clayey-silty and silty-sandy ground are perfectly suited (Maidl *et al*, 1996). The range of soils, which can be excavated using an EPB, can however be extended using soil conditioning.

1.1.3 Soil conditioning in tunnelling and pipe jacking

The term soil conditioning refers to the use of suitable additives (conditioning agents) in various proportions to alter the soil properties of the excavated spoil. Conditioning agents have been used extensively in drilling and tunnelling operations for many years. Particularly in tunnelling and pipe jacking, the performance of tunnelling machines is enhanced using proper ground conditioning and lubrication agents (Milligan, 2000a). Recent experiences in mechanised tunnelling have revealed the prime importance of ground conditioning agents in the excavation process from the tunnel face to the spoil handling (Milligan & Marshall, 1998; Pellet & Castner, 1998). Soil conditioning is applied in relatively long drives and in difficult ground conditions, where fully mechanised systems are used. Some case studies are presented in the last section of this chapter.

Soil conditioning agents are usually bentonite-based slurries (Thomson, 1993), sometimes mixed with various types of polymer as well as foams. Foams were introduced in the tunnelling industry in the late 1970's in Japan with EPB machines (Maidl *et al*, 1996). Today, apart from the physical and chemical requirements associated with the performance of the various agents and chemical additives, environmental issues must also be taken into account. The latter means compliance with both safety-in-use and disposal regulations.

Soil conditioning agents improve the performance of several of the TBM parts and may be introduced at various points as discussed in the following sections.

Tunnel face:

At the tunnel face, the main role of soil conditioning agents is to reduce the friction between the cuttings and the cutting tools of the machine's cutter head. The reduction of friction decreases wear and torque requirements for the cutting head. This, in turn, results in lower operational cost and longer life for the components of the machine.

In slurry shields, the conditioning agent (bentonite suspension) creates a 'filter cake' which supports the tunnel face and makes the ground impermeable. In EPBs, soil conditioning agents can reduce the permeability of the soil in order to allow the excavation to take place in a controllable way, in coarse-grained water bearing soils.

In all cases, the soil conditioning agent should be introduced at the point of cut as early as possible to allow sufficient mixing with the ground.

Machine head:

The main objective is to reduce friction within the machine head and to create a more homogenous mass so that coggings are avoided. Reducing friction again results in a reduced wear within the head. It also decreases the power requirements for the cutter head to turn the excavated material into a suitably plastic mass. Creating a more plastic and homogenous excavated mass improves its workability and consequently, allows for better control of the pressure changes at the face of the tunnel. This, in turn, appears to improve the stability of the tunnel face and provides better control of ground movements thereby contributing to safer working conditions for the personnel in the tunnel. In slurry shields, the excavated material falls into an excavation chamber filled with slurry, which is placed behind the cutting head.

In EPBs, the addition of conditioning agents is necessary so that the excavated material can be transformed into an earth-slurry supporting the tunnel face. The excavation chamber is also filled with the excavated material and at this stage, can be conditioned with suitable agents. It is important to note that the interior of the excavation chamber should be designed in such a way as to provide the best possible mix of soil and additives. The ports on the cutting head must ensure early mixing of the conditioning agents with the excavated

material. At the cutting head, each injection point should have its own delivery line in order to prevent blockages. This mainly concerns the face ports that are more prone to blockages.

A high advance rate is achieved due to the improved flow characteristics of excavated material through the cutter head and the lubrication of the moving parts.

Spoil handling:

Soil conditioning agents also affect the handling process by reducing the wear of the parts of the spoil removal system. In slurry shield machines, the spoil is pumped out from the face to the surface separation plant. In order to transport the spoil efficiently with the minimum pipe and pump wear at the required velocity, the slurry must have the optimal flow characteristics. For example, thixotropic properties of the bentonite slurry are useful so that in case of a circulation halt, spoil remains in suspension without settling out in the pipes. The reduction in the friction losses in the pipes, valves and pumps results in lower power consumption and savings in energy.

In slurry shield machines, the last stage of the excavation process is the separation of the spoil from the slurry. The addition of conditioning agents facilitates the separation process. Adding special flocculating or deflocculating agents can also enhance separation. The final spoil contains less fine material after it has been processed in the separation plant and therefore is in a more suitable state for disposal. In slurry shields, the excavated material is removed hydraulically and is separated from the support medium (bentonite) in a separation plant. This is the major disadvantage of using slurry shield machines on account of environmental hazards and the high cost involved should the soil contain a high percentage of fines (Herrenknecht, 1994; Maidl *et al*, 1996).

In EPB shields, screw conveyors achieve the removal and the transportation of the excavated material from the pressurised excavation chamber to the tunnel exit under atmospheric pressure. The removal rate is very significant because it is related to the rate of advance. Ideally, the two rates should be compatible, otherwise loss of the support pressure at the tunnel face occurs. When the soil in the excavation chamber has not reached a sufficiently low permeability, a further injection of conditioning agents in the screw conveyor prevents excessive flows of water. An important detail with regard to the design of screw conveyors is their position in the excavation chamber. When the screw conveyor is located at the bottom of the excavation chamber, it is easier to empty it. The spoil should be

in a suitably plastic state in order to allow controlled extrusion through the screw conveyor without causing excessive wear or consumption of power (Milligan, 2000b).

Sometimes the same type of conditioning agent is used to achieve different material properties. For example, in the excavation chamber of an EPB machine, the aim is to make the soil more plastic and workable usually by adding water. However, afterwards excessive water in the screw conveyor can create problems (Milligan, 2000b).

In *Table 1.1*, the application of soil conditioning agents with tunnelling machines is summarised. In this table, TBMs include the open or shield mode machines suitable for rock conditions whereas slurry shields and EPBs, are principally for soft ground conditions. Specifically, in EPBs, the addition of conditioning agents extends their range of application (*Table 1.2*) as described in the ensuing paragraphs.

The suitability of the various types of conditioning agents depends on the different ground conditions encountered. For example, in clays, when bentonite slurries are used, the addition of polymers makes them more effective. However, if polymers are used alone, they will disappear into the formation without providing any lubrication (Lyon, 1999a).

In sands with gravels or poor rock and in sandy-silty soil, foams can be used as conditioning agents. When cobbles and gravel are encountered, polymer additive with foam (0.1 to 3 % per volume) is necessary. The addition of foam offers two major benefits: increased compressibility and reduced permeability.

In fine-grained soils, foam can be enhanced with natural polymers, which prevent water absorption. This helps to prevent clogging and balling. Milligan (2000b) noted that in stiff over-consolidated clays, the addition of agents makes clay more plastic. However, it is difficult to estimate how much water must be added to reduce the undrained shear strength. If too much is added, then it can turn the clay to slurry whereas insufficient water can make the clay stiffer and would then need extremely high power to remould it.

In high plasticity clays, a large quantity of water is required to sufficiently change the water content and therefore, the shear strength. In this case, the danger is the creation of large chunks of clay in a softened soil matrix that will clog up the machine and the conveyor (Milligan, 2000b). For intermediate plasticity clays, the best practice is to create a rubble of

intact clay blocks in a ‘matrix’ of polymer foam, which inhibits water absorption but allows clay blocks to slide around each other.

1.1.4 Soil conditioning agents for EPB machines

This section describes the soil conditioning agents used with EPBs. These soil conditioning agents are typically foams, water or oil based mixtures with bentonite clay or polymer suspensions.

In EPBs, the role of soil conditioning agents is to improve the soil properties by both increasing compressibility and reducing shear strength and permeability. The objective is to make soil more plastic with low internal friction and low permeability. Failure to satisfy the above criteria, results either in blockages at the cutting head, clogging or problems in transporting. Without soil conditioning agents the use of EPBs would be limited to fine-grained soils (Maidl *et al.*, 1996).

The common materials used with EPBs are bentonites, foams and polymers. Polymers and bentonite slurries are introduced into the soil in a liquid form, usually as thixotropic fluids. It is of prime importance that the exact quantity of the additives is precisely predetermined.

Bentonite slurries used in tunnelling industry are made by mixing bentonite and water. They have thixotropic properties, forming a gel at concentrations 3-6 % per volume (Lyon, 1999a). The name bentonite is used to characterise a range of clay minerals: primarily potassium, calcium and sodium montmorillonites. Montmorillonites consist of thin flat sheets of clay particles and have the ability to absorb water and to swell. Water is absorbed onto the external and internal sheet surfaces due to their low bonding energy. Calcium ions provide a stronger bond than the sodium ones and swell less. In tunnelling practice, sodium bentonite is preferred because it is the most dispersing type, showing higher viscosity than the other types for the same slurry density. Bentonite slurries can be used as a means to enhance the capacity of the slurry to carry the excavation debris (Lyon, 1999b).

Polymers are made from small chemical compositions, known as ‘monomers’, through a chemical process, in which the monomers are linked together to form large long chain molecules. Polymers are used separately or in addition to bentonite, to form suitable

slurries. Some types of natural polymers such as cellulose sugars, starches and proteins can be used in tunnelling. In addition to these, synthetic polymers such as polyacrylamides (PA), carboxymethyl cellulose (CMC) and polyanionic cellulose (PAC) can be used. Synthetic polymers have been developed in the petroleum drilling industry as an alternative to bentonite slurries. When used with bentonite, they improve the ability of bentonite slurries to form ‘filter cake’ and to maintain a dispersed structure. However, polyacrylamides and their derivatives are very important as soil conditioning agents (Milligan, 2000b) and have been used particularly with EPBs with foam or bentonite as face stabilisers (Babendererde, 1998). The role of the polymers is the inhibition of the ground from absorbing water, dehydration and (when used with oil) the lubrication of the tunnel or shaft. Water absorbing polymers like partially hydrolysed polyacrylamides (PHPA), can be used with foam in small proportions to ‘plastify’ coarse-grained soils.

Foams as conditioning agents are presented in Section 1.2

1.2 Foams

1.2.1 General

Foams are defined as a dispersion of gas bubbles in a liquid or solid in which at least one dimension falls within the colloid size range (1-1000 **mm**). Thus, foams typically contain either very small bubbles or more commonly, quite large ones separated by thin liquid films (lamellae). The detailed study of foams is beyond the scope of this thesis; here only some basic aspects of foam behaviour are presented.

The dispersed phase of the foam is usually called the internal phase, whereas the continuous phase, external. Foams can be depicted two-dimensionally as a structure in which foam is between two phases: on the bottom, there is bulk liquid and above this, in a second bulk phase, gas. The gas phase is separated from the thin liquid-film by a two-dimensional interface. The region that encompasses the thin film and the two interfaces on either side of the film is conventionally defined as lamella (*Figure 1.2*).

Foam can be formed in a liquid, if bubbles of gas are injected and the liquid between the bubbles can drain away. In pure liquids, gas bubbles will rise and separate according to

Stokes' law. The foam structure will be unstable because there will be no thin-film persistence. Persistence can be achieved by adding surfactants, which transform the bubbles into foam cells. In these cases, the foam contains gas, liquid and a foaming agent. The stability (persistence) of the foam is related to the film thinning and the coalescence process. The stability is determined by a number of factors (Bikerman, 1973): gravity drainage, capillary suction, surface elasticity, viscosity, electric double layer repulsion, dispersion force attraction, steric repulsion and proper surfactants.

The interfacial properties in foams are of prime importance because the gas bubbles have a large surface area. Even a modest surface energy per unit area can become a considerable total surface energy. As the bubble size decreases, the total surface area increases and consequently energy has to be added to the system to achieve dispersion of small bubbles. The energy can be either mechanical and/or chemical by adding the proper surfactant (Schramm & Wassmuth, 1994).

The role of surfactants is to reduce the surface tension. Surfactants are chemical compounds, typically short-chain fatty acids that are either amphiphilic or amphipathic. The most favourable orientation of these molecules is at surfaces or interfaces so that each part of the molecule can reside in the fluid for which they have greater affinity. In this way, they create monolayers at interfaces. The surface absorption of a surfactant at the interface acts against the normal interfacial tension.

Surfactants are classified according to the nature of the polar (hydrophilic) part of the molecule (*Figure 1.3*). In an aqueous solution, dilute concentration of surfactants act as normal electrolytes but as their concentration increases, their behaviour alters. The surfactants behaviour can be explained in terms of the formation of organised aggregates of large numbers of molecules called micelles. In micelles the lipophilic parts of the surfactants associate in the interior of the aggregate and leave the hydrophilic parts to face the aqueous medium. The concentration at which micelle formation becomes significant is called the critical micelle concentration (cmc) (*Figure 1.4*) and it is a property of the surfactant but this depends on the nature of hydrophilic group and the surface (Porter, 1994). The range of Molar values of the cmc for typical surfactants is between 10^{-5} and 10^{-1} . Above a certain temperature, which is called the Krafft point, the solubility of some micelle-forming surfactants increases due to the maximum reduction in surface or interfacial tension occurring. The Krafft point is the temperature at which the cmc is equal

to the saturation solubility (Moroi, 1992). Surfactants are classified based on the charge carried by the polar head group: anionic, cationic, non-anionic and amphoteric.

Immediately after foam generation, there will always be a tendency for liquid to drain due to the force of gravity. The liquid will drain by flowing downward through the existing liquid films, which constitute the interior of the lamellae. The gas bubbles will not be spherical and at this point, the capillary forces will become competitive with the forces of gravity. The pressure differences between the plateau area force the liquid towards the plateau area, initiating the thinning process, which in turn, will lead to film rupture and the collapse of the foam.

The initial requirements for foam formation are low surface tension and surface elasticity. Schramm and Wassmuth (1994) noted that greater elasticity tends to produce more stable bubbles, but a restoring force is needed in order to produce persistent foams and counteract the 'overwhelming effects' of the gravitational and capillary forces. If a surfactant-stabilised film undergoes a sudden expansion, then immediately the expanded portion of the film must have a lower degree of surfactant absorption than unexpanded portions because the surface area has increased. This local surface expansion provides surface tension, which increases the resistance for further expansions. The resisting force exists under the condition that surfactant absorption equilibrium has been established in the film. This is known as the Gibbs-Marangoni effect, where a tension force counteracts film rupture (*Figure 1.5*). The durability of the thin layer is dependent on the surface elasticity, which is a dynamic phenomenon; many surfactant solutions display dynamic surface tension behaviour.

Another aspect of foam behaviour is the electric double layer. The interfaces on each side of the thin-film are equivalent so that any interfacial charge will be equally carried on each side of the film. If a foam film is stabilised by ionic surfactants, then their presence at the interfaces will induce a repulsive force that opposes the thinning process. The magnitude of the force will depend on the charge density and the film thickness.

Gas bubbles can be stabilised entirely by the repulsive forces created when two charged interfaces approach each other and their electric double layers overlap. Schramm and Wassmuth (1994, p. 28) noted that "when the interfaces that bind a foam lamella are electrically charged, the interacting diffuse double layers exert a hydrostatic pressure that

acts to keep the interfaces apart". The net pressure difference between the gas phase (bubbles) and the bulk liquid from which the lamellae extend is called 'disjoining pressure'. This pressure is the total of electrical, dispersion, and steric forces that operate across the lamellae.

1.2.2 Foam properties

The term "foam" implies the mixture of foam concentrate with water and air. Until recently, protein-based foaming agents were deemed to be more suitable than the synthetic ones for tunnel operations because they tend to retain the water for longer, producing more stable bubbles (Cash & Vine-Lott, 1996). Protein-based foams consist of protein-based agents and a glycol-based booster. Protein-based agents, in turn, consist of various sources of hydrolysed protein (animal blood, horn and hoof meal, soya beans, waste fish and corn gluten), solvents and stabilizers (Lyon, 1998). However, synthetic foams, which are composed of anionic hydrocarbons, solvents and stabilizers (Lyon, 1998), have been improved and are becoming very popular. Synthetic foams consist of synthetic detergent and a glycol-ether booster. In both types of foaming agent, a soluble polymer can be added together with other special site-specific additives like corrosion inhibitors, solvents and anti-freeze agents.

Regardless of the foam type, a very crucial parameter, which determines foam persistence, is the bubble size. Bubbles have diameters greater than 10 mm. Foam stability is not necessarily a function of bubble size, although there may be an optimum size for an individual foam type. Foams should not be characterised in terms of a single bubble size because there is a size distribution, which can be represented by a distribution function. Generally, the smaller the air pores, the more stable the foam will be. The size of the bubbles depends on the dilution rate, the density of the foam, the foam generator and the mechanical conditioner (Cash & Vine-Lott, 1996).

A bubble size distribution that is weighted toward smaller sizes represents the most stable foams. In such cases, changes in the bubble size distribution curve with time yield a measure of the stability of the foams. The bubble size distribution also has an important influence on the viscosity, which increases as the size reduces. This happens because the enlarged interfacial area and the thinner films increase the resistance to flow. The viscosity

will also be higher when the bubble sizes are relatively homogeneous, which is when the bubble size distribution is narrow rather than wide (Schramm & Wassmuth, 1994).

It must be mentioned that the existence of a different phase – solids - alters the behaviour and the properties of the foam. The presence of dispersed particles can increase or decrease foam stability, which can be achieved by having a bulk viscosity enhancement, so that a stable dispersion of particles in the solution will be created. In addition, another mechanism is present when the particles are not completely wetted with water. In this case, particles tend to collect at the interface in the foam where they may add to the mechanical stability of the lamellae. Intermediate contact angles between 40 and 70° appear to be optimal for solid-stabilised foams (*Figure 1.6*). The easiest way to control foams is by adding a suitable surfactant but they can be very costly (Porter, 1994) and for this reason, should be used carefully. Foam control is achieved by using additives called anti-foams, which prevent the formation of foam, and de-foamers, which cause collapse of the already formed foams.

1.2.3 Testing foamed soil

There are various tests available to evaluate the foam properties and their effectiveness in soil conditioning. Various test procedures have been developed based on experience and previous applications of foams mainly in the petroleum industry. The bulk properties of the foams can be determined through standard testing as suggested by ASTM (Schramm & Wassmuth, 1994). Generally, foam stability is tested through one of three methods:

- lifetime of single bubbles
- steady-state (dynamic) foam volume under given conditions of gas flow
- rate of collapse of a (static) column of foam generated

For tunnelling applications, Quebaud *et al* (1998) recommended some simple tests to characterise foam:

- The generation test to study the relationship between the generation pressure of the fluid in the generator with the foam flow rate
- The consistency test in order to quantify the foam quality (bubble size)
- The half-life test to measure the time necessary for foam to lose half of its solution
- The compressibility test to understand the foam behaviour in a confined environment under pressure variations

Similar to the half-life test is the “quarter drain time” test, in which the volume of the liquid produced by the degradation of the foam is collected in a measuring cylinder. The term “quarter drain time” refers to the amount of time required to achieve 25% liquid drainage from the foam structure.

The compressibility of the foam can be measured by varying the air pressure applied to a foam volume. The test uses a transparent cylinder filled with foam, on which air pressure p is applied. Assuming that the law $PV=\text{constant}$ applies, the expansion ratio ER at absolute pressure p related to ER_a at atmospheric pressure p_a is:

$$(ER-1) p = (ER_a - 1) p_a \quad 1.2.1$$

The expansion ratio ER is defined as the ratio of the total volume of foam tested to the volume of liquid required to produce that foam.

It must be noted that the rheological properties of foam are sensitive to each test. Thus, for tunnelling applications it is better for the foam to be tested mixed with the soil. There are some special tests which can be carried out that assess the water content, slump, torque resistance (adhesion test), sedimentation and permeability:

1. Foam penetration test

The objective is to determine the penetration of the injected foam into the ground in front of the cutter-head. Excessive penetration will result in excess foam consumption and the support pressure provided may be inadequate; if the penetration is insufficient, there is the risk of ground water inflow. The apparatus used in this test forces foam to penetrate a soil sample in a test cylinder against a back pressure. Quebaud *et al* (1998) reported that initial penetration of about 30 mm into the sample was almost instantaneous. The results, however, cannot be applied directly to the tunnel machines because the conditions and the mechanics differ considerably (Milligan, 2000b).

2. Mixing test

There are different mixing tests for foamed soil (Decon, 1996; Quebaud *et al*, 1998; Condat, 1998) but all of them are based on the same procedure: a system of blades stirs the soil in a pan or tank and the power input required for the mixing is measured. Afterwards

foam (with or without another additive) is added and the reduction in power consumption is measured. Bezuijen *et al* (1999) and Bezuijen (2000) carried out some mixing tests in an experimental chamber, under confining pressure, in an attempt to simulate the EPB conditions.

3. Slump test

Simple slump tests (as those performed on fresh concrete) can give an indication of the plasticity of the soil. Quebaud *et al* (1998) suggested that a slump of 12 cm is required to provide a mixture with the optimum characteristics for plastic flow in an EPB. Maidl (1995) and Jancsecz *et al* (1999) also noted, after carrying out this type of test, that foam made the soil more plastic.

4. Permeability test

Permeability can be measured in a constant head permeameter (for coarse-grained soils) and in a hydraulic compression cell or (for fine grained-soils) special techniques such as constant flow rate permeability tests (Zhang *et al*, 1998) can be employed. Foamed soil is less permeable than ordinary soil by over two orders of magnitude as Quebaud *et al* (1998) and Bezuijen *et al* (1999) reported.

5. Compressibility test

Compressibility can be assessed in a cylinder similar to that used in foam penetration testing (Milligan, 2000b). Alternatively, foamed soil specimens can be tested in a hydraulic compression cell under different vertical pressure.

6. Adhesion/friction test

According to Quebaud *et al* (1998), measurement of the friction angle can be achieved on a sloping stainless steel plate. Alternatively, this can be achieved by using a shear box (Jancsecz *et al*, 1999) or a ring shear apparatus in order to measure the continued sliding over an interface under confining pressure (Milligan, 2000b). This test aims also to measure the adhesion between the foamed soil and metal surfaces.

7. Cone Penetrometer test

This test determines the effect of different foaming agents on clays. The apparatus consists of a metallic cone, which falls down into the soil sample and the penetration depth is

measured. Jancsecz *et al* (1999) in the Izmir tunnel project noted that the more foam or the higher the foaming agent concentration added to the soil, the higher the penetration depth.

TBM manufacturing companies in Japan, Germany and UK have carried out research on the effect of foams in tunnelling. More advanced research in this area was undertaken in Germany (Maidl, 1995), in France (Quebaud, 1996) and in the Netherlands (Bezuijen *et al*, 1999; Bezuijen, 2000). The German and French projects centred on foamed soil properties and the influence of different proportions of foaming agents on soils. The Dutch project had quite a complex experimental set-up. The effect of foam on soil was studied in an apparatus, in which the excavation process was simulated. The results showed the relationship between the shear strength of the soil and the porosity. The addition of the foam increased the porosity and decreased the permeability by replacing the pore water. Research on foamed soil in the UK started recently at Oxford University. The aim of this study is to evaluate the mechanical properties of different soil conditioning agents (foam, bentonite and polymers) as well as their effectiveness when mixed with different soils. The project focuses on coarse-grained soils.

1.3 Current Practice in the Use of Foams in Tunnelling

Excavating, mixing and handling the excavated soil results in a waste of energy and wear of the moving parts of the EPB machine. The addition of a relatively cheap conditioning agent such as foam can lead to significant reductions in the torque required for the cutting and transportation of spoil. The benefits of using foam are presented in this section along with several case studies.

1.3.1 Main issues using foam with EPBs

Foams are used with EPB machines in fine-grained soils. In coarse-grained soils, the permeability of the soil is the crucial parameter and should not exceed 10^{-5} m/s (Herrenknecht, 1994). EPB TBMs operate more effectively when the soil immediately ahead of the cutter and in the excavation chamber forms a 'plastic' plug, which prevents water inflows and ensures face support. Foam appears to integrate very well with the soil. When foam is added, the bubbles lower the density of the earth slurry and reduce the

friction among soil particles. Reduction of the ground internal friction leads to a reduction in power requirements.

Foam must be added onto the face so that it mixes with the soil before the air bubbles start to disintegrate. A foam-generating unit produces foam where the foam solution is swirled up with compressed air and then is injected through nozzles in front of the cutting wheel or into the excavation chamber. Based on site experience, the conditioning unit should be mounted as closely as possible to the injection point (Cash & Vine-Lott, 1996; Mauroy, 1998). Additionally, the injection points should be as close as possible to the cutter head (Moss, 1998).

As stated in Section 1.1.3, one of the main objectives of adding foam to the face is to create an impermeable layer. In the case of bentonite slurries, this can be achieved after the consolidation of the slurry, which becomes an impermeable membrane. However, in low permeability soils, the ability of bentonite slurries to form the ‘filter cake’ falls (Herrenknecht, 1994). Foam can be used with EPBs, in any type of soil, provided that the final permeability of the foamed soil is not over 10^{-5} m/s . By adding anionic-active water absorbent polymers such as PAs, the soil particles are coated, creating a three-phase system (Herrenknecht & Maidl, 1995). In front of the cutting wheel, foam displaces free pore water out of the soil and thus the polymers can be absorbed. Hence, the watertightness of the recently developed three-phase system lies considerably above that of the natural ground.

Another benefit of using foam is the increased compressibility of the soil. As a result, the bulk modulus of the ground mixture is lowered so that it is possible to control the support pressure at the tunnel face (Maidl *et al*, 1996). If the pressure in the excavation chamber is dropped, the gas phase within the structure will expand and the ground will deform. As the volume of soil is relatively small and well-confined in the excavation chamber, small differences in the proportion of foam:excavated soil can be used as a rapid response measure to a sudden change of ground conditions at the tunnel face.

The major advantage of using foam instead of bentonite-based conditioning agents is that a significantly smaller volume of extra liquid is added to the natural water content of the muck. This, in turn, results in a smaller volume of excavated material. As 90% of foam consists of air, which will escape entirely after only a few days, the original consistency of the ground can be restored very quickly. The other 10% of foam consists of solution which

is 90-99% water and the rest, foaming agent and polymers (Maidl *et al*, 1996). Laboratory tests (DECON, 1996) showed that the best performance in tunnelling operations can be achieved by using a mixture of 10% solution: 90% air. The same report revealed the dependence of the foam stability on the temperature as well as the ratio of solution:air.

The foam expansion rate (FER), otherwise known as expansion ratio (ER), is an important parameter in measuring the effectiveness of the liquid concentration in producing foam. It is also important to know the foam injection ratio (FIR) or mixing ratio, which is the ratio of volume of foam over the volume of excavated soil. On site, the FIR should be varied significantly in different ground conditions (Kusakabe *et al*, 1999):

Environmental issues are becoming increasingly important when it comes to tunnelling practice. The trend is to use biodegradable materials such as low toxicity protein-based foams. There are some standards procedures to evaluate the toxicity and biodegradability of foams. It should be mentioned, however, that these tests are designed for fire-fighting foams, for which a large variety of types exists in the market. One of the main benefits of using foams in tunnelling is that foam dissolves with time when the air disappears and the foaming agents are biodegradable. On the other hand, polymers, which can be used with foams, degrade very slowly but recently degradable polymers based on natural materials are becoming popular (Lyon, 1999b).

However, information on the environmental impact of soil conditioning agents is limited. This is because there is no standard test procedure to assess the suitability of the existing products. The problem is becoming evident in the case of pipe jacking, where the slurry is disposed in the muck and part of it is used for lubrication and consequently will remain in the ground. Furthermore, the cost of disposal increases when the material contains either toxic or non-biodegradable materials because additional remedial treatment is required. Rapid degradation may be problematic because as Milligan (1999, p. 13) noted “if run-off enters water courses, the degradation reaction may de-oxygenate the water”. Conditioning agents that are based on natural materials like guar (slimming aid), xanthan (a constituent of tomato ketchup) or locust bean gel are environmentally safe. The solvents based on oil as well as the fluorocarbons in foams are considered to be potentially dangerous.

1.3.2 Case studies

Peron & Marcheselli (1994) first reported the use of foam in sandy-gravelly soils for a shallow tunnel of 8.0 m diameter in Italy. The foam system was developed by Obayashi in Japan. The proportions of the foam concentrate were 1.5% foaming agent and 0.7% of cellulose polymer stabilizer in water. The proportion was foaming solution 100 l : air 600 l (@1.9 bar). The FIR was from 60 to 80% in dry soil and from 50 to 60% in water bearing ground.

Another situation where foam was used was the Valencia metro tunnels (Wallis, 1995). The tunnel was beneath the ground water table, in alluvial sands and gravels with about 15% fines and some lenses of stiff silty clay. EPB was fitted with injection ports for both bentonite and foam. After experiencing problems using bentonite as the conditioning agent, it was found that the use of foam produced a more homogenous and compressible material. The average consumption was about 500 l of foam per m^3 excavated, of which only 18 l were foaming solution, compared to 220 l/ m^3 of bentonite. The FIR ranged from 25 to 35%. The foam mixed with the soil reduced the power and the torque needed to turn the cutting wheel by the order of 20%. Herrenknecht and Maidl (1995) also referred to the same case as evidence of the benefits of utilising foam.

Webb and Breeds (1997) reported another successful use of foam in a tunnel, with a water head of up to 18.3 m, driven through mixed ground. Various proportions of a water-absorbing polymer were used (0.5 to 2%) together with foam and bentonite. Mauroy (1998) reported the positive effect of using foam as a soil conditioning agent in reducing cutter-head torque for a 7.7 m diameter tunnel in clay. The foam had an expansion ratio of 20 and was injected through different ports at the cutter-head and into the excavation chamber and the screw conveyor. Babendererde (1998) also referred to the same project noting a cutter-head torque reduction of over 50% and thrust force reduction from 2000 to 1200 t.

Another successful case of use of foam with polymer and bentonite (Jancsecz *et al*, 1999) was the construction of part of the Izmir rail transit tunnels. The 6.5 m diameter EPB was driven through a wide variety of soil conditions such as sandy silts, sands and clay under water table. In silty sand and clay foam (with bentonite) of about 300 to 500 l/ m^3 , an ER of 6 to 10 was used. In a second drive in the same formation, due to clogging of the foam injection pipes, the soil conditioning agent was switched from foam to bentonite slurry. In

sandy soil, the ER was increased from 12 to 15. In silty soil (sea-side), foam was utilised only when needed to keep the water away and to make the muck less ‘sticky’. The polymer consumption varied between 0.01 and 0.5 kg/m³ of excavated soil. Bentonite was used instead of foam during the stoppages because of break-downs or maintenance. The authors concluded that the use of foam in combination with bentonite and polymer improved considerably the performance of the EPB machine in terms of productivity, cost and safety.

There are also several references on the benefits when EPBs are used with soil conditioning agents. Pellet and Castner (1998) reported the benefits of soil conditioning in also reducing the face resistance. Maidl (1999) noted the success of using EPBs with foam in the Netherlands in layered silty and clayey sands under earth pressure conditions reaching 350 kPa. Maidl and Jonker (2000) also discussed the increased flexibility and adaptability of EPBs using foam in the Netherlands. They also noted that due to high pressure, transportation by screw conveyor could not be guaranteed, which is why a mixed system with conveyor belt and slurry pipe was used. In the mass-transit tunnelling project in Singapore (Reilly, 1999), EPBs were used with foam and polymer or with foam and bentonite, under face pressure varying from 150 to 360 kPa in mixed ground. The results were an impressive reduction in required torque as well as low settlements. Melis (1999) reported that for Madrid Metro project, the overall cost of utilising EPB did not exceed that of other tunnelling methods and at the same time was faster.

Problems using foam and polymer with EPBs were reported by Doran and Athenoux (1998). The problems encountered were in glacial tills with water-bearing lenses under pressure 2.2 bar and in hard fractured clays. The main difficulty faced was to control the water content in the low plasticity clay and consequently excessive wear was recorded. In those conditions, the slurry mode of operation was considered preferable.

1.4 Summary of the effects of the conditioned soil properties on EPB performance

In the previous sections the properties of various soil conditioning agents and their role in modifying the ground properties in tunnelling applications were presented. In this section, the effect of the foamed soil properties, particularly on the improvement of the EPB

performance, is summarised. The three fundamental properties of the ground examined are compressibility, permeability and shear strength. In the ensuing paragraphs the influence of each soil property on the operation of EPBs is discussed.

1.4.1 Compressibility

The increase of the compressibility of the soil in the pressure chamber through the addition and mixing of conditioning agents, improves the workability and the homogeneity of the spoil. A more compressible and 'plastic' material in the pressure chamber enables the bulkhead to be responsive to pressure fluctuations, resulting in a better control of the stability of the face. The main benefit is that if the material in the pressure chamber is very incompressible then small fluctuations in extraction rate cause large pressure changes. Increase in compressibility causes a "softer" response in which the pressure in the chamber can be more easily kept constant.

1.4.2 Permeability

Reduction of soil permeability at the face minimises the possibility of face collapse due to water inflow. Successful control of the permeability of the spoil in the pressure chamber allows a suitably plastic consistency to be achieved. This is also important in the spoil removal stage where an effectively impermeable spoil can be remoulded in the pressure chamber and extruded through the screw conveyor without allowing inflow of ground water. Particularly in stiff clays, the aim is to form a rubble of intact blocks, in a matrix of foam which inhibits uptake of water by the clay.

1.4.3 Shear strength

The shear strength of the soil affects the wear of moving parts and cutting tools. Decreasing the angle of shearing resistance of the soil at the face results in a reduction in wear due to the reduced resistance to cutting. Reduced resistance results in reduction of wear and torque and consequently, significant savings in energy. Another function of the conditioning agents is the lubrication of the cutting parts which in turn reduces the working temperatures and extends the life of moving parts such as the cutter-head, cutters and screw conveyor.

Reduced resistance in shear improves the workability of the spoil once it enters in the pressure chamber and the screw conveyor. However, if the shear strength is reduced too much than it may not be possible to sustain the necessary pressure gradient in the screw conveyor.

1.5 Research Objectives

In the UK, individual contractors have investigated foamed soil behaviour in an attempt to provide solutions to specific construction projects. To this end, the Research and Technical Committee of the Pipe Jacking Association (PJA) in collaboration with Oxford University initiated a research project at the end of 1998 on soil conditioning and lubrication in tunnelling and pipe jacking. The Civil Engineering Group at Oxford University, with the assistance of the PJA, EPSRC and water companies, has been carrying out research on pipe jacking for more than 14 years in total. The current project is at stage six of the whole research programme and its objective is to produce guidelines on the effectiveness of various soil conditioning agents in tunnelling applications and to specify suitable assessment procedures for soil conditioning agents. The correlation of the laboratory tests with data from active tunnelling projects will establish a set of test procedures for assessing soil conditioning agents under various ground conditions. Further understanding of foamed soil behaviour will benefit the tunnelling and pipe jacking industry.

The objective of this thesis is to explore and assess the behaviour of foam/sand mixtures. In order to investigate the basic foamed sand mechanism, tests on the fundamental soil properties - compressibility, permeability and shear strength of soil – were carried out. The aims of the research project are broken down as follows:

- to produce foam in-house, suitable for further testing
- to assess the foam produced and compare different kinds of foaming agents
- to carry out basic compressibility and permeability tests on foamed soil and demonstrate the effect of the different conditioning agents on sands with relevance to 1.4.1 and 1.4.2.
- to carry out direct shear strength tests and assess the shear strength changes with relevance to 1.4.3

- to provide an initial explanation of the mechanism governing foamed soil behaviour based on these preliminary tests

It must be noted that in the literature there are no reports of experimental work on foamed soil using standard soil mechanics equipment. No 'simple' theoretical framework has been developed to explain foamed soil behaviour due to the nature of its complexity. Research has focused primarily on simulation and description of the process rather than on explaining the foamed soil behaviour.

Chapter 2. Sample Preparation and Properties

2.1 Equipment Set-up

2.1.1 Small scale testing

In Chapter 1 the objectives of the project were identified. In this chapter, several small-scale mixing tests carried out on foam/sand mixtures are discussed. These initial tests provided a first indication of the suitability of the specific experimental equipment and procedures.

Generally, small-scale tests offer some benefits over larger scale testing:

- High stresses can be imposed without requiring special safety procedures or measures.
- The sample can be considered homogenous.
- It is a fast way to establish an initial datum of performance of the foamed soil against which decisions for the suitability of larger equipment can be made.

Small-scale testing included mixing, compression, permeability and shear-box tests. Mixing tests were performed in order to study the behaviour of the foam-soil as well as to evaluate the importance of foaming agents when introduced to a cutting surface such as a mixer paddle. However, the way of mixing sands with grout is of prime importance for non-uniform size mixtures (Scharz & Krizek, 1994).

Compression tests were carried out to study the volume change characteristics of the foamed soil together with changes in compressibility and permeability. Shear-box tests were performed to assess the shear strength changes of the soil after the addition of foam.

At the outset, it was unclear whether small-scale tests would be sufficiently conclusive. The main advantage of testing larger samples is that in some cases, they provide more reliable and reproducible results since a larger volume of soil is placed away from the boundaries, minimizing the interference with them.

2.1.2 Soil mixer

Initially, some large-scale trials were carried out by using second-hand equipment to mix soil and foam. The aim was to test whether mixing sand with foam would provide any significant reduction in power consumption. In order to study the stated problem an experimental laboratory system had to be set-up. A large soil-mixer machine, of about $\frac{3}{4} m^3$ capacity, together with a foam generator would comprise the initial experimental set-up. Considerable time and effort was required to make the foam-generator operational and compatible with the large soil mixer. However, due to the difficulties in operating the equipment and experimenting with different mixtures, the author employed a small single-phase soil mixer of 4.56 l capacity (*Figure 2.1*). This soil mixer was reliable and of a convenient size so that it could be used together with the other apparatus for small scale testing. In order to measure the power input required to turn the paddle, an electronic wattmeter was connected in parallel to the soil mixer. The set-up is shown in *Photo 2.1*.

2.1.3 Foam generator

Many difficulties were experienced in bringing the second-hand foam-generator to an acceptable operating level and various obstacles were faced in accessing a similar capacity system from the marketplace. The main problem was the fact that the foam generator was initially designed for industrial use and consequently the compressed air requirements exceeded the capacity of the laboratory compressed air supply line. Due to the poor air:liquid mixture (2:1 to 3:1) the foam produced was of poor quality (not dry enough). Therefore, the author decided to develop a foam generator in-house, suitable for small scale testing. Considerable effort was invested in making a simple yet effective, new foam generator.

The author designed the new foam generator specifically for the small-scale tests and bearing in mind the available space within the civil engineering laboratory (*Photo 2.2*). The basic design requirements were that:

- The generator ought to be constructed as soon as possible using spare parts and components.
- It had to be a simple design - robust and preferably portable without requiring complex electrical equipment.

- The size had to be such that it would allow small-scale testing, using the available soil mixer.
- It should produce stable foam at a rate compatible with the capacity of the testing equipment.

Figure 2.2 shows the basic design as it was conceived by the author. The foam generator consists of the following parts:

- A cylindrical high pressure tank of 144 mm internal diameter, 525 mm external height and 7.0 l capacity, filled with fluid
- A 'Venturi' Inverter to mix the liquid and the air, a sketch of which is shown in *Figure 2.2*
- A smaller metallic cylinder of 125 mm diameter and 175 mm height called the mechanical conditioner, filled with small pieces of perforated tube (*Photo 2.3*)
- Two main circuits, the high pressure air circuit and the fluid circuit
- Various regulators and pressure gauges

The liquid consisted of water and the foaming agent (concentrate). The foam generator operates by mixing solution (liquid) with compressed air at a proportion of 10:90. Literature within the field cites similar proportions (DECON, 1996; Maidl *et al*, 1996). The solution consists of water, the foaming agent (concentrate dissolved in water) and in some cases, a small amount of polymer. In every case, the water comprised 95-99% of the solution. The high air pressure system was necessary in order to create a mixture of air and fluid. Foam concentrate and water were mixed into the pressure tank. The prescribed proportions are presented in Section 2.1.4. The solution was then pressurised through the inlet valve on the top of the tank with compressed air. It was of prime importance that the pressure in the tank was less than that of the air circuit in order to achieve satisfactory mixing.

Another important aspect is that the fluid and the compressed air had to be mixed before reaching the mechanical conditioner. This was achieved by mixing the compressed air with the fluid in a 'Venturi' Inverter (*Photo 2.4*). This component has an internal configuration consisting of a T-shape pipe system (see sketch in *Figure 2.2*). As the compressed air goes through the larger L-shape pipe, it generates a difference in pressure across the main pipe and in turn sucks fluid from the smaller pipe. The proportion of air in the mixture was high resulting in the creation of foam. However, the foam had to be conditioned in the

mechanical conditioner in order to produce relatively stable 'single size' foam. The diameter (15 mm) of the perforated tubes (*Photo 2.3*) in the mechanical conditioner appeared to be critical to the creation of foam bubbles of appropriate size (less than 1.0 mm). The maximum pressure of the air system was 7 bar and the operating pressure was 1.8 bar. The generator delivered foam at a rate of 2-4 l/min at atmospheric pressure.

The exact proportions of air:liquid under pressure were not known as this would have required two separate mechanical flow-meters. However, after each trial the ER was measured (See Section 2.1.4). The proportion of the foam concentrate to water was calculated for each test as the mixing took place in the pressure tank. The proportions and the masses of water and concentrate were taken into account to derive the amount of foam concentrate used in every test.

2.1.4 Foam testing

The aim was to have the foam generator produce the required amount of foam of acceptable quality. The foam quality can be assessed from the foam ER and the drainage time.

It appeared that high viscosity foam agents required a pressure difference between the air circuit and the pressurised tank. The production rate was estimated and the ER was calculated by filling up the drainage pan with the foam.

There are no standard tests for assessing the quality of foaming agents for tunnelling applications. The suitability of the foam as a conditioning agent is determined from the ER, which is the ratio of a measured volume of foam over the volume of the liquid required for its production. The measured volume is the volume of a drainage pan. For this purpose, a drainage pan of 2242 ml capacity was made in the workshop. At the bottom of the drainage pan, there was a shut-off valve in order to control drainage. During each test, the pan was filled up with foam and afterwards, the foam was left to drain out into a measuring cylinder. The ER ranged between 5 and 40. PP90 foam and especially Versa foam gave higher ERs as well as a drier, "shaving" foam in comparison to the other foam agents. Quebaud *et al* (1998) noted that an ER of greater than 7 is considered adequate for tunnelling applications.

Another measure of the foam quality is the drainage time *i.e.* the time required to drain out a certain quantity from the drainage pan. However, the drainage time measured for every compression test (see Chapter 3) varied, as the ER was not constant. The drainage time for half life test (50% of the drainage volume measured) varied between 15 and 25 min.

2.2 Materials Used

2.2.1 Sands

Two different types of sand were used in order to test the effect of the foam on different size material. The sands were uniform so that when they were mixed with foam, produced a homogenous mixture. Furthermore, the behaviour of uniform sands is more likely to be sensitive to changes of one particular parameter whereas in well/gap-graded soils the different shapes and particle sizes when mixed with slurry tend to add inter-particle mechanisms.

The two types of sands were fine and coarse sand (*Photo 2.5*). The coarse sand was Leighton Buzzard silica (yellow) 14/25. This is a very uniform sand (coefficient of uniformity $CU = 1.3$) with angular grain shape $G_s = 2.65$ and mean particle diameter $d_{50} = 0.85\text{ mm}$. Minimum and maximum void ratios for the coarse sand were 0.49 and 0.79 respectively (Bolton, 1986). The fine sand was Leighton Buzzard silica DA 81DF. It is also a very uniform material ($CU = 1.4$) with $G_s = 2.65$ and mean particle diameter $d_{50} = 0.165\text{ mm}$. Minimum and maximum void ratios for fine sand were calculated as 0.61 and 0.91 respectively, after measuring the dry density at the loosest and the densest states.

2.2.2 Foaming agents

Five different types of foam agent were tested. The foam generator was able to operate with all of them producing acceptable quality micro-foam. Different proportions of foam:water were tested under different air pressure. The types of foam tested included:

- Angus – Fire P90 (protein based foam agent).
- Angus - Fire PP90 (protein based foam agent with polymer).
- CETCO SC200 (synthetic polymeric foam agent).

- CETCO Drill-Terge (synthetic polymeric foam agent).
- CETCO Versa VSX foam agent (synthetic polymeric foam agent).

In addition to these, the CETCO InstaPac 425 a polymer (PHPA) was used as well as a special synthetic oil (VCP) for drilling applications. SC200 and Terge Drill were tested adding an anionic polymer (CETCO InstaPac 425) at about 0.05% to the foam concentrate. The role of the polymer is to absorb water, to cover the sand particles providing adhesion as well as to contribute to the creation of a homogenous mixture.

However, after carrying out some compression tests (see Chapter 3), only one type of foaming agent, based on the CETCO Versa foam, was used in compression and shear-box tests. The author decided to concentrate on one foaming agent and investigate the effect of other parameters based on the fact that compression tests (see Chapter 3) on the same sand but using different types of foaming agent showed quite similar behaviour.

It was difficult to draw from the literature a method of calculating the required proportion of the foaming agent and polymer in the foam solution. Initially, different proportions of foaming agent for fine and coarse sand were utilised, based on field experience. After some trials, the final foam solution consisted of VSX ‘Versa’ foaming agent 3% per volume, VCP oil with Instapac425 and SC200 (this polymer mixture was conventionally named by the author as ‘FOP’) 0.7% per volume. The role of ‘FOP’ is to act as a ‘booster’ enhancing the bubble production. The foam generator tank had a capacity of 7.0 l and consequently the total quantity used was 210 ml of foaming agent and 50 ml of ‘FOP’. This mixture appeared to produce foam with a stable bubble size. From a first microscopic inspection, the size of the foam (‘Versa’ foaming agent 3% with ER = 15) bubbles produced was in the range of 0.1 to 1 mm. This mixture was used for both sands.

2.2.3 Bentonite and polymer

A very important and commonly used soil conditioning agent is bentonite. Attention was focused on testing the previous sands, enhanced with bentonite slurry alone and in combination with other conditioning agents. The bentonite used was the CETCO Hydraul-EZ type bentonite. This is a sodium montmorillonite-type bentonite able to swell to about 10 times its original volume. The proportion of bentonite powder to water is critical for the rheological characteristics of the produced bentonite slurry. The presence of dispersed

particles, like bentonite powder in water, alters the flow characteristics and this effect, which is reflected by the viscosity, is strongly dependent on the concentration of particles. After some trials, it was decided that the bentonite slurry should be around 5% per weight (mixture of bentonite powder to water at a proportion 5:95). In tunnelling applications, the bentonite slurry dosage should be enough to fill the theoretical porosity of the sand more than one time, in order to be able to create the impermeable 'filter cake'. The theoretical porosity n' is that of the dry sand at a loose state and is given by the formula:

$$n' = e_{max} / (1 + e_{max}) \quad 2.2.1$$

where e_{max} is the maximum voids ratio of the dry sand defined as the ratio of voids volume in soil structure over the solids volume. The porosity is related to the water content:

$$n' = w G_s / (1 + w G_s) \quad 2.2.2$$

where w is the water content and G_s , the specific gravity of soil particles. The theoretical porosity for fine sand was 0.476 and for coarse sand 0.441, after applying Equation 2.2.1. Thus the volume of the bentonite slurry was:

$$V_{slurry} = \alpha n' V_{sand} \quad 2.2.3$$

Where α values, ranged from 0.5 to 1.9, are shown in *Table 2.1*. Calculations are based on several compression tests (see Chapter 3). The quantity of bentonite used in those tests was 80 g for the coarse sand whereas 60 g for the fine sand.

It is convenient to use the bentonite slurry voids ratio e_{bs} , which can be defined as the ratio of the water used (V_w) over the volume of the bentonite V_{bs} :

$$e_{bs} = V_w / V_{bs} \quad 2.2.4$$

The volume of bentonite can be calculated knowing the specific gravity (2.35) and the mass of the bentonite. For the compressibility tests (see *Table 2.1*), the bentonite slurry voids ratio varied between 17 and 31.

Lyon (1997, p. 18) states that bentonite's ability to swell is due to the presence of montmorillonite, which "consists of crystal lattices of sheets of molecules or atoms that are thinner and more readily separable in water than those of other clays". Montmorillonite provides greater surface area upon which water molecules may be absorbed. The presence of calcium in the water reduces the effectiveness of bentonite because calcium ions have a higher charge valence and therefore hold the crystal lattices of sheets more tightly allowing less dispersion in water. The water used for the mixing was tap water with a measured pH between 6.5 and 6.8. However, better mixing was achieved when the water had a pH between 7 and 8. The presence of calcium was detected by adding a tiny proportion of ammonium oxylate. The water was treated with caustic soda (NaOH) or soda ash (Na_2SO_4) so that the pH reached 8.

In all cases with coarse sand and in some with fine sand (see Chapter 3), a small proportion (25-60 ml) of a polymer mixture 'WOP' (Water:VCP Oil:Polymer) was added. In each test, the quantity of dry sand used was between 1500 and 2000 g. In the case of coarse sands, the addition of 'WOP' helped to produce a more homogenous foamed soil by creating a high viscosity fluid matrix. The initial proportions were (4:1:1) respectively, and the dosage from 0.01 to 0.04 ml of 'WOP' mixture per g of dry sand. The addition of this mixture was necessary in the cases where the water content of the sand was more than 27-35%. 'WOP' was added during mixing in the soil mixer bowl as a 'pre-conditioner', prior to the addition of foam. The performance of the 'WOP' mixture improved when the proportion of oil:polymer changed from 4:1 to 2:3. The final 'WOP' dosages used were 25 ml for the fine sand and 50 ml for the coarse sand (10 ml and 20 ml polymer InstaPac425 respectively). In the case of coarse sand, this quantity was the minimum required to achieve a homogenous mixture in the mixer bowl so that a representative slurry sample could be tested. However, when bentonite slurry was added, the effectiveness of the 'WOP' mixture decreased. It must be mentioned that PHPA polymer and oil were not volatile; after putting a specimen of predetermined quantity in the oven at 120°C for 24 hours, the mass remained was 97 and 98% respectively. Thus, in the calculation of the voids ratio (see Chapter 3) both of the additives were taken into account as part of the water fraction in the voids.

Slurry bulk density was calculated indirectly by measuring the amount of water in the sample (Chapter 3). The slurry bulk density in the mixer bowl was measured with an instrument called a 'mud balance'. It consisted of a base upon which is balanced a graduated arm with a cup, lid, knife edge, level vial, rider and counterweight (Lyon, 1997).

The slurry was poured into the cup until it filled it up. Moving the rider, until level on arms indicated level, balance was achieved. The density of the various mixtures varied significantly. Foamed mixtures with either coarse or fine sand were less dense compared to those with bentonite. For foam/sand mixtures, the bulk density varied between 1.05 and 1.65 kg/l depending on the foam quantity and the presence of bentonite.

A measure of the viscosity of the slurry may be made with the Marsh funnel. Viscosity characterises the flow properties of the mixture. The Marsh funnel has a diameter of 150 mm at the top, tapering over a distance of 300 mm to a smooth bore tube 50 mm long with an inside diameter 4.8 mm. Over half of the top opening is a wire screen with apertures of 1.6 mm. The time (in seconds) required for a certain quantity of slurry (1500 ml) to pass through exit tube is measured using the Marsh funnel. The measurement in the case of fine sand with bentonite was about 45 whereas in the case of coarse sand with bentonite was about 59.

2.3 Foam/Sand Mixing

2.3.1 Foamed soil samples

Four types of tests were carried out: mixing tests, compressibility tests, permeability tests and shear strength tests. Samples were prepared following the same procedure for every type of test. The soil mixer bowl was filled with sand in a dry state. Afterwards, water was added in a proportion that gave a mixture of prescribed water content. The dry sand mass was between 1500 and 2000 g.

The mixing sequence of the different materials was of prime importance. Particularly in the case of the bentonite slurry, the polymer mixture had to be prepared outside the mixing bowl. The prescribed quantity of bentonite powder was mixed with distilled water (pH 7.5) in a separate pan. Then the polymer mixture was added and mixed with the bentonite slurry until visual uniformity was achieved. This sequence was important in preserving the effectiveness of the polymer in retaining water. Afterwards, the mixture was poured over the saturated sand into the soil mixer bowl. Where foamed soil was tested in combination with bentonite and polymer, the bentonite slurry was mixed with saturated sand first and then foam was added.

After the foam was produced, it was tested to measure the ER. The elapsed time between production and testing was kept to a minimum. The required quantity of foam was estimated by measuring the time and the production rate (*ml/min*) after collecting the foam in a pan of known volume.

The slurry was mixed in the soil mixer at the lowest mixing speed. Higher speed did not improve mixing and would not have been representative of real-life conditions. Mixing was considered ‘completed’ when it appeared to be homogenous following a visual inspection.

The test procedures for compression and shear-box tests are described in the following chapters.

2.3.2 Foam/sand mixing test

One of the main objectives of adding foam in an EPB machine is the reduction of the wear in the moving parts as well as the reduction of the required torque. This is vital in reducing power consumption as well as wear of the cutting wheel. This effect has been studied on an experimental scale (DECON, 1996) using large, industrial size equipment. In an effort to achieve similar behaviour through the reduction of power required to mix the soil, the author set-up an experiment using the soil mixer and foam.

It must be noted that these tests did not intend to simulate real conditions but to obtain an indication of the reduction of mixing power. Thus, the aim was to measure the input power consumption needed to rotate the mixer paddle when different combinations of materials were mixed in the mixer bowl. The fine sand was mixed with different quantities of water and the power input was measured in each case.

Two different mixing tests were carried out. In the first set, the power consumption was measured for different water contents (*Table 2.2*) while in the second, the influence of foam was tested and the relative power reduction was measured (*Table 2.3*). In each case, water content w was calculated as:

$$w = M_w / M_s \quad 2.3.1$$

Where M_w is the water mass and M_s is the solids mass. In the above definition, solids mass includes the non-volatile component of the foaming agent, as it is described in Section 3.3.1. Although there would be an argument for including the non-volatile fraction with the solid rather than liquid, the above is the more practicable definition for experimental purposes as it can be obtained from conventional wet and dry mass measurements. In all tests, the dry sand mass was 1500 g. The fundamental volume-mass relation for every soil is:

$$S e = w G_s \quad 2.3.2$$

Where S is the degree of saturation, e is the void ratio and G_s is the specific gravity. The degree of saturation is defined as the percentage of the voids that contain water and the non-volatile component as it is described in Section 3.3.1. Foam quantity in the mixture was evaluated by introducing the FIR defined as the ratio of the volume of foam injected into the mixture over the total volume of the mixture.

Figure 2.3 shows the power consumption of water-sand mixtures at different water content. The power consumption is related to the torque required to turn the mixer paddle and consequently to the shearing resistance of the soil mixture. It is evident from *Figure 2.3* that for all tests the power requirement peaks at a certain water content. This occurs at a water content of about 27%, which indicates according to Equation 2.3.2, a degree of saturation of about 78.6%, assuming the maximum void ratio (0.91). For an unsaturated soil, this is close to the limit of a continuous air phase (Fredlund & Rahardjo, 1993). The lower dashed line represents the ‘air’ power consumption P_{air} , which is the power required by the mixer to rotate the paddle.

In the second batch of tests (*Table 2.3*), foam was added. The power reduction due to foam can be assessed from the relative power requirement. The relative power requirement Pr can be defined as the ratio:

$$Pr = (P_f - P_{air}) / (P_{ws} - P_{air}) \quad 2.3.3$$

Where P_f is the measured power with foam and P_{ws} is the power measured with wet sand. *Figure 2.4* shows the plot of relative power requirement in foamed sand against FIR. The

water content in these tests was between 27 and 33 %. The relative reduction in power requirement reached 100% in some cases. However, when FIR exceeded 0.32 the power reduction did not show further improvement.

The variation of the relative power requirement of the various soil mixtures is shown in *Figure 2.5*. The vertical axis is the relative power increase ΔP with respect to P_{air} :

$$\Delta P = 100 (P - P_{air}) / (P_{ds} - P_{air}) \quad 2.3.4$$

where P is either P_{ws} or P_f while P_{ds} is the power measurement for mixing dry sand. The relative power increase in the case of foamed soil is much lower than that of wet sand. The required power increases slightly as the water content increases for the foamed sand case (*Figure 2.5*). The values in *Table 2.4* were the averages calculated from the water-sand mixing tests (*Table 2.2*) and foam-water-sand mixing tests (*Table 2.3*). P_{air} was considered to be constant (110 W).

The mixing tests demonstrated the positive effect of adding foam to a wet sand mixture by reducing the required power input required. It appeared that this behaviour occurred after a certain quantity of foam was introduced to the mixture. Additionally, the beneficial effect of foam is more significant at a range of water content between 22% and 30%, for this particular type of sand. The power reduction provides an indication that foam when mixed with sand reduces the internal friction of the mixture and consequently, its shear resistance. The implication of this behaviour in terms of compressibility, permeability and shear strength will be discussed in the following chapters.

Chapter 3. Compression Tests

3.1 Compressibility of Foamed Soil

3.1.1 Introduction

Classical soil mechanics refers to soils fully saturated with water. However in many cases, soils are not fully saturated, and the voids are filled with water and air or even gas. These soils are defined as unsaturated and their behaviour differs significantly from that of saturated soils. The relative quantities of water and gas within unsaturated soil are of prime importance since they alter the basic soil structure considerably, resulting in different mechanical behaviour. Thus, unsaturated soils can be classified depending on the degree of saturation; when it is low, the gas phase is continuous but the water discontinuous, forming menisci at particle contacts. When the degree of saturation is high, the water is continuous but the gas forms discrete bubbles. These extreme cases of unsaturated soils are likely to behave differently (Wroth & Houlsby, 1985).

Assuming that soil particles and pore water are incompressible, the volume changes in a saturated soil are due to the water flow. In the case of unsaturated soils, volume changes are due to water and air flow as well as to air compression during loading. At this stage, foamed soil can be considered a special type of unsaturated soil.

In recent decades, considerable effort has been invested in the study of unsaturated soils. The most important finding was that the concept of a single effective stress was invalid in describing the volume change behaviour for unsaturated soils. Bishop and Blight (1963) first used two independent stress variables ($\sigma - u_g$) and ($u_g - u_w$), where σ is the total applied stress and u_g , u_w the pore air and pore water pressures respectively. Fredlund and Morgenstern (1976, 1977) analysed the unsaturated soils as a four phase material, considering the fourth phase as the air water interface (contractile skin). They carried out experiments verifying the uniqueness of a three dimensional surface with three independent state parameters: the voids ratio e , the net total stress ($\sigma - u_g$) and the matric suction ($u_g - u_w$).

When there is air in the voids, fluid menisci form at inter-particle contact points. Two types of pore water can be recognized: bulk water and capillary water acting on single soil particles. In this situation the effects of changes in capillary water pressure and total stress are independent: the former induces variations of normal stresses at the inter-particle contact points and the latter still acts as in the saturated soil case (Rampino *et al.*, 1999). Thus, two independent stress state variables are necessary to describe the soil behaviour: the total net stress and the matric suction. An unsaturated soil will undergo volume change when the net normal stress or the matric suction variable changes in magnitude. For unsaturated soils containing water and air, Fredlund and Rahardjo (1993) described extensively the subject by presenting different concepts for volume change theory.

Another case of ‘non-saturated’ soils is gassy soils. These soils form in the seabed if it contains undissolved gas, typically methane nitrogen or carbon dioxide. The degree of saturation is high and the gas is usually in the form of discrete bubbles which are much larger than the normal void spaces (Wheeler, 1988). Considerable research has been undertaken at Oxford University to investigate the behaviour of these soils, the findings of which are presented in Wheeler's (1986) and Thomas' (1987) theses. However, the experimental work demonstrated that these soils do not satisfy the unsaturated soil model of a single compressible fluid. The behaviour was explained (Thomas, 1987) by adopting a double compressibility model. Thomas (1987) showed that in the case of gassy soils, unlike other unsaturated soils, the gas pressure was not governed by the pore water pressure. The only restraint was that the menisci had to hold a gas pressure between a maximum and a minimum value of capillary pressure. More recently, in Canada, Grozic *et al.* (1999) carried out undrained triaxial tests on loose gassy sand. The results revealed that sand strain softens and experiences flow liquefaction.

3.1.2 Volume changes and pore fluids

One of the fundamental aspects of soil behaviour is the volume change properties. In conventional soil mechanics, volume change theory is formulated by constitutive relations. The volume change constitutive relations are equations which relate the stress state to the deformation state variables. Several forms of the volume change constitutive equations have been developed for saturated as well as unsaturated soils.

Volume change theory can be expressed in a compressibility form. The compressibility of saturated soil is described by Terzaghi's one-dimensional consolidation theory. The derivation of the equation is based on the conservation of the mass of water flowing through an element of saturated soil. The theory can be found in standard textbooks.

Generally, the volume change of a phase is related to a pressure change by its compressibility C as:

$$C = - dV / V dp \quad 3.1.1$$

where V is the total volume and dV/dp is the volume change with respect to a pressure change dp . The negative sign is used in order to give positive compressibility in Equation 3.1.1. In classical soil mechanics, the compressibility of the skeleton is defined by using the volume change coefficient m_v with respect to changes in net normal stress for one-dimensional consolidation. In compressibility form, constitutive equations can be written as:

$$\mathbf{De}_v = m_v \mathbf{Ds}_v' \quad 3.1.2$$

where \mathbf{De}_v is the compressive volumetric strain and m_v is the coefficient of volume change with respect to a change in normal effective stress \mathbf{Ds}_v' .

The mechanical behaviour of an unsaturated soil under compression is governed by the change in pressure of its main components: air, water and soil. Pore pressures (air and water) are generated after loading under undrained conditions. The applied total stress is carried by the soil and pore fluid (water and air) depending upon their compressibility. Thus, the induced pore air and pore water pressures are related to the applied total stresses. The excess pore pressures will dissipate if pore fluids (water and air) are allowed to drain (drained conditions).

In soil mechanics volume and volume changes can be represented by the voids ratio e and the change in voids ratio \mathbf{De} respectively:

$$e = V_v / V_s \quad 3.1.3a$$

$$\text{and } \Delta e = e_i - e_f \quad 3.1.3b$$

where V_v is the volume of voids in the soil structure, V_s is the volume of solids, e_i the initial and e_f the final voids ratio. In this thesis, the volume of voids includes the water, the gas and the volatile component of the liquid foaming agent (FOP) and the additive WOP, whereas the volume of solids includes all the non-volatile components.

Fredlund and Morgenstern (1976, 1977) visualised unsaturated soils as a four-phase mixture, with two phases that come to equilibrium under applied stress gradients (soil particles and contractile skin) and two phases that flow under applied stress gradients (air and water). The total volume change of the soil element must be equal to the sum of volume changes associated with each phase. If the soil particles are assumed to be incompressible, the continuity requirement for the unsaturated soil can be stated as follows:

$$\Delta V_v / V_o = (\Delta V_w + \Delta V_g) / V_o \quad 3.1.4$$

Whereas V_v/V_o is the volumetric strain which can be used as a deformation state variable and defines the soil volume change resulting from the deformation. The volume of contractile skin is assumed to be negligible. Equation 3.1.4 can be written in a form using the voids ratio:

$$\Delta e = \Delta e_g + \Delta e_w \quad 3.1.5$$

This expression can be used to determine the relative reduction of the two phases (water/gas) after the completion of the compression stage. For example, Fredlund and Rahardjo (1993) noted that in some cases where the air volume becomes less than approximately 20% of the voids, air dissolving in water significantly affects the compressibility of the air-water mixture. However, this is not the same in the case of foamed soil where the air (gas) void ratio is generally higher.

On the other hand, the compressibility model for gassy soils had two modes of deformations, as was presented by Thomas (1987). The first mode of deformation was due to the local shear behaviour and the compression and dissolution of the gas which accompanied changes in total stress. The second mode of deformation was due to overall

drainage or shear behaviour of the saturated matrix and was caused by changes in consolidation stress. According to the same author (p. 248) "a gassy soil behaves as a saturated soil containing discrete compressible solid inclusions". He also noted that time-dependent volume changes that occurred under undrained conditions, such as local consolidation around gas voids and the dissolution of gas into pore water, were difficult to separate from the volume changes due to the dissipation of pore water pressures.

Matric suction appears to be one of the main stress variables that affects an unsaturated soil. However, matric suction can be described using the Kelvin equation; for unsaturated soils the pore air pressure is related to the value of the pore water pressure and their difference depends upon the surface tension T between air and water without taking into account any effect of the vapour pressure:

$$u_a - u_w = 2T/R \quad 3.1.6$$

where u_a is the air-pore pressure, u_w is the water-pore pressure and R is the radius of curvature of the formed air water menisci. The above equation provides a qualitative description of the dependency of matric suction on the bubble size. However, Fredlund and Rahardjo (1993) noted that it is almost impossible to measure the radius of curvature. Furthermore, a macroscopic compressibility model incorporating satisfactorily the above relationship has yet to appear in the literature.

3.1.3 Scope and objectives

In Chapter 1, it was stated that one of the main benefits of using foam in tunnelling is the increase in the compressibility of excavated soil. The increased compressibility improves the EPB's productivity and efficiency allowing for better control in the whole excavation process. Creating a 'plastic' spoil with reduced stiffness allows the machine to be more responsive to sudden changes of pressure at the face of the tunnel.

After reviewing the literature, it became evident that there is no unified theory for the compressibility behaviour of soils containing water and gas in various proportions. Particularly for foamed soil, experimental data is lacking. Bearing this in mind, the primary objectives of the volume change study were to:

- quantify the volume changes under vertical loading in a hydraulic cell (Rowe cell)
- correlate volume change characteristics with the type of loading (undrained-drained) and with time and evaluate the difference between different combinations of conditioning agents
- identify the mechanics of the particular behaviour that results from the use of foam

The apparatus, the procedure and the results of the tests are presented in the following sections.

3.2 Compressibility Tests in Rowe Cell

3.2.1 Description and calibration of the apparatus

Compressibility tests were performed in a 75 mm diameter Rowe cell (*Figure 3.1*). This choice of apparatus was based on some advantages that the Rowe cell offers over the conventional oedometer, which can be summarised as follows:

- Larger samples can be tested compared to oedometer testing.
- Permeability can be measured directly with a proper set-up.
- It has a hydraulic loading system and control facilities. Control of the drainage at the bottom enables loading to be applied in an undrained manner, allowing development of the pore pressure. This also allows the initial immediate settlement to be measured separately from consolidation settlement.
- The sample can be loaded either by applying uniform pressure over the surface ‘free strain’ or through a rigid plate, which maintains a loaded surface plane and is known as ‘equal strain’.

Additionally, the Rowe cell was available immediately and the author brought it to operational condition in a relatively short amount of time. It must be noted that if a larger Rowe cell had been used, a higher proportion of foam:soil and a bigger volume sample could have been tested. The benefit lies in the fact that more reliable data can be acquired. However, a larger Rowe cell would require a larger sized soil mixer.

The experimental set-up is shown in *Figure 3.2*. It consisted of the 75 mm diameter cell, a pressure transducer to measure the applied pressure, appropriate signal conditioning units, an LVDT (linear variable differential transformer) to measure changes in height.

Furthermore, there was an air/water pressure interface system to convert the operating air pressure to hydraulic pressure, a sensitive pressure regulator (0-60 psi) as well as the various valves, tubes (4 mm) and fittings (*Photo 3.1*). The maximum allowable vertical pressure of this set-up was 240 kPa.

The pressure and the displacement of the diaphragm were measured electronically through a Data Acquisition Unit (DAU). The DAU provided power to the transducers, amplified the return signal and stored it in memory. The unit was controlled by a PC that enabled to access the data at any time during test. Data were retrieved at the end of each test for subsequent processing. Measurements were taken at a rate of one per second.

Two types of calibration are required in compression tests. The first type of calibration is to determine the relationship between the output from the transducers and the parameters being measured. The LVDT was calibrated using a caliper and the pressure transducer was calibrated against a digital pressure indicator, Druck DPI 600. Calibration curves described the correlation between measured voltage and applied pressure as shown in *Figure 3.3*. The other type of calibration is the system compliance. System compliance concerns the diaphragm displacement correction. In this case, a diaphragm calibration test was performed to measure the deflection of the diaphragm itself. A dummy sample of mild steel was placed and after applying load, the displacement was measured. Strain was measured as diaphragm displacement over sample height. The load-displacement curves (loading-unloading) gave a strain less than 0.5% within the range of 50 to 220 kPa (see *Figure 3.3*). The deformation of the diaphragm was deducted from the measured deformation. The fluctuation of the recorded values was of the order of 1 to 2%.

Furthermore, a test was performed pressurising the cell using water, at the test maximum pressure (226 kPa), in order to measure possible leakage from valves, seals and diaphragms. During some trials, leakage was observed through the O-ring seal and before the cell cap was placed and bolted. This brought to light a problem, which later had to be taken into account during quality control of the results (see Section 3.3.2).

3.2.2 Test procedure

The type of test conducted was with ‘equal strain’ loading and single drainage at the bottom. The procedure followed for the compressibility tests was as follows:

The sintered bronze porous discs were placed beneath the diaphragm to collect water draining vertically from the sample. The average permeability of the discs was in the order of 10^{-6} m/s. These discs provided rigidity and uniformity of loading pressure on the top surface. Before each test, they were boiled in de-ionised water for at least 20 min in order to saturate them. In the cell base, a ‘vyon’ porous plastic was fitted in the central drain hole. This fitting had to be replaced every few tests with fine sand, as it tended to be clogged due to the presence of fines.

As soon as the foamed soil was well-mixed (about 2 min), the Rowe cell was prepared. The outlet at the base level was filled with water in order to flush out all the air. The first sintered bronze porous disc was placed above the base. The second was positioned after the sample had been poured into the cell. The discs were porous to allow drainage but at the same to prevent clogging of the outlets by the finer material. The upper disc also provided ‘rigidity’ and allowed a uniform displacement to be applied to the whole surface of the specimen. The foamed soil was poured into the cell (still in a very loose state). Finally, the cover was lowered carefully to sit onto the flange without entrapping air or causing pinching. Attention was given to ensure that the diaphragm flange lay perfectly flat on the body flange.

The LVDT was set on the top of the settlement drainage rod and the initial readings were recorded. As the pressure valve was on, the pressure regulator was adjusted to low values (less than 10 kPa). Prior to each test, in order to de-air the hydraulic system, the bleed valve on the top of the cap was opened so that any trapped air bubbles were driven out of the system.

With the valve of the diaphragm pressure line closed, the pressure was adjusted with the regulator to the value of the first loading stage. In total nine loading stages were carried out in each test and four unloading stages. The sequence was (14.1, 20, 28.3, 40, 56.6, 80, 113.1, 160, 226.2, 113.1, 56.6, 28.3, 14.1 kPa) for the Series I tests. For the subsequent tests

the sequence in the unloading phase was altered to give a better distribution (20, 28.3, 40, 56.6, 80, 113, 160, 226, 160, 80, 40, 20 kPa). It is recommended (Head, 1994) in conventional oedometer tests that the successive load values be double that of the previous stage (in other words the load increment is equal to the load already applied). Due to the high compressibility of the foam, the author considered that a close spacing of points would be more appropriate, thus the load increment was factored by $\sqrt{2}$.

Initially, some tests were performed with the bottom outlet valve kept continuously open during the loading stage (fully drained). The rest of the tests were carried out in two stages: undrained and drained stage. In the former, the bottom outlet was closed and the load was applied. After the immediate settlement was completed, the outlet was opened and the consolidation was recorded. The vertical pressure was increased to the next increment as soon as the LVDT measurements reached a steady value. However, some tests were performed using equal time intervals. During the unloading stage, the bottom outlet was left open.

Before and after the test, the sample was weighed and the water content, dry density and the voids ratio were determined. The procedure's shortcomings are presented in Section 3.4. The height was measured with a caliper before and at the end of the test at different radial positions and the average was considered to be the mean height of the sample.

3.3 Tests Results

3.3.1 Calculation procedure

To simplify the analysis of tests results, the compression tests are listed in date order. Tests marked with letter 'f' stand for the fine sand tests whereas those with the letter 'c' stands for coarse sand. In total, 47 different tests were carried out, primarily on fine sand and foam. Four different foaming agents were used as well as different proportions of bentonite and polymer for fine and coarse sand. The first tests were fully drained tests (*f01-f13*); the rest had an undrained stage and then were drained at each loading step. The results from the consolidation tests after processing are presented in *Table 3.1*. Tests are numbered in date order together with some data about the materials used and some comments derived from the testing procedure. As is noted in the remarks' column, some tests are characterised as

inconclusive due to rather high discrepancies in the measurements, and this will be explained in the next section.

One objective of compression tests was to determine the volume change difference for various conditioning agents as can be expressed by the voids ratio. The total voids ratio consists of two components: the gas voids ratio e_g and the water voids ratio e_w , which can be expressed as:

$$e_g =$$

$$\frac{\text{Volume of Gas} + \text{Volume of the Volatile Component of the Mixture}}{\text{Volume of Solids}}$$

and

$$e_w =$$

$$\frac{\text{Volume of Water} + \text{Volume of the non-Volatile Component of the Mixture}}{\text{Volume of Solids}}$$

The volatile and the non-volatile component of the mixture refer to the quantity of the polymer and oil used, as stated in Section 2.2.3. The following procedure was followed for the calculation of voids ratio.

The (bulk) density of the sample at any time was:

$$\mathbf{r} = M / V \quad 3.3.1$$

where M was the mass of the sample and V its volume. The mass was measured on a scale and the volume was deduced after measuring the height of the sample at the beginning or at the end of the experiment. The area of the sample remained constant during the test. Knowing the density, the dry density \mathbf{r}_d could be calculated as:

$$\mathbf{r}_d = \mathbf{r} / (1 + w) \quad 3.3.2$$

where w was the water content measured from a sub-sample at the beginning of the test (the procedure will be explained later in this section). The same measurements were carried out at the beginning and at the end of each test.

The voids ratio (for the initial or final conditions) can be calculated as:

$$e = (G_s \mathbf{r}_w / \mathbf{r}_d) - 1 \quad 3.3.3$$

where G_s is the specific gravity of solids in which the non-volatile component of the additives (FOP and WOP) was included. According to Vertugo and Ishihara (1996) for loose soil, the calculation of voids ratio through the water content and dry density is more reliable than that through the height measurements. Assuming that during the test the cross section area of the sample remained constant, the equivalent height of solid particles was:

$$H_s = H_o / (1+e_o) \quad 3.3.4$$

where H_o was the initial height of the sample (measured) and therefore, the difference in voids ratio at each stage with regard to the initial conditions was:

$$\mathbf{D}e = \mathbf{D}H / H_s \quad 3.3.5$$

where $\mathbf{D}H$ is the measured (LVDT) change in height. The voids ratio at each stage was:

$$e = e_o - \mathbf{D}e \quad 3.3.6$$

However, the difference in voids ratio consisted of the difference in gas voids ratio e_g and the difference in water voids ratio e_w (as defined in previous page) is:

$$\mathbf{D}e = \mathbf{D}e_g + \mathbf{D}e_w \quad 3.3.7$$

The difference in water voids ratio was calculated by measuring the water volume in the drained stage. Thus, combining equations 3.3.5, 3.3.6 and 3.3.7, the difference in gas voids ratio at any loading stage was:

$$\mathbf{D}e_g = \mathbf{D}H / H_s - \mathbf{D}e_w \quad 3.3.8$$

Furthermore, knowing the amount of water in the final stage, the water voids ratio together with the gas voids ratio were determined:

$$e_w \text{ final} = e_w \text{ initial} - D e_w \quad 3.3.9a$$

$$e_g \text{ final} = e_g \text{ initial} - D e_g \quad 3.3.9b$$

After determining the water voids ratio at the beginning and the end of each increment, the gas voids ratio was also calculated. The final voids ratios were the final values of the last unloading stage. The initial values of ratios were those calculated at the beginning of each test.

A measure of the one-dimensional deformability of the soil per unit thickness is the volume change coefficient m_v which can be calculated knowing the incremental voids ratio difference de :

$$m_v = de / dS_v (1+e) \quad 3.3.10$$

where dS_v was the incremental vertical pressure change.

For each stage, graphical plots of settlement and volume change against time can be obtained. The settlement (compression) against time graph is used to derive the time corresponding to 90% of compression t_{90} , which is necessary in order to determine the coefficient of consolidation c_v :

$$c_v = T_{90} H^2 / t_{90} \quad 3.3.11$$

where H is the drainage path, equal to the mean sample height at the particular stage and t_{90} is the equivalent time of 90% consolidation. T_{90} is a time factor equal to 0.848 (for single drainage with equal strain loading) derived from a theoretical consolidation curve (Head, 1986). The coefficient c_v is usually expressed in m^2/year . It must be noted that for the compression tests, the analysis was dependent on an overall behaviour and the calculated t_{90} value was calculated assuming a curve fitting technique based on ‘averaged’ degree of consolidation. This approach is explained in relation to evaluation of permeability, in Section 3.5.

A typical example of the spreadsheet calculations made for tests of foamed fine sand with bentontite and polymer mixture ‘WOP’ is *Table 3.2*. On the first page of the spreadsheet, the measured quantities before mixing are presented and represent the initial proportions of the materials added in the mixer bowl. Each material (sand, foam, bentonite slurry and polymer ‘WOP’) is expressed in volume and mass of its basic components (air, water and solid). The measure (input) values are highlighted. The column marked ‘Proportion’ shows the consumption of each material in the mixture. For example, ‘Proportion’ 0.95 indicates that 95% of the initial material quantity was used for mixing. In the box entitled ‘Mixture’, all the materials are expressed in mass and volume, according to their volatility. For water and air, the volatile fraction is 100%, whereas for oil and PHPA, 2 and 3% respectively. The box at the bottom right hand corner of the spreadsheet displays the most important indices: the water content, the degree of saturation, the voids ratio, the FIR and the bulk density.

On the second page of the spreadsheet, the calculations made at the beginning and at the end of the text, based on measurements, are presented. Again, the measured (input) values are highlighted. On the right hand side of the second page, in the ‘Computed values’ box, the initial and final values of the water and gas voids ratio are depicted. In the same box the initial and the final mass of water is also given. These values have been deduced from the measurement data, according to the calculation procedure described in Equations 3.3.4 – 3.3.7. The compressibility coefficient is calculated for each compression stage applying Equation 3.3.10. The permeability coefficient is calculated in some of the compression stages, where it was possible to do so (See Section 3.5).

During mixing part of the air in the foam was lost, thus the voids ratio in the mixture e_o was lower than that of the sample e_i . In the ensuing section, the methodology used to explain the uncertainty in measurements is discussed.

3.3.2 Quality control

The measurements taken in the tests include an element of redundancy which allows certain cross-checks to be made. Quality control of the results was necessary to evaluate the range of error during the whole process of the compression tests.

The main concern was the derivation of the final voids ratio value and the shape of the curve voids ratio *versus* vertical stress, which reveal the compressibility characteristics of the foamed soil. However, the question which arose was how much confidence can one assign to the absolute value of the final voids ratio provided that there are some water gains or losses during the process. A simplified sketch of the procedure is shown in *Figure 3.4*. Discrepancies are expressed as water mass differences corresponding to loss or gain of water during the process.

A critical parameter in determining the initial or the final voids ratio e is the water content w , which is defined as the ratio of water mass over the solids mass.

$$w = M_w / M_s \quad 3.3.12$$

The mass of solids includes the non-volatile component of the additives as described in Section 3.3.1. Water content was measured at the beginning and at the end of the test from a sub-sample. It was assumed that the water content in the sub-sample would be the same as that in the cell and that in the mixer bowl. However, the values calculated and those derived from the mixing proportion were not exactly the same.

There were three ways to calculate the initial water content. The first was through the measured quantities put in the mixer bowl. In that case, the water content could be defined as (*Table 3.2*):

$$w_o = \frac{\text{total mass of the volatile component}}{\text{total mass of the non-volatile component}}$$

Another way was by applying the Equation 3.3.12, after putting a sub-sample in the oven for 24 hours, measuring the mass reduction and calculating the water content w_i .

Finally, the third way applied to tests without foam where saturation S was 100%. The water content is related to the voids ratio at all times using the following expression:

$$w G_s = e S \quad 3.3.13$$

Furthermore, for the conditions of Rowe cell compression tests, it can be safely assumed that at any time:

$$De/(1+e) = DH /H \quad 3.3.14$$

The initial estimated water content w_{ie} can be deduced from Equations 3.3.13 and 3.3.14 using the final values:

$$w_{ie} = w_f + DH (w_f + l/G_s) / H_f \quad 3.3.15$$

where w_f is the final measured water content, H_f is the final measured height of the sample, G_s is the specific gravity of the solids and DH the measured compression of the test.

The discrepancy between the various water contents in the mixture w_o , w_i and w_{ie} was expressed in water mass (g) that should be added or removed in order to match these numbers. In the case of foam tests, a comparison was made between w_o and w_i . The calculated discrepancy dM_w was:

$$dM_w = dw M_s \quad 3.3.16$$

where dw was the water content difference ($w_o - w_i$, $w_i - w_{ie}$ and $w_o - w_{ie}$) and M_s the mass of solids which was:

$$M_s = M_i / (1+w_i) \quad 3.3.17$$

With M_i , the initial measured mass of the sample.

Another way to calculate the discrepancy between the measured and calculated values is by examining the degree of saturation at the beginning of the test. The comparison is between the degree of saturation S_o based on the mixture material proportions and the degree of saturation calculated at the beginning of the test S_i . In this case, the equivalent difference in height of the water can be calculated from the initial degree of saturation S_i

$$dH_w = dS e_i H_i / (1+e_i) \quad 3.3.18$$

where the difference dS is

$$dS = S_o - S_i \quad 3.3.19$$

The initial degree of saturation S_i is calculated from:

$$S_i = w_i G_s / e_i \quad 3.3.20$$

The initial voids ratio can be calculated as:

$$e_i = (G_s r_w / r_d) - 1 \quad 3.3.21$$

where r_d is the dry density (Mg/m^3) of the sample. The difference in water mass is

$$dM_w = G_w p_w A dH_w \quad 3.3.22$$

where A is the cross sectional area (mm^2) of the sample. This type of check calculation involves not only the water content but also the discrepancy in the height of the sample and therefore the absolute value is higher.

The whole procedure is depicted in *Figure 3.4* in an effort to clarify the sequence of the process. As can be seen in the 'Quality Control' spreadsheet in *Table 3.3*, the differences in water can be compared with the amount of water expelled during compression tests. This is an indication of the relative error expressed in water loss. In order to accept or reject a test, the above two types of errors are compared with the aforementioned discrepancies, which were derived from the experimental procedure.

Discrepancies in the measurements can be explained in a number of ways. In order to quantify the discrepancies, the author tried to express them as loss or gain of water mass (see *Table 3.3*).

- The measurement error of the caliper was of the order of $\pm 0.5\ mm$. This affected the final height measurement and consequently, the initial height.

- When the cell cap was placed, the sample was compressed because of the weight of the cap, and furthermore, some water (of the order of 5 ml) may have been lost. The leakage came from the base O-seal ram, which could not be sealed perfectly until the top cap bolts were tightened. Consequently, the sample was drier than assumed to be.
- The existence of water in the drain outlet increased the water content in the cell compared to that in mixture. This was because before pouring the sample into the cell, the drain outlet had to be de-aired. The air was flushed out and then the base sintered disc was filled with water.
- At the beginning or at the end of the test, during the assembly or the disassembly of the cell, some quantity of water might be present on the cell edges, increasing the weight of the sample. As a result, the initial (or final) measured mass of the sample was greater than expected.
- The proportions of the various materials in the mixture differed slightly than those in the Rowe cell. This led to the first type of error where the water content in the mixture w_o was different than that measured from the sub-sample. Particularly with coarse sands or where the initial quantity of water was much higher than that needed to saturate the sand, after the addition of the conditioning agent (either bentonite or foam), the mixture in the bowl failed to be homogenous. In this case, the water content in the sample as well as in the sub-sample was not the same as in the mixture.

Tests were performed on saturated sand, wet foamed sand with or without polymer as well as foamed sand with polymer and bentonite. In each case different volume changes were measured. The results of Quality Control evaluation are depicted in *Tables 3.4 - 3.5*. For each test, a number reflects the estimated gains or losses of water. The convention is positive differences mean that the sample was drier than the mixture. As can be seen in the tests marked with the letter 'A' the differences are negligible, whereas in the tests marked with letters 'A?' and 'R', the differences were substantial. The latter tests were not initially rejected but their results were treated with scepticism. However, the average difference in mass of water was quite small overall.

3.3.2 Compression variation with time

The variation of compression with time was one of the important outcomes from each foamed test. It was expected that the presence of gas would alter the shape of the curve

compared to that of saturated sand and would reflect the increase of compressibility. In *Figures 3.5 - 3.8* the plots of compression against time are presented for some typical foamed fine sand tests. The undrained stage was first and then the drained followed. The undrained stage usually lasted some seconds; this time was enough to compress the gas phase at the particular pressure. As soon as LVDT measurement indicated no further settlement, the valve at the bottom of the Rowe cell was opened, water drained out and as a result, consolidation settlement took place, under drained conditions.

As can be seen in the *Figures 3.5*, the most significant compression took place in the range of low vertical stresses (20-40 kPa) for a typical foamed fine sand test (*f22*). It is interesting to note that after the increment of 56.6 kPa, the settlement was almost exclusively during the undrained stage. However, this type of behaviour was not observed in the case of foamed bentonite fine sand or when polymer was added (see *f46*). When foam and polymer was used, compression appeared to occur in both stages irrespective of the vertical stress. As is shown in the series of *Figures 3.8*, compression still occurred at high stresses. In particular the bentonite foamed sand appeared to require a longer time to consolidate (clearly shown for *f39* and *f40*, demonstrating that the bentonite affected the rate of consolidation in the stages over 80 kPa - see *Figures 3.6 - 3.7*).

The behaviour of the soil sample during consolidation in response to a single load increment is investigated further by plotting a graph of settlement against square root of time. This is important in order to assess the consolidation rate and indirectly, soil permeability. Plotting the drained stage compression against the square root of time and applying one of the standard curve fitting techniques, the coefficient of consolidation can be determined (Head, 1986). As will be shown in the 'Permeability Evaluation' (Section 3.4), the standard technique was not applicable in most of the cases due to the shape of the curve. In many cases, the curve was either flat or it appeared alternatively to have two parts: one steep and linear (large compression) and the other quite flat (small compression).

3.3.3 Void ratio variation with vertical stress

Volume change behaviour can be quantified by plotting the void ratio against the applied total vertical stress. The addition of polymer and/or bentonite altered the foamed soil behaviour to a different extent. The results are grouped according to particle size and

whether they include foam, polymer or bentonite. The graphs depict the void ratio against the logarithm of vertical pressure. For foamed fine sand tests, only the compression stage is shown for illustration purposes. However, the unloading stage did not significantly change the final value of voids ratio.

Fine sand:

Tests marked as Series I are those with foaming agents P90, PP90 and SC200. Those grouped as Series II are those using 'Versa' foam. *Figures 3.9 - 3.12* show Series I/II tests together with a typical saturated fine sand test (*f04*). For fine sand compression, fine sand was tested at different water content and at different densities. In the first type of test, dry loose sand was poured into the cell filled with water, creating sediment and achieving a denser state than that of the other wet sand test. In the second type of test, a sand sample of the prescribed water content was poured into the cell after having been mixed in the soil mixer. In each graph, the minimum as well as the maximum voids ratio for the dry sand are presented for comparison purposes. These values are referred to as a relative density of 0 and 100% respectively.

Figure 3.9 shows the voids ratio variation with vertical pressure for various foaming agents. (tests *f05-f13*). The curves follow the same pattern, starting at a high voids ratio and ending up clearly at a point above the maximum voids ratio for sand alone. A different marker is used to depict the main foaming agents (P90, PP90 and SC200). Different starting/ending points reflect differences in foam quantity and the ER. However, in order to reduce the number of parameters, it was decided to focus on one type of foaming agent to investigate the behaviour of the foamed soil whilst changing the other parameters. *Figures 3.10 - 3.11* depict tests with Versa foam (Series II), using different foam quantities and ER. For the purposes of enhancing illustration, the low FIR (less than 35%) tests are separated from the high FIR (more than 35%). Details about materials proportion in these tests can be found in *Table 3.1*. *Figure 3.12* shows all series II tests.

In *Figure 3.13* the graphs of the average values for these two groups (Series I and Series II) are depicted. In the same graph the average high and low FIR values are plotted. The results show clearly that the higher the quantity used, the larger the difference in voids ratio for samples tested under the same loading conditions. This is illustrated in *Figure 3.14* where volume changes are plotted against FIR.

Non-foamed tests are shown in *Figure 3.15*. The introduction of polymer increases the compressibility of soil. In the case of bentonite with polymer, the initial voids ratio was quite high (*f39*). Some tests were carried out with bentonite and polymer. The behaviour of test *f39* seemed quite different from that of *f30* or *f31* but similar to bentonite with coarse sand (*c33* - *Figure 3.15*). When foam is added the increase in compressibility is evident (*f40*) as is shown in *Figure 3.18*.

For tests with foam and polymer ('WOP') the initial water content was higher and the loading stages lasted longer. Tests *f46* and *f47* were almost identical and the sole difference was the time intervals at each loading stage: for *f46* the duration of the test was 1 hour whereas for the *f47* it was 10 hours. For *f45* the duration was 50 hours but there were only three loading stages (*Figure 3.19*).

Coarse sand:

In the case of coarse sand, foam was added with polymer ('WOP'). This was necessary because otherwise the sample would not be homogenous; the foam quantity was not enough to create the homogenous structure seen in fine sand. Due to the size of the cell, a higher proportion of foam could not be tested. A higher proportion of foam in the soil was needed to reach a void ratio similar to those of fine sands.

Non-foam coarse sand tests showed similar behaviour to the non-foam fine sand tests. In bentonite with polymer tests (*c33*, *c42*), the final voids ratios were higher than those of bentonite sand tests (*c37*, *c34*) as shown in *Figure 3.15*. For tests *c33* and *c34*, the amount of bentonite and water used was reduced.

The foam effect can be seen in *Figure 3.17* where foamed soil (tests *c27* and *c28*) is compared with saturated coarse sand (test *c24*). Again, in all figures the maximum and the minimum voids ratio are depicted in each graph for comparison purposes. Coarse sand in foamed tests gave final voids ratios well above their loosest dry state. All tests using coarse sands were performed under undrained/drained conditions.

Bentonite tests showed similar behaviour to fine sand tests. *Figure 3.17* shows the voids ratio variation with pressure for two bentonite coarse sand tests (*c35* and *c44*) with different proportions. Due to the addition of water both started at high voids ratio but the end point

differed significantly. It is interesting to compare these graphs with the non-foam test with bentonite and polymer: *c37* and *c42* differ significantly but their shape is similar.

3.3.4 Void ratio variation

Examination of volume changes in terms of voids ratio differences is a simple way to acquire a first insight into what kind of interaction happens between gas and water. It is important to detect what happens to the free gas in the sample during the compression. The actual behaviour of the foamed soil at the beginning and at the end of the test can be described following the change of certain 'special' voids ratios. These are the water voids ratio e_w , the gas voids ratio e_g and the 'matrix' voids ratio e_m . The water voids ratio is defined as:

$$e_w = V_w / V_s \quad 3.3.23$$

where V_w is the water volume, which includes the volatile component of the additives (FOP and WOP) and V_s is the solids volume which includes the non-volatile component of the additives (FOP and WOP). The gas voids ratio is:

$$e_g = V_g / V_s \quad 3.3.24$$

where V_g is the gas volume. The 'matrix' voids ratio is actually the water (liquid) voids fraction in the mixture and can be expressed as:

$$e_m = V_w / (V_g + V_s) \quad 3.3.25$$

The total voids ratio measured at the beginning and at the end of each test is:

$$e = e_g + e_w \quad 3.3.26$$

The above analysis assumes that the gas dissolution in water is negligible. An illustration of the 'special' voids ratios is depicted in *Figure 3.20*.

Table 3.6 presents all the voids ratios and volume changes for the foam tests. *Figures 3.22* show the correlation between the changes in matrix voids ratio and gas voids ratio with the total volume changes. The plots suggest a strong link between gas voids ratio and the total volume changes but no correlation between matrix and total volume changes.

In order to examine what happens in the two phases (water and gas) the curves of the voids ratio against time were used. The data are incomplete since measurements were not made to allow determination of gas and water voids ratios at every stage. *Figures 3.21* show the voids ratio variation with time for some foamed fine sand tests. The compression of the gas phase appears to be much higher for low pressures and follows the same pattern for these tests. Volume changes due to gas compression were larger than those due to water exclusion, as *Figures 3.21* show for tests f40, f41, c44, f46 and f47. The exception was test f43 where the water volume change appeared to be larger.

Figures 3.23-3.26 depict the voids ratio against pressure. Here, only the initial and the final values based on measurements are presented. Therefore, results are plotted only for start and end points as in an attempt to reveal the general trend of the gas and water voids ratios. It is evident that while the trend is a reduction of gas voids ratio, the amount of this reduction differs over the same pressure gradient (212 kPa). For foamed tests without other agents (f14 - f25), the gas voids ratio appeared to be dependent on the initial foam quantity: the higher the FIR and consequently the initial voids ratio, the greater the reduction. The same behaviour was noted for polymer foamed tests (f41-f47) indicating that gas volume changes were not directly affected by the presence of polymer.

In the case of foamed sand, after the compression of the soil, the gas voids ratio did not reach zero value. In addition, the final proportion of gas to water voids ratio was higher than the initial one in most cases, demonstrating that at the end of the test the soil was drier than before the test. However, for some tests (f40, c44, f45, f46 and f47) where polymer or bentonite was added at high FIR, the outcome was that the sample ended up wetter. In most cases, the gas voids ratio decreased, particularly when values approached unity. When the percentage of gas in the mixture was low, the gas voids ratio appeared to change slightly (decrease or even increase but this could be due to fluctuation of the measurement).

3.4 Permeability Evaluation

One of the important effects of soil conditioning agents is the decrease of soil permeability. Foamed soil is an unsaturated soil in this context and the accurate determination of soil permeability of unsaturated soil requires special equipment and procedures. When a soil is unsaturated, an air phase is present and the water flow channels are drastically modified compared to those in saturated soil. In an unsaturated soil the water phase is bounded partially by solid particles and partially by an interface with the air-phase (Jury *et al*, 1991).

Conventional methods of direct measurement such as constant head and falling head techniques estimate the permeability of saturated soils by measuring the flow rates. These techniques can be modified for testing unsaturated soils in order to take into account the presence of air. Similar research concerning the permeability of wall barriers and the hydraulically tight geological deposits led to the use of special techniques like the flow-pump technique for measuring low permeabilities (Zhang *et al*, 1998).

For this project, the primary objective was the evaluation of foamed sand permeability compared to saturated sand. Tests were carried out in a Rowe cell under constant head on sands with and without foam as a preliminary assessment of foamed soil permeability. The author wanted initially to test the relative reduction of soil permeability when mixed with foam under external pressure.

3.4.1 Indirect evaluation

Permeability formulae:

Indirect evaluation of the soil permeability was possible because both sands were uniform. Soil permeability is influenced by such factors as particle size, voids ratio, composition, fabric and degree of saturation. The first four are closely interrelated and they cannot be isolated. For coarse-grained soil, composition and fabric have little effect on permeability (Lambe & Whitman, 1979).

Permeability is directly related to the pore structure parameters such as the voids ratio. There are single relationships between permeability and particle size, which can be applied

to coarse-fine sands. An approach to estimating the permeability of a coarse grain soil is given by the empirical Kozeny-Carman equation (Head, 1994):

$$k = 2 e^3 / f S^2 (1+e) \quad [m/s] \quad 3.4.1$$

where f is particle shape factor (from 1.1 to 1.4) and S is the specific surface of grains:

$$S = 6 / (d_1 d_2)^{0.5} \quad 3.4.2$$

where d_1 and d_2 are the mean diameters of a non-rounded sand particle. The voids ratio depends on the density state of the sand.

Alternatively, Hazen's method can be used. In this case, the permeability k is given by a formula, which again is applicable to uniform sands and the result may be in error by a factor of 2 either way (Head, 1994):

$$k = 0.01 (D_{10})^2 \quad [m/s] \quad 3.4.3$$

where D_{10} is the effective size in mm representing 10 % by weight passing from the grading curve.

The calculations for both fine and coarse sand are shown in *Table 3.7* together with two grading curves. For the Kozeny – Carman equation the maximum voids ratios were used. The calculation of the product of particle shape factor times the square of specific surface was based on the particle size distribution for the two types of sands. Sands were dry sieved in a series of sieves with aperture from 1.18 mm to 0.063 mm .

Determination from consolidation tests:

In the case of an indirect evaluation of permeability, absolute precision is not an issue because several parameters enter into the relationship of the rate of consolidation - permeability (Lambe & Witman, 1979). Some results can be drawn from the series of foamed soil tests during the drained stage of each load increment. From consolidation tests in Rowe cell, permeability was calculated indirectly through the coefficient of consolidation c_v and the volume change coefficient m_v , as:

$$k = c_v m_v \mathbf{g}_w$$

3.4.4

where \mathbf{g}_v is the water unit weight equal to 10 kN/m^3 . The coefficient of consolidation can be calculated from Equation 3.3.11 and is dependent upon the drainage path of the sample and the time required to complete the consolidation. This can be achieved by plotting out compression with time, as shown in *Figures 3.5 - 3.9*. For the determination of the time t_{90} , the square root method was used applying the appropriate slope factor (1.15) (Atkinson *et al*, 1995). The calculation took into account the linear part of each graph; the tangent line is extrapolated until it reaches the time axis. From that point a second line with a slope of 1.15 was drawn until it cut the curve, defining a point on the curve with same abscissa and ordinate t_{90} . A typical example is shown in *Figures 3.27*, test f39.

In some cases the standard technique of determining the permeability can be used, by plotting out the measured compression against the square root of the time required to complete this compression. However, as stated earlier, the ‘compression against time’ graphs did not follow a consistent pattern for the different loading stages. Consequently, it was questionable whether the calculation could produce reliable permeability results in most foamed soil tests. For the saturated sand tests, permeability determination was not feasible due to the rapid rate of consolidation. With foamed coarse sands, permeability was also very difficult to determine for the same reason. In foamed fine sand, the curves were sometimes smoother but still showed in some cases, a ‘dual’ behaviour. As can be seen for example in test f46 in *Figures 3.27*, there is a ‘stepping’ behaviour with sudden falls and then flat regions suggesting no settlement for a period of time.

A possible cause of this behaviour was the presence of foam in the soil; as the pressure increased water drained out carrying bubbles (visually inspected). The remaining bubbles in the sample could have rearranged themselves or even changed shape so that again the available channels for the water to flow were blocked. The same cycle could have been repeated until the consolidation was completed. Thus, it might be possible that there were two permeabilities characterizing the foamed soil for the different regions.

3.4.2 Permeability tests in Rowe cell

Direct measurements of foamed soil permeability were carried out in the 75 mm Rowe cell. The experimental set-up was presented in Section 3.2. Initially the author tried to carry out tests adopting the ‘falling head’ principle but after some unsuccessful trials, the idea was abandoned. It was decided to shift to the ‘constant head’ principle, which applies to coarser material (Head, 1994). Instead of having a constant head cell, a ‘Marriotte bottle’ was used. The ‘Marriotte bottle’ was made in the workshop and it comprises two plexiglas tubes of different diameters, of which the smaller is mounted inside the larger. It works at atmospheric pressure and provides the constant head. Initially two sintered discs were used but soon it became apparent that due to their low permeability, it was difficult to calculate the combined permeability of the system discs-soil sample. To overcome the problem, two fine meshes were utilised together with two perforated plates (*Photo 3.2*). The plates were made in order to distribute the water flow uniformly over the entire cross section area of the sample. The water used both in the ‘Marriotte bottle’ as well as in the system was de-aired before each test.

As soon as a sample was placed in the cell, the pressure was applied. After consolidation had taken place, the bottom outlet was connected with the ‘Mariottte bottle’ permitting (de-aired) water to pass through the sample. The combined permeability of the system was calculated as:

$$k_c = q_c / A \ i_c \quad 3.4.5$$

where A , was the cross section area of the soil, q_c was the flow rate (ml/s) measured from the Rowe cell outlet and i the hydraulic gradient defined as :

$$i = dh / L \quad 3.4.6$$

where dh was the piezometric height above the outlet and L , the height of the sample (distance). Assuming that the flow was normal to the surfaces, the combined permeability of the system sample and meshes could be defined as:

$$k_c = (L_1 + L_2 + L_3) / (L_1/k_1 + L_2/k_2 + L_3/k_3) \quad 3.4.7$$

where $k_1 = k_3 = 0.83 \times 10^6 \text{ m/s}$ and $L_1 = L_3 = 0.3 \text{ mm}$ are the permeability and the thickness of the two similar meshes respectively whereas k_2 and L_2 represent the permeability and the height of the sample after the consolidation stage.

Firstly, the permeability of the two meshes was determined by running the test without a sample. The permeability of the sample when tested was:

$$k_2 = k_c k_1 L_2 / \{k_1 (2L_1 + L_2) - 2k_c L_1\} \quad 3.4.8$$

However, the solution of Equation 3.4.9 becomes unstable when:

$$k_1 (2L_1 + L_2) @ 2k_c L_1 \quad 3.4.9$$

The summarized results presented in *Table 3.8* were carried out using meshes and discs. The average time for reaching a steady outflow was 3 min for fine foamed sand and 4 min for coarse sand. With both sands, polymer mixture ‘WOP’ was used.

All tests were performed at 20 kPa vertical pressure. The pressure was such that it was greater than the applied head so that it could prevent any water leakage of water upwards through the diaphragm. Some small inevitable losses of pressure head due to friction and turbulence in the connecting tubing were considered negligible compared to the hydraulic head and were not taken into account.

3.5 Discussion of Test Results

3.5.1 Foaming agents

The new foam generator requires some improvements in order to produce constant quality foam. However, it was very promising that the foam generator was able to deal with all types of foam concentrate. It seemed that the quality of the foam was dependent on the quality of the foam agent, the proportion of the air:liquid mixture and the pressure under which the air and the fluid is delivered.

Different foaming agents did not exhibit impressive differences. The most important variables as stated, were the proportion of the foaming agent and the volume of foam produced (for example FIR) and less significant was foaming agent type or its ER, at least for the tested range size of bubbles. The latter contradicts the view that synthetic foams behave completely differently from protein-based foams. In order to achieve the same texture of ‘shaving foam’, different quantities of foaming agents had to be used. For example: P90, 10% and PP90, 5% by weight. With Versa foam this was achieved using a tiny proportion of polymer mixture and 3% foaming agent.

The behaviour of the various foam agents appeared to be quite similar. Different proportions of concentrate:water were tested based on manufacturers’ recommendations. Any increase in the amount of foam also produced more compressible material. Versa foam showed the most stable behaviour in terms of the foam quality produced. A small increase in the quantity of foaming agent used from 5% to 7% improved stability. Synthetic foams did not leave any visual trace on the soil after some period on the sample. PP90 produced the most stable foam bubbles in terms of drainage time. The latter has to be confirmed by measuring and comparing the drainage time for the same ER. It was noted, however, that this did not affect the compressibility characteristics. P90 and ‘Versa’ foam were lighter foams whereas the PP90 and SC200 (after adding IP425 agent) were heavier. An increase in concentrate quantity did not always improve the foam quality. Particularly with PP90 and SC200 the concentrate was first dissolved into a beaker with water and afterwards was poured into the foam generator pressure tank.

Foam manufacturers claim that the pore water is displaced by the foam and absorbed by the polymers. There was no evidence that polymeric foam (PP90) offered better stability in the soil matrix. All foams appeared to be remarkably stable after the mixing tests; soil particles seemed to integrate in the foam system quite well. Further study of the effect of foaming agents on foamed soil matrix may demand microscopic inspection.

3.5.2 Volume change behaviour

Clearly, the addition of either foam or bentonite increases the initial voids ratio due to the addition of a considerable volume of water. It was evident that the added polymer affected

the compressibility of the soil in every case. Based on these tests, some further conclusions can be drawn.

As stated earlier, the displacement due to the undrained loading was the immediate settlement. This was due to the collapse of the foam bubble and the closure of voids. At the same time the pore water pressures increased and some gas could have been forced into solution. The amount of gas, which went into solution, was assumed negligible. At the drained stage the water was expelled with some of the gas, the pore water pressures dropped to zero and consolidation took place. In the unloading stage, some bubbles were recreated, increasing the voids ratio slightly. The volume change during the undrained stage can be seen in the context of Boyles law: $PV=constant$ assuming that no change in temperature took place. The law applies to ideal gases but it can be utilized in this case. In addition, using Henry's law, the concentration of gas dissolved in the liquid (the amount of gas forced into solution) can be estimated.

For foamed fine sands, even though the slopes differed, the final voids ratio was well above the loosest state of the dry sand as well as that of the curve of saturated sand tested under the same conditions. The difference in the final voids ratio was attributed to the presence of foam in the soil even after the test was completed. This was confirmed by visual inspection of the sample after the test, when the texture of the sample is different from that of wet sand. The final load increment was insufficient to squash all the bubbles, which appeared to be able to withstand pressures of the order of 200 kPa. It must be noted that in some cases, where the compression was not as large as it was expected to be, this was attributed to the friction between the top sintered disc and the side walls of the Rowe cell.

The coefficient of volume compressibility does not follow a clear trend. For some tests the first stage show high values of compressibility whereas in some others it shows lower values for the same amount of foam. This is due to a small amount of compression that occurs in some cases after placement of the cell cover. It would be expected that the compressibility decreases as the consolidation progresses and the sample becomes stiffer. However, this did not always happen at each stage, especially in the bentonite tests.

Foam and fine sand seemed to integrate quite well when the water content of the saturated sand before the addition of foam was less than 32% (that meant saturation 100%, assuming the sand in the bowl was in its loosest state). Above that quantity, the surplus of water in the

mixer bowl degraded the added foam very quickly. This was evident in tests *f41-f47*. Test *f22* showed higher compressibility in the early loading stages due to a high proportion of foaming agent (7%) at less than 35% water content. Test *f36* showed very low compressibility (the dosage was 400 ml - 3% 'Versa' foam).

When polymer was added the voids ratio differences were higher (see *Table 3.6* tests *f40 – f41*) than those for foamed soil. However, this was not necessarily related to the addition of polymer. Tests *f43* and *f45* lasted longer than the usual foamed soil tests. This introduces time as an important parameter, which should be taken into account. It must be noted that the addition of the polymer was considered necessary in the cases where foam was tested with bentonite. The role of polymer was to 'dehydrate' the bentonite slurry and homogenize the mixture. Otherwise, the excess water in the mixture would degrade the foam very quickly and consequently, the conditions would be similar to that of mixing bentonite slurry with sand. Due to the restricted size of the cell, high proportions of foam could not be tested with coarse sand.

The addition of bentonite increased the proportion of fines so that the sand could be considered a gap-graded material. Foamed coarse sand followed the behavioural pattern of foamed fine sand and showed more compressible behaviour than the saturated coarse sand. As stated in Section 3.3, the addition of bentonite increased the voids ratio significantly. At the end of the compression stage the final voids ratio was well above that of dry sand (*c37, c44*). It should be noted that for the test *c44* very little water was collected so it was questionable whether the duration was such as to allow the consolidation to be completed. When bentonite was added, the change of the gas voids ratio appeared inconsistent. In these cases, volume changes were independent from drainage. It became evident that the choice of time scale for each test was of prime importance in the cases where bentonite slurry mixtures were tested. Saturated sands with or without foam can be tested considerably faster than sands with polymer and bentonite slurries. Particularly with bentonite slurry, which was actually clay, considerably more time was required for the mixture to consolidate to avoid misleading results.

Most of the foamed samples tended to be drier at the end of the test compared to the non-foam samples. These values (depicted in *Figures 3.23 - 3.26*) were deduced from initial and final measurements whereas those presented in *Figures 3.21* came from measurements of the drained water mass during consolidation testing. Comparing these two calculations for

the same tests, it was evident that the final values were not entirely consistent. In the latter case, this was due to measurement discrepancies as well as to the fact that the gas bubbles expelled with the drained water were not taken into account. Thus, these plots did not provide any conclusive evidence on the dissolution of gas or on how much gas was expelled by the water. It was impossible to isolate the effects of each parameter when knowing only the initial and the final conditions.

3.5.3 Foamed soil structure

Some tests did follow a similar pattern but additional information is needed in order to draw any conclusion. It can be safely assumed that this micro-foam mixed with fine sand creates a material whose properties differ from that of the wet sand. As the foamed sample dried, after a 24-hour exposure to atmospheric conditions, the texture seemed to return to its original appearance. The question that arose was whether the sand particles were attached to each other or whether they were completely coated with foam, and under which vertical pressure the soil particles regained contact with each other.

Foam tests displayed different behaviour from non-foam tests. The injection of the foam was critical in increasing the initial volume of the mixture as well as the compressibility of the soil. The difference lies in the presence of the gas bubbles within the structure of the soil. However, the structure of the foamed soil containing gas bubbles can vary depending primarily on the relative size of the bubbles and the soil particles. The impression was that the bubble size, compared with that of the sand particles, was of the same order. Foam bubbles when mixed with soil fell within the range of 0.1 to 1 mm whereas for the soil particles, the mean size ranged from 0.16 to 0.6 mm. When the bubbles were smaller they could fit within the normal void spaces without affecting the structure whereas when they were bigger their effect was significant because they created "cavities" larger than the original structure. The latter case was likely to be more representative of the situation that occurs when foam is mixed with soil, where the large expansion of the volume is attributed to the mixture of the high voids ratio.

An attempt to provide a qualitative explanation of the behaviour of foam/sand mixture through the introduction of the matrix voids ratio, was unsuccessful. This index was aimed at modelling the foamed sand as a mixture consisting of two types of particles, the sand

grains and the bubbles. If the gas bubbles are considered to be 'particles' within the foamed soil structure, then the matrix voids ratio determines the available 'packing' of these particles. However, the matrix voids ratio failed to reveal any trends in the behaviour of the foam/sand mixture.

Changes in total stress have a marked effect on gas volume changes and consequently on gas pore pressure, if it is accepted that Boyle's law holds for foamed soil. In the undrained stage as the total stresses increased, gas bubbles were squashed and as result, this produced some reduction in the size of the foam or air bubbles. However, under the drained stage it was likely that the decrease in pore water pressure restored, to some extent, the size of the bubbles since there was evidence of gas remaining at the end of some tests.

The conventional approach to modelling of unsaturated soils may be unsuitable to describe fully the behaviour of the foamed soil. The main question was what happens when applied pressure compressed the bubbles and some of them burst and/or decreased in size. In some cases, all the remaining bubbles might have reduced in size so that the final voids ratio fell below the maximum dry sand value and thus the soil particles came in contact with one another. For example, the presence of the polymer mixture 'WOP' which provides dehydration and lubrication in the mixture, appeared to affect the final voids ratio. The addition of bentonite altered the compressibility behaviour considerably by introducing a fraction of fine material in the mixture. The permeability of the foamed sand appeared to be lower than that of sand but there is a quite wide range between the measured values and those derived from the compression tests.

Chapter 4. Direct Shear-box Tests

4.1 Shear Strength Parameters

4.1.1 Shear strength and dilatancy

One of the fundamental properties of soil is the shear strength. The basic laws of frictional behaviour state (Lambe & Whitman, 1979) that the shear resistance between two bodies is proportional to the normal force between the bodies and is independent of their dimensions. In soils, shear strength is the shear resistance that can be mobilized among soil particles in order to resist a relative movement between the particles. The shearing resistance in a granular material is defined through the angle of internal friction and the main objective of the direct shear tests is to determine that quantity.

The stress state in a soil can be represented by Mohr's circle. A line tangent to these circles can be drawn defining the failure plane. The soil fails when the applied shear stress exceeds the shear strength of the soil. For saturated soils, the most common failure criterion is the Mohr-Coulomb condition:

$$\mathbf{t} = c' + (\mathbf{s} - u_w) \tan \mathbf{f}' \quad 4.1.1$$

where \mathbf{t} is the shear stress, \mathbf{s} represents the normal stress on the failure plane, u_w is the pore water pressure, c' is the shear strength intercept ($= 0$ for coarse grain soils) and \mathbf{f}' the effective angle of internal friction. A measure of the soil's ability to withstand applied shear stress is the shear strength envelope. Equation 4.1.1 defines a line referred to as the failure envelope. However, Lambe and Whitman (1979) noted that the failure as defined by the Equation 4.1.1 may or may not be the plane upon which shear strains become concentrated when the soil fails.

For plane strain experimental conditions, as in shear-box testing, at failure the soil satisfies the following equation:

$$\mathbf{t}_f = \mathbf{s}_f \tan \mathbf{f} \quad 4.1.2$$

where t_f and s_f are shear and normal stresses respectively. The above equation is a straight line, which can be fitted to a tangent to the Mohr circle as the failure envelope. It must be noted that this approach assumes that the horizontal plane through the shear-box is identical to the theoretical failure plane. Depending on the state of stress and the initial voids ratio, the angle of friction f may be the peak (f_{peak}) or the critical (f_{crit}). The latter characterizes the state where the sand strains without changing in volume.

The effect of relative density and moisture content on the shear strength of coarse grain soils has been recognised for some time (Bishop, 1966; Lambe & Whitman, 1979; Maeda & Miura, 1999). However, for unsaturated soils, Equation 4.1.1 has to be modified to take into account the stress state variables ($s - u_a$) and ($u_a - u_w$). Fredlund and Rahardjo (1993) extended the Mohr-Coulomb failure envelope, introducing an intercept at a specific matric suction in place of c' and an additional angle which indicates the rate of increase in shear strength relative to the matric suction. In this framework, the shear strength equation for an unsaturated soil is an extension of the shear strength equation of a saturated soil. Soil strength usually decreases with increasing water content for fine-grained soils. One reason for this is that bonds that hold particles together in structural units are weakened as more water is absorbed (Marshall *et al*, 1996).

The state of compaction of coarse grain soils can be defined by using the relative density index I_D :

$$I_D = (e_{max} - e) / (e_{max} - e_{min}) \quad 4.1.3$$

when $e = e_{min}$, and $I_D = 1$ the soil is in the densest possible state whereas at the loosest state, is represented by $e = e_{max}$ and $I_D = 0$. Bolton (1986; 1987) presented a relative dilatancy index correlating the friction angle and relative density:

$$f_{peak} - f_{crit} = 5I_R \quad [^\circ] \quad 4.1.4$$

with

$$I_R = 5I_D - 1 \quad 4.1.5$$

for low confining pressures. Bolton (1986) noted that in plane strain the contribution of dilation to peak strength (maximum) is represented by the correlation:

$$\mathbf{f}_{peak} = \mathbf{f}_{crit} + 0.8\mathbf{y} \quad 4.1.6$$

Sands tested in shear under confining stress exhibit volume change behaviour. The shear strength of a soil is defined in terms of stress developed at the peak of a shear stress shear strain curve. However, this curve does not always have a distinct peak point. In a loose state, the soil contracts until it reaches the critical state at the critical voids ratio (when continued shearing takes place). When the soil is in a loose state during shearing it becomes denser and its volume is reduced.

In direct shear-box tests, an upward movement of the shear box implies an increase in volume or dilation. This corresponds to a negative volumetric strain, according to the usual soil mechanics convention. The angle of dilation is an indication of the rate at which the sample changes in volume as it is sheared. Conventionally, an expansion of soil during shearing corresponds to a positive dilation. Dilation can be defined as the negative rate of increase of volumetric strain \mathbf{e} with shear strain \mathbf{g} .

$$\mathbf{y} = \tan^{-1} (-d\mathbf{e} / d\mathbf{g}) \quad 4.1.7$$

For direct shear tests, the dilation effect can be taken into account by calculating the work input due to the two components of shear strength, friction and interlocking:

$$\mathbf{t} du = \mathbf{m}\mathbf{s} du + \mathbf{s} dv \quad 4.1.8$$

The friction coefficient \mathbf{m} (Taylor's energy correction factor - Taylor, 1948) can be calculated as:

$$\mathbf{m} = (\mathbf{t}/\mathbf{s}) - (dv / du) \quad 4.1.9$$

where $dv/du = \tan^{-1}(\mathbf{y})$ is the dilation rate with \mathbf{y} , the dilation angle.

4.1.2 Objectives of the study

The shear-box test is the simplest way to investigate the shear stress-strain behaviour of a soil and determine the angle of friction. The vertical stress and the shear stress acting on the central horizontal plane of the shear box are obtained by dividing the normal force and horizontal force respectively by the cross sectional area of the sample. After calculating the absolute values of shear stress t and horizontal u and the vertical v displacements, the friction angle f will be:

$$t/s = \tan f \quad 4.1.10$$

where f is the mobilised friction angle value at the end of the travel of the box. For the shear-box tests carried out, f was the friction angle at critical state. It must be borne in mind that the friction angle measured in shear-box tests on a soil sample is not the true inter-particle angle of friction.

As stated in Chapter 1, reduction of the shear strength of the excavated soil brings about reduction of the required torque to rotate the cutting wheel. Therefore, the shear strength was one of the fundamental mechanical properties of foamed soil of importance in tunnelling. Shear strength is expressed as the angle of shearing resistance (Equation 4.1.10) and assuming no excess pore water pressure can develop in sands, effective stresses are equal to the measured total stresses (Head, 1994).

In order to assess the shear strength of the foam soil, some direct shear-box tests were carried out. The objectives of the study were to:

- quantify the absolute values of friction angle of foamed sand
- compare the results with saturated sands and evaluate the differences
- discuss the results in relation to compressibility tests in order to draw some conclusions towards furthering the understanding of foamed soil behaviour

These preliminary tests were conducted assuming at this stage, that the calculated strength parameters were not affected by the scale of the tests. Additionally, foamed samples were considered homogenous.

4.2 Apparatus and Experimental Procedure

4.2.1 Description of the apparatus

The apparatus used (*Photo 4.1*) was of the type widely available in the UK for routine testing of dry and wet sands. The procedure described is the rapid test determination of the shearing resistance of the sand sample in a predetermined plane.

The shear-box comprised a drive unit, shear-box assembly, shear-box carriage and a load hanger. The shear-box body comprised two halves: the upper half on which a ‘swan-neck’ yoke was mounted and the lower half (*Figure 4.1*). The two halves could temporarily be fixed together by means of two clamping screws. These screws were removed before the start of the test. At the bottom of each of the halves, there was a retaining plate. Two lifting screws enabled the upper half of the box to be lifted slightly so that the shearing could take place between soil surfaces. The sample was placed between a top and a lower grid plate, enabling the shearing forces to be transmitted uniformly along the length of the sample (Head, 1994). The loading pad was placed above the top grid plate through which the vertical load was transferred to the sample.

4.2.2 Test procedure

For the foamed soil tests, the sample preparation procedure was similar to that described in Chapter 3. The sample of the foamed soil was prepared in the bowl of the soil mixer. Soil was firstly saturated with water and then the required quantity of foam was added. Afterwards, the foamed soil was poured into the shear-box.

After ensuring that the shear-box parts were clean and dry, the shear-box body was assembled prior to the placement of the sand sample. For saturated sand tests, water was added into the space between the carriage and the shear-box.

A thin film of grease was applied on the surfaces and around the grid plate, which had to be placed in such a way that it would sit horizontally on the specimen. This was an important detail because, particularly with foamed coarse sand tests, the top grid plate tended to tilt. Water content and mass determination were measured prior to the addition of the vertical load from the mixer-bowl.

Each specimen within the shear-box body had dimensions 60 mm x 60 mm and its height varied 30 to 35 mm. Apparatus assembly was completed when the shear-box and its components were in position and the gauges set to zero. The horizontal displacement u was determined by measuring the difference of the two gauges (reading to 0.01 mm) whereas the vertical movement during the test was measured directly with a gauge (reading to 0.001 mm).

The required normal stress was calculated from the added vertical load. Then the vertical load was added progressively onto the yoke hanger. Four different vertical load levels for fine/coarse sand and seven different ones for the foamed sand were induced. The normal stress was calculated by measuring the vertical load on the sample.

The vertical pressure on the specimen was:

$$\mathbf{s}_n = W/L^2 \quad 4.2.1$$

Where W was the force on the sample and L was the length of the shear-box. The mass required to produce a stress \mathbf{s}_n was given by:

$$W_{req} = \mathbf{s}_n L^2 - W_h \quad 4.2.2$$

where W_h was the mass of the hanger and the loading pad. Thus the required mass for the 60 mm x 60 mm specimen was:

$$W_{req} = 0.367 \mathbf{s}_n - W_h \quad [kg] \quad 4.2.3$$

$$W_h = 5.84 \quad [kg] \quad 4.2.4$$

with $\mathbf{s}_n = 28.3, 40, 56.6, 80, 113, 160, 226 \text{ kPa}$.

The selection of the sequence for the above loading combinations was made to be consistent with the loading steps of the compressibility tests. The rate of horizontal displacement was controlled by the electrical motor and the drive unit at 0.3 mm/min.

The shear stress corresponding to a load dial reading for the 60 mm x 60 mm specimen was:

$$t = C R/3.6 \text{ [kPa]} \quad 4.2.5$$

where R is the readings and C is the calibration factor of the loading ring ($C = 3.21 \text{ N/division}$). The ring was calibrated against a 10 kN force calibrating machine (Instron 4204).

All readings were set at zero before carrying out each test. Prior to commencing shearing, the specimen was left to consolidate under the vertical load, for several minutes. The end of the consolidation was determined from the vertical gauge readings. Once the shearing began, readings were taken initially every 10 divisions of the displacement dial gauge, but after a 2 mm displacement, the number of readings was reduced to one every 20 or 50 divisions. This was because the rate of change in horizontal and vertical displacement was higher at the initial stages. Shearing was completed when the full length of travel of the box had been reached (almost 8 mm).

After the end of each test, the load and specimen were removed and the apparatus was disassembled. The final water content, the dry density and the final voids ratio were determined in a manner similar to that for compression tests, as described in Chapter 3.

4.3 Shear-box Test Results

A total of 28 tests were performed in the small shear-box. Of these, 18 were on foamed sands. Details of the tests and all the results are presented in *Table 4.1*. The purpose of these shear-box tests was to evaluate the shear strength of the foamed sand compared to that of saturated sands. It must be noted that for all fine sand tests the same type of foaming agent was used. The aim was to test specimens of the same FIR at different normal stresses. Deliberately, in some cases FIR varied between 30.8 and 41.2% for fine sands and between 28.7 and 39.8% for coarse sands. ER varied between 15 and 18. The tests quoted as ‘f’ referred to fine sand and those referred as ‘c’ to coarse sand.

An example of the shear-box calculation procedures followed is shown in *Table 4.2* (for test *f74*), and it is in a similar format to the spreadsheet for compression test *f40* in *Table 3.2*. The main difference lies in the second page of the spreadsheet where calculations at the beginning and at the end of the test, based on the measurements, are presented. In the box on the top of the page, the summary of the critical parameters are shown including friction angle, friction coefficient and dilation angle. In the box entitled ‘Sample measurements & Calculations’ three measurements were taken for each test: at the beginning, after consolidation and at the end. However, in the consolidation stage, it was only possible to measure the height of the sample.

4.3.1 Shear stress variation with displacement

All tests for fine sand as well as for coarse sand are shown in the series of *Figures 4.2 – 4.11*. The shear strength was expressed as the ratio of shear stress over the applied normal stress. This ratio represented friction angle f (see Equation 4.1.2). Shear strength was plotted against deformation along the horizontal axis (horizontal displacement u). Additionally, the vertical deformation v was plotted against the horizontal deformation u . Negative values of vertical deformation meant movement upward (dilation) and opposite to the direction of the applied vertical force. Thus, in all figures dilation is depicted as negative in the vertical axis and the contraction as positive.

Fine sand exhibited contractive behaviour without a distinct peak value (*Figures 4.2*). The only exception was test *f52*, tested at vertical pressure of 56.6 kPa. For the coarse sand the behaviour observed was dilation in most cases, as shown in *Figures 4.3*. However, test *f60* (vertical pressure at 28.3 kPa) showed the highest dilation value. The ratio of shear stress over normal stress for coarse sand was higher in all cases with the exception of test *f52*.

In foamed tests both sands behaved similarly. For fine sands at low vertical stresses, shear strength was extremely low exhibiting dilative behaviour (*Figure 4.4*). For vertical pressure 40 kPa (test *f72*) the friction angle was much higher than that of the two tests at vertical pressure 28.3 kPa. *Figure 4.5* shows the behaviour of two tests under the same normal stress (*f73, f74*) with different FIR ratio. The difference in the final values of the angle of friction was very small. At higher normal stress (*Figure 4.6*), tests *f75* and *f76* both appeared to contract but the final values of the angle of friction differed significantly. An

even larger difference was recorded in the case of higher normal stresses (160 and 226 kPa) as is shown in *Figure 4.7*.

The shearing behaviour of coarse sands followed similar patterns. *Figure 4.9* shows the variation of shear strength and vertical displacement against horizontal deformation for low normal stress (28.3 and 40 kPa). It is evident that in comparing tests *c80* and *c81* there was a significant difference in shear strength, whereas the shear strength of *c82* lay between these two values. Tests *c83* and *c84* were performed under the same normal stress but their FIR was different (*Figure 4.9*). At higher normal stress levels (80 and 113 kPa), the difference in shear strength was also significant as *Figure 4.10* depicts. Test *c85* also showed a dilative behaviour. At even higher normal stress levels (160 and 226 kPa), the final values of the angle of friction appeared to be constant and in both cases the soil contracted significantly (*Figure 4.11*).

4.3.2 Shear strength parameters against vertical pressure

Foamed sand shear strength in relation to that of sand shear strength is presented in the series of *Figures 4.12 – 4.13*. For all tests, the angle of friction *f*, the dilatancy dv/du as well as the friction coefficient *m* were deduced by calculating the values at large displacement. These values were those corresponding to at least 6 mm horizontal travel of the shear-box. *Figures 4.12 – 4.13* display these indices plotted against normal stress.

Observing the values of the friction coefficient in *Figures 4.12 – 4.13*, it is evident that for both sands the shear strength was reduced when foam was used. *Figures 4.12* show that the values of friction coefficient of fine sand (dark dots) are quite steady (between 26.08 and 28.46°) with the exception of test *f52*. The white dots represent the foamed sand tests and they are spread across the range of 6.76 to 22.95°. The foamed sand friction coefficient lies below that of fine sand in all cases. *Figures 4.13* reveals similar patterns for coarse sand tests. In this case, coarse sand (dark dots) values lie within the range of 31.43 to 33.23°. In the graph for foamed coarse sand (white dots), the values lie in two ‘regions’: the first shows quite low values of friction coefficient (from 6.72 to 17.0°) and is characterized by low density values, and the second shows higher values closer to those of wet sands (from 25.37 to 31.78°).

4.4 Discussion on the Results

4.4.1 Test procedure and measurements

Tests were performed in two stages: the first stage was the consolidation under drained conditions after the addition of vertical load and the second stage involved shearing. Measurements of water content and sample weight were taken only prior to the assembly of the shear box (initial values) and at the end of each test. Thus, the determination of water content and mass of the sample during the intermediate stage (consolidation) was not feasible. The measurement of the sample height at the beginning of the test was also problematic at times. This was because, after having placed the yoke on top of the load pad, the slightest movement brought about an additional settlement. The initial settlement differed significantly from test to test and this produced varied initial densities in similar samples. Measurement discrepancies were more likely to affect the deduced densities and consequently the computed voids ratio values, which were more sensitive to changes.

Another problem encountered was the fact that the initial measured water content tended to be significantly less than that estimated for the saturated sand tests. This was likely to be attributed to the fact that a sub-sample of reduced water content was taken from the main sample in the mixing bowl. For foamed tests, this was not the case because the sample was unsaturated after the addition of foam and the water content measurements were accurate.

The author used the same foaming agent for both sands and in the case of coarse sand, a polymer mixture ‘WOP’ (see in Chapter 2) was added. FIR did not vary considerably because the author wanted the foam quantity used to be comparable with that of compression tests. Furthermore, it was impossible to test at higher FIR, due to the restricted dimensions of the test apparatus. In some trials with higher FIR and after the consolidation stage, the sample ended up having insufficient height due to excessive settlement.

4.4.2 Shear strength and relative density

Both types of sands when mixed with foam exhibited low values of shear angle. The shear behaviour of foamed sand also followed a similar pattern irrespective of the level of normal stress. Jancsecz *et al* (1999) reported the positive effect of foam in reducing the shear strength of sandy clay in a shear-box.

It is apparent from *Figures 4.12 – 4.13* that in the case of saturated sands, the coefficient of friction as well as the shear strength values remained steady irrespective of normal stress. Foamed test values are spread over a wider range. Values are scattered and therefore no specific trend or distribution can be assigned to them. There was one exception, test *f77* (7.42°), which could not be attributed to the different FIR. Higher FIR tests exhibited lower shear strength but the reduction was small; this is evident when comparing test *f70* (5.57°) with test *f71* (8.03°) and test *f73* (17.55°) with test *f74* (13.5°). For coarse sand in low stresses there was a distribution of friction values from 6.21° to 31.2° (for tests *c80* and *c81* with different FIR), but at higher normal stresses (over 113 kPa), the friction angle became steady around 23 to 24° .

A possible explanation lies in the fact that testing began at different densities. Generally, tests were carried out at low densities where the sands were in a very loose state. This explains why voids ratio values were so high before the test. Dilation was observed only in some cases and cannot be directly correlated with FIR or normal stress; it occurred in some specific tests under certain combinations of normal stress and density.

One of the characteristics of the foamed sands was the significantly high value of the initial and final voids ratios, which were higher than in the loosest dry sand state. As a result, when the conventional definition of relative density (Equation 4.1.3) is applied to the foamed sands, it yields negative values. This raised the question as to whether Bolton's correlation (Bolton, 1986) was applicable to foam/sand mixtures. Bolton's correlation (see Equations 4.1.4 and 4.1.6) applies to conventional sands within a range between the minimum and the maximum relative density.

In *Figures 4.14 – 4.15*, friction angle is plotted against relative density for fine and coarse sand tests. These graphs compare the experimental results obtained by shear-box tests with Bolton's data. The top graphs in *Figures 4.14 – 4.15* show the shear strength ***m*** against the relative density together with the critical state values as stated in Bolton's (1986) paper. The dark dots are Bolton's values corresponding to a relative density of 0 to 20%. The bottom graphs in *Figures 4.14 – 4.15* show the variation of shear angle ***f*** with relative density. The L-shaped line defines Bolton's correlation (Bolton, 1986) with minimum and maximum dry densities of the sand. The dark dots are the original Bolton's plane strain values. These values correspond to relative densities of 0 to 100%. Bolton's correlation assumes that the

angle of friction falls with reducing the relative density. In this correlation, this reduction does not continue below the critical state friction angle attained at about a relative density of 20%.. Fine sand test results lie at the edge of Bolton's line whereas foamed sand results lie in the area beneath that line. The relative density of foamed soil is scattered over a wide range of negative values from -3 to 0. It is evident from the graph (*Figure 4.14*) that there are two distinct regions: one for the fine sand and another for foamed fine sand. A similar trend is shown in results plotted for coarse sand tests. Again coarse sand without foam lies within Bolton's correlation range whereas foamed coarse sand covers a wide area extending from -2.5 to 0 (*Figure 4.15*).

The dependency of density on shear strength was demonstrated in *Figures 4.14 – 4.15*, which depict shear strength against relative density. Foamed sand tests results lay below the region of minimum dry sand density, at a very loose state and exhibiting in some cases extremely low shear strength. It appears also that the relative location of each test depends on the degree of saturation: as the degree of saturation increases the relative density rises approaching the saturated sand values. To illustrate this point, the final saturation values are depicted beside each test in *Figures 4.14 – 4.15*. Low saturation is associated with a high percentage of gas in the final state and with high FIR. It is evident that for tests with high FIR (tests *f75, f77, c80* and *c84*) the shear strength was much lower than that of the other tests, revealing a dependency of FIR to shear strength.

Volume changes during the consolidation stage were greater than those during the shearing stage. This was expected since the primary aim of shear-box tests was the determination of shear resistance and consolidation was a necessary stage, which had to be taken into account as it had a marked effect on the foamed sand structure.

The very low values of shear strength observed in some tests give an indication of the peculiar mechanism governing the foam action. It appeared that in some tests, irrespective of the range of normal stress applied, foam integrated well with the sand, reducing the shear strength. The bubbles were able to withstand vertical as well as shear forces. High voids ratio at the end of shearing can be attributed to the bubbles' ability to change shape and size during the process.

Another outcome of the shear-box testing pertained to the use of 'matrix' voids ratios, which failed to provide an insight to the shear behaviour of foam/sand mixtures. The idea of

introducing an index for foam/sand mixtures similar to Bolton's relative density index I_R in order to incorporate the effect of bubbles on foam/sand mixtures was unsuccessful. This was because the ratio of final gas volume to the final water volume varied significantly and therefore no conclusions on the relationship between foamed sand voids ratio and shear strength could be drawn.

Chapter 5. Concluding Remarks

5.1 Summary of Findings

This thesis describes the experimental work carried out in that Civil Engineering Laboratory at Oxford University and presents the findings as preliminary research investigating foamed sand behaviour. The work centred on establishing an initial assessment of foaming agents as well as determining the fundamental foamed sand properties (compressibility, shear strength and permeability). The conclusions derived from test results are presented here.

5.1.1 Main Findings

The most important findings of this study are derived from the experimental results and can be summarised as follows:

- Foam/sand mixtures of high FIR when tested in Rowe cell exhibit high volume changes and can sustain high vertical pressure whilst retaining high final voids ratio (higher than the loosest dry state). It appeared that the foam/sand mixture has a composite action: the sand itself would have been compacted to a much lower density and the foam would have been crushed at such stress levels. This was a remarkable finding since it was unexpected that such high ratios could be sustained at that stress level. As stated in Chapter 1, the high compressibility of the sand/foam mixture is an encouraging finding for tunnelling applications, demonstrating that foam integrates well with sand and is able to retain gas bubbles at pressure over 200 kPa. Such high pressures are likely to occur in the pressure chamber of an EPB machine.
- Sand/foam mixtures at moderate/high FIR when sheared exhibit extremely low values of shear strength. This too is an unexpected result because even though the shear strength-strain curve levels off at the end of the tests, it still lies well below the large displacement values of conventional sand tests. Shear-box results demonstrated that foam reduced shear strength of the foam/sand mixture. This is a very promising finding because, as stated in Chapter 1, the reduction of the shear resistance of the foam/sand mixture results in a reduction of power requirements and wear of the moving parts in a

EPB. However, in tunnelling applications the reduction of the shear strength should be controlled, otherwise a very low friction angle of the spoil would create problems in the screw conveyor because the spoil would flow through it too easily.

- Permeability of sand/foam mixtures showed a ten-fold reduction compared to that of the saturated sand. Reduced permeability contributes to a better control of the spoil in the pressure chamber as well as in the screw conveyor of an EPB machine (see Chapter 1).

5.1.2 Other observations

- Fine and coarse silica sands performed in a similar way exhibiting comparable behaviour when mixed with foam. However, the particle size appeared to play an important role as far as the absolute values of the fundamental properties were concerned.
- The foam generator was designed and assembled specifically for this project. Important issues concerning foam generator design included selection of the mechanical conditioner and the high pressure air circuit.
- Results did not appear to be dependent upon the type of foaming agent utilised. It was the quantity of foam used, expressed as FIR, which appeared to be more significant. The type of foaming agent affected the drain time in terms that protein based foaming agents last longer than synthetic ones. ER did not appear to affect directly compressibility results. It is of prime importance to note that the conclusions drawn concerning the foaming agents are related to the foam generator used.
- In some fine sand tests and in all coarse sand and bentonite tests, a mixture of polymer-oil mixture ('WOP') at prescribed proportions was added to the mixture. In the case of bentonite, polymer was mixed with bentonite slurry prior to mixing to achieve homogeneity as well as dehydration since excessive water quickly degrades foam when mixing foam with sand, some of the foam volume was lost. As a result, the true FIR for each sample was lower than that estimated from the mixing proportions.

- The first type of test carried out on foamed fine sand involved the measurement of power reduction during mixing. Tests were performed in the soil mixer bowl by mixing the power input for different combinations of water content and FIR. It became apparent that the reduction of power input was significant in every case particularly when foamed fine sand values were compared with the unsaturated fine sand ones (with a saturation degree around 70%).
- Compression tests provided the basic framework for the evaluation of the volume changes in the behaviour of foamed sand. The addition of bentonite altered the behaviour of foamed soil, but before further conclusions can be drawn, further testing is required. Polymer with excessive water, when added to foamed fine sands, had a negative effect on foam, facilitating its degradation. In these tests final values of voids ratio fell within the range of dry sand densities. Additionally, when polymer and bentonite were used, time appeared to affect the results since in these cases, consolidation stages lasted much longer.
- Shear-box results were not entirely consistent in all cases, showing considerable differences in measured shear strength but always showing (in some cases extremely) lower values than those of saturated sand samples. Another interesting outcome was the fact that test results could be presented along with Bolton's correlation are displayed in the same graph. Foamed sand lay in a region below Bolton's range.

5.2 Recommendations for Future Work

Further experimental work is required in order to establish a level of confidence that would be sufficient to understanding the behaviour of the foamed soil. Due to the complexity of foamed soil behaviour, the author believes that an additional number of experiments are necessary to test the findings of this study.

A larger size apparatus will enable different proportions of the mixing materials to be tested and consequently will extend the range of information. It will also allow well-graded sands to be tested so that the effect of other parameters such as particle size, texture and mineralogy of particles can be examined. It appeared that the presence of other conditioning agents like bentonite and polymer altered the foam/sand mixtures. Some of the critical

parameters like bentonite dosages or initial water content and time effects have already been identified, but further testing is needed to reassess their impact.

In terms of equipment, a larger Rowe cell (252 mm) and a larger shear-box would be more suitable. For the latter, the author has modified an existing shear-box, details of which can be found in *Figure 5.1*. A next stage could be triaxial testing. This would allow the sample to be tested under uniform pressure and the relationship between volumetric strain and applied isotropic stress to be obtained. In this case, the main issues to be considered initially would be sample preparation and the selection of the strain rate.

A conceptual approach to the foamed sand mechanics can be achieved by deriving a model consistent with experiment results. A complete analysis of foamed sand behaviour would have to include some numerical modelling. The derived model should provide a sound explanation of the mechanism, which allows the foamed soil to retain its loose structure as well as shedding light as to under which conditions it can withstand high pressures. Finally, experimental results should be verified in the field through trials and measurements in-situ.

The results presented here demonstrated that foam had an apparent effect on sand by increasing compressibility and decreasing the permeability and shear strength of the foam/sand mixture. The pipe jacking and tunnelling industries have shown strong interest in the research associated with foams and work in this field is expected to carry on.

References

1. **Anagnostou G. & Kovari K., 1996.** "Face stability conditions with Earth-Pressure-Balance shields." *Tunnelling & Underground Space Technology*, Vol. 11, No 2, April-June pp. 165-177.
2. **Angus Fire.** Trade literature.
3. **Atkinson J.H., Anagnostopoulos A.G., Clayton C.R.I., Bonnechere F., Head K.H., 1995.** "Incremental loading oedometer test on water-saturated soil". Workshop 2: standardisation of laboratory testing, in the 11th European Conf. on Soil Mechanics & Foundation Engineering, Report no ETC5-N.95.6.
4. **Babendererde L.H., 1998.** "Developments in polymer application for soil conditioning in EPB-TBMs." *Conf. Proc. 'Tunnels and Metropolises'*, Negro J. & Ferreira (eds.), Balkema, Vol 2, pp. 691-695.
5. **Babendererde S., 1991.** "Tunnelling machines in soft ground: a comparison of Slurry and EPB shield machines." *Tunnelling and Underground Space Technology*. Vol 6, No 2, April-June, pp.
6. **Bezuijen A., Schamimie P.E.L., Kleinjan J.A., 1999.** "Additive testing for EPB shields." *Proc. of 12th conference on Soil mechanics and Geotechnical Engineering*, Amsterdam, June, Vol. 3, pp. 1991-1996.
7. **Bezuijen A., 2000.** "Model experiments using foam." Research report No BF51010, GeoDelft, September.
8. **Biggart A.R., 1999.** "A quiet revolution". *Tunnels & Tunnelling International*, Vol 31, No 5, May, pp. 18-22.
9. **Bikerman J.J., 1973.** "Foams." Springer - Verlag. New York
10. **Bishop A.W. & Blight G.E., 1963.** "Some Aspects of Effective Stress in Saturated and Partially Saturated Soils". *Geotechnique*, Vol. 13, No3, pp.177-197.
11. **Bolton M.D., 1986.** "The strength and dilatancy of sands." *Geotechnique* Vol 36, No 1, pp. 65-78.
12. **Bolton M.D., 1987.** "The strength and dilatancy of sands. Discussion" *Geotechnique* Vol 37, No 2, pp. .219-236.
13. **Condat, 1998.** Trade literature.
14. **Cash T. & Van Lott K.M., 1996.** "Foam as a tunnelling aid: its production and use." *Tunnels & Tunnelling International*, April, pp. 22-23.
15. **Decon, 1996.** "Decon foam project. To establish the effect of using foam as a method of aiding tunnelling operations." Confidential document.
16. **Doran S. R. & Athenoux J., 1998.** "Storebaelt tunnel – geotechnical aspects of TBM selection and operation". *'Tunnels and Metropolises'*, Negro J. & Ferreira (eds), Balkema, Vol 2, pp. 761-766.
17. **Fredlund D.G. & Morgenstern N.R., 1976.** "Constitutive relations for volume change in unsaturated soils". *Canadian Geotechnical Journal*, Vol. 13, pp. 261-267.
18. **Fredlund D.G. & Morgenstern N.R., 1977.** "Stress state variables for unsaturated soils. *Proc. ASCE*, Vol. 103, No GT5, pp. 419-466.

19. **Fredlund D.G. & Rahardjo H., 1993.** "Soil mechanics for unsaturated soils." John Wiley & Sons, New York.
20. **Grožić J.L., Robertson P.K., Morgesten N.R., 1999.** "The behaviour of loose gassy sand". Canadian Geotechnical Journal, Vol 36, pp. 482-492.
21. **Head K.H., 1992.** "Manual of soil laboratory testing. Soil classification and compaction tests." 2nd edition, Vol 1, Pentech press, London.
22. **Head K.H., 1994** "Manual of soil laboratory testing. Compressibility, shear strength and permeability." 2nd edition, Vol 2, Pentech press, London.
23. **Head K.H., 1986.** "Manual of soil laboratory testing. Effective stress tests." Vol 3, Pentech press, London.
24. **Herrenknecht, 1999.** Trade literature.
25. **Herrenknecht M, 1994.** "EPB or Slurry machine: the choice." Tunnels & Tunnelling, June, pp. 35-36.
26. **Herrenknecht M. & Maidl U., 1995.** "Applying foam for an EPB shield drive in Valencia" Tunnel 5/95 pp. 10-19.
27. **ISST, 1998.** Trenchless Technology Guidelines. ISTT
28. **Jancsecz S. & Steiner W., 1994.** "Face support for a large mix-shield in heterogeneous ground conditions." Conference Proc. "Tunnelling '94", IMM & BTS, Chapman & Hall, London UK, pp. 253-257.
29. **Jancsecz S., Krause R., Langmaack L., 1999.** "Advantages of soil conditioning in shield tunnelling: Experiences of LRTS Izmir". Proc. of the Conf. Challenges for the 21st century, Allen *et al.* (eds), Balkema, Rotterdam, pp 865-875.
30. **Jones M., 2000.** "Micro modifications give macro improvements." Tunnels & Tunnelling International, December, pp. 38-40.
31. **Jury W.A., Gardner W.R., Gardner W.H., 1991.** "Soil Physics." 5th edition, John Wiley & Sons.
32. **Kusakabe O., Nomoto T., Imamura S., 1998** "Geotechnical criteria for selecting mechanised tunnel system and DMM for tunnelling." Panel discussion. Proc. of the 14th Intern. Conf. on Soil Mechanics and Foundation Engineering in Hamburg, Balkema, Rotterdam Vol 4, pp. 2439-2440.
33. **Lambe T.W. & Whitman R.V., 1979.** "Soil Mechanics, SI version." John Wiley & Sons, New York.
34. **Lyon J., 1997.** "Drilling manual". CETCO Europe.
35. **Lyon J., 1998.** "Polymers, bentonite and fluid injection". The New Amalgamated Tunnelling and Construction Magazine, April, p. 72.
36. **Lyon J., 1999a.** "Drilling Fluids". No-Dig International. Vol 10, No 2, February pp. 20-25.
37. **Lyon J., 1999b.** "Pipe jacking fluids". Tunnels & Tunnelling International, July, pp. 24-26.
38. **Maidl U., 1995.** "Erweiterung der Einsatzbereiche der Erddruckschilde durch bodenkonditionierung mit Schaum." PhD Dissertation Ruhr-University Bochum, Germany.

39. Maidl U., Herrenknecht M., Anheuser L., 1996. "Mechanised shield tunnelling". Ernst & Sohn, Berlin.
40. Maidl U., 1999. "Design features of the Botlek rail tunnel in the Betuweroute". Tunnelling and Underground Space Technology. Vol 14, No 2, April – June, pp. 135-140.
41. Maidl R.B. & Jonker J.H., 2000. "Dutch courage". Tunnels & Tunnelling International, Vol 32, No 6, June, pp. 29-31.
42. Marshall T.J., Holmes J.W., Rose C.W., 1996. "Soil Physics". 3rd edition. Cambridge University Press.
43. Mauroy F, 1998. "New developments in earth pressure equipment for boring underground transit lines in France (VAL)". 'Tunnels and Metropolises', Negro J. & Ferreira (eds), Balkema, Vol 2, pp. 697-701.
44. Melis M.J., 1999. "Client viewpoint. Madrid Metro Extension". Supplement, Tunnels & Tunnelling International, Vol 31, No 3, March, p vii-xiii.
45. Melis M.J., 1999. "EPBM performance. Madrid Metro Extension". Supplement, Tunnels & Tunnelling International, Vol 31, No 3, March, p xxi-xxii.
46. Milligan G.W.E. & Marshall M., 1998. "Pipeline resistance in difficult ground conditions". Pipe Jacking Seminar, Wolfson College, Oxford University, September.
47. Milligan G.W.E., 2000a. "Lubrication and soil conditioning in pipe jacking and microtunnelling". Tunnels & Tunnelling International, July, pp. 22-24.
48. Milligan G.W.E., 2000b. "Soil conditioning and lubrication in tunnelling, pipe jacking and microtunnelling. A State-of-the-art review". August. Web site: <http://www-civils.eng.ox.ac.uk/research/pipejack.htm>.
49. Moss A., 1998. Personal communication.
50. Moroi Y., 1992. "Micelles. Theoretical and applied aspects". Plenum Press.
51. Pantian N.S., Nagaraj T.S., Raju P.S.R.N., 1995. "Permeability and Compressibility behaviour of bentonite-sand/soil mixes". Geotechnical Testing Journal, ASTM, Vol. 18, No 1, March, pp. 86-93.
52. Pellet A.L. & Kastner R, 1998. "Comparison of microtunnel jacking force theoretical calculation and experimental data". 'Tunnels and Metropolises', Negro J. & Ferreira (eds), Balkema, Vol 2, pp. 733-738.
53. Peron J.Y. & Marcheselli P., 1994. "Construction of the 'Passante Ferroviario' link in Milan, Italy, lots 3P, 5P and 6P, excavation by large earth pressure balanced shield with chemical foam injection". Conference Proc. "Tunnelling '94", IMM & BTS, Chapman & Hall, London UK, pp. 679-707.
54. Porter M.R., 1994. "Handbook of Surfactants". 2nd edition, Blackie academic & Professional.
55. Rampino C., Mancuso C. Vinale F., 1999. "Laboratory testing on an unsaturated soil: equipment, procedures, and first experimental results" Canadian Geotechnical Journal, Vol 36 pp. 1-12.
56. Reilly B.J., 1999. "EPBs for the North East Line Project". Tunnelling and Underground Space Technology. Vol 6, No 2, April-June, pp. 491-508.

57. **Qian X., Gray D.H., Woods R.D., 1993.** "Voids and granulometry: effects on shear modulus of unsaturated sands". ASCE Journal of Geotechnical Engineering, Vol 119, No 2, February, pp. 295-314.
58. **Quebaud S., Sibai M., Henry J-P., 1998.** "Use of chemical foam for improvements in drilling by earth pressure balanced shields in granular soils". Tunnelling and Underground space Technology, Vol. 13, No.2, pp. 173-180.
59. **Quebaud S., 1996.** "Contributions a l'étude du percement de galeries par boucliers à pression de terre: Amélioration du creusement par l'utilisation de produits moussants" PhD thesis, University of Sciences and Technologies of Lille, France.
60. **Schramm L.L. & Wassmuth F., 1994.** "Foams: Basic principles". Chapter 1 from 'Foams: Fundamentals and applications in petroleum industry'. Schramm L.L. (ed.), Advances in chemistry series 242, American Chemical Society.
61. **Schuppener B., Amar S., Kavvadas G., 1995.** "Determination of soil permeability by constant and falling head." Workshop 2: standardisation of laboratory testing, in the 11th European Conf. on Soil Mechanics & Foundation Engineering, Report no ETC5-N.94.38.
62. **Schwarz L.G. & Krizek R.L., 1994.** "Effect of preparation technique on permeability and strength of cement-grouted sand". Geotechnical Testing Journal, ASTM, Vol 17, No 4, December, pp. 434-443.
63. **Taylor D.W., 1948.** 'Fundamentals of Soil Mechanics'. John Wiley & sons, New York.
64. **Thomas S.D., 1987.** The consolidation behaviour of gassy soil. D.Phil. Thesis, Oxford University, Jesus College, Trinity term.
65. **Thomson J.C., 1993.** "Microtunnelling and Pipejacking". Blackie academic & professional.
66. **Vertigo R. & Ishihara K., 1996.** "The steady state of sandy soils". Soils and Foundations, Vol 36, No2, pp. 81-91.
67. **Wallis S., 1995.** "Foaming success at Valencia". World Tunnelling, October.
68. **Webb R. & Breeds C.D., 1997.** "Soft ground EPBM tunnelling – west Seattle Alki tunnel." Conference Proc. "Tunnelling '97", IMM & BTS, Chapman & Hall, London UK, pp. 501-514.
69. **Wheeler S.J., 1986.** "The stress strain behaviour of soils containing gas". D.Phil thesis, Oxford University, Balliol College, Hilary term.
70. **Wheeler SJ., 1988.** "A conceptual model for soils containing large gas bubbles". Geotechnique, Vol 38, pp. 389-397.
71. **Wroth C.P., & Housby G.T., 1985.** "Soil mechanics: property characterisation and analysis procedures". Proc. 11th Int. Conf. Soil Mechanics & Foundation Engineering, San Francisco Vol 1, pp. 1-55.
72. **Zeng X., Wu J., Young B.A., 1998.** "Influence of Viscous Fluids on Properties of Sand" Geotechnical Testing Journal, ASTM, Vol. 21, No 1, March, pp. 45-51.
73. **Zhang M., Takahashi M., Morin R.H., Esaki T., 1998.** "Theoretical Evaluation of the Transient Response of Constant Head Flow-rate Permeability tests". Geotechnical Testing Journal, ASTM, Vol. 21, No 1, March, pp. 52-57.

TABLES

Table 1.1: Application of soil conditioning agents in mechanised tunnelling (Milligan, 2000b)

Location	TBMs	Slurry Shields	EPBs
Tunnel face	Lubricate cutters/discs; Reduce wear and power requirements	Improve slurry properties; reduce wear and power requirements	Lubricate cutters; reduce wear & power requirements; reduce water inflows
Machine head	Improve muck flow; reduce friction-wear	Prevent clogging; reduce wear with abrasive soils	Make soil more plastic; prevent clogging & re-compaction; reduce wear & friction provide, pressure fluctuations
Spoil handling system	Reduce water content; improve handling	Improve dispersion of soil in slurry; reduce wear; improve performance in separation plant	Produce plastic state in spoil; reduce permeability, friction, wear & power requirements, water content of muck; prevent excessive water flow
Spoil tip	Improve spoil quality for easier disposal or/and re-use in construction	Improve spoil quality for easier disposal or/and re-use in construction	Improve spoil quality for easier disposal or/and re-use in construction
Tunnel bore	Support tunnel bore; provide lubrication	Support tunnel bore; provide lubrication in Pipe Jacking	Support tunnel bore; provide lubrication in Pipe Jacking

Table 1.2: Use of soil conditioning agents in EPBs (Milligan, 2000b)

Soil type	Mining characteristics	Treatment
Plastic clays	Tend to reconstitute with little loss of strength in machine chamber	High dosage of foam at head to keep excavated material as separate pieces
Laminated, silty or sandy clays	Break up better, but still tend to reconstitute, slightly abrasive, form plug	Possibly none other than water to reduce shear strength to acceptable value; in stiffer clays, medium dosage of foam at head. Possibly add lubricant to foam to reduce abrasion.
Clayey sands and gravel	Flow easily, may form plug if fines content in excess of 10%; highly abrasive	Add lubricant polymer at head to reduce wear; add water - absorbing polymer at screw if required to form plug and control water inflow
Silty fine sands	Do not flow, do not form plug, allow ground water inflow, highly abrasive; problems increase with larger particle sizes	Foam with polymer additive to stiffen foam and provide lubrication; approximate dosage rates for polymer:
Sand / gravel		<ul style="list-style-type: none"> • Silty sands, 0.1% • Sands/gravel, 0.25% • Gravel/cobbles, 1-3%
Gravel / cobbles		
Cobbles and boulders	Tend to congregate in clumps in head and/or jaw screw.	Large dosages of additive to keep cobbles separate in head and provide water control and lubrication

Table 2.1: Bentonite slurry voids ratio and coefficient a for bentonite compression tests

compression test		$V_{sat.sand}$	$V_{bentonite}$	V_{water}	e_{bs}	a
fine sand $n = 0.476$	<i>f30</i>	1375	17.0	300	17.6	0.48
	<i>f31</i>	1405	17.0	300	17.6	0.47
	<i>f32</i>	1455	34.0	400	11.8	0.63
	<i>f39</i>	1455	25.5	750	29.4	1.12
	<i>f40</i>	1455	25.5	800	31.4	1.19
coarse sand $n = 0.441$	<i>c33</i>	1315	25.5	350	13.7	0.65
	<i>c34</i>	1355	25.5	400	15.7	0.71
	<i>c35</i>	1355	25.5	400	15.7	0.71
	<i>c37</i>	1375	25.5	650	25.5	1.11
	<i>c42</i>	1405	34.0	900	26.5	1.51
	<i>c44</i>	1355	34.0	1100	32.4	1.90

Table 2.2: Water/sand mixing tests - Power consumption [W]

sample	<i>w</i>	0%	10%	20%	30%	40%
1500 g dry fine sand	<i>test1</i>	112	120	129	123	
	<i>test2</i>	111	120	127	120	
	<i>test3</i>	115	123	128	126	
	<i>test4</i>	119	124	131	129	
	<i>test5</i>	111	122	128	127	
	<i>test6</i>	114	126	131	127	
	<i>test7</i>	116	123	127	125	
	<i>test8</i>	117	125	131	130	
	<i>test9</i>	115	124	131	123	
	<i>test10</i>	113	123	129	127	
	<i>test11</i>	114	125	128	121	
	<i>test12</i>	119	128	134	124	
	<i>test13</i>	118	128	134	124	
	<i>test14</i>	119	129	136	126	
average	Pds & Pws	115.2	124.3	130.3	125.1	115.5
in air	Pair	110	110	110	110	110

Table 2.3: Foam/water/sand mixing tests

sample 1500 g (566 ml) dry fine sand				Power consumption [W]				FIR =	Pr =
test	water [ml]	foam [ml]	foam/sand	Pair	Pds	Pws	Pf	Vf / (Vw+Vs+Vf)	dPf/dPws *
t001	450	100	0.098	110	115	124	119	0.086	0.643
t002	450	200	0.197	109	114	125	118	0.158	0.563
t003	450	300	0.295	108	114	123	115	0.219	0.467
t007	500	300	0.281	109	115	128	116	0.219	0.368
f05	450	400	0.394	109	117	132	114	0.272	0.217
f06	450	500	0.492	106	112	123	111	0.319	0.294
f07	450	750	0.738	112	119	129	113	0.412	0.059
f08	450	500	0.492	109	113	123	112	0.319	0.214
f09	450	500	0.492	109	115	127	113	0.319	0.222
f10	450	750	0.738	114	119	126	114	0.425	0.000
f11	480	1000	0.956	113	118	124	113	0.483	0.000
f12	450	500	0.492	113	120	132	115	0.319	0.105
f13	450	750	0.738	110	116	126	113	0.412	0.188
f14	450	400	0.394	108	113	127	110	0.272	0.105
f15	450	600	0.591	108	117	131	108	0.347	0.000
f16	400	500	0.518	109	114	128	112	0.341	0.158
f17	450	800	0.787	113	119	124	113	0.443	0.000
f18	450	800	0.787	110	115	123	110	0.445	0.000
f22	450	900	0.886	112	118	124	116	0.470	0.333
average:				110.1	115.9				
at w = 27%				109.0	114	128.0	112.0		
at w = 30%				110.1	116.0	126.2	113.4		
at w = 33%				111.0	116.5	125.5	114.5		
								$* dPf = Pf - Pair$ $dPws = Pws - Pair$	

Table 2.4: Water/ fine sand mixture - Relative power increase

spesific gravity	Gs =	2.65	2.65	2.65	2.65	2.65	2.65
water mass [g]	Mw =	0	150	300	400	450	500
soil mass [g]	Ms =	1500	1500	1500	1500	1500	1500
water content	w =	0.0%	10.0%	20.0%	26.7%	30.0%	33.3%
voids ratio	e =	0.91	0.91	0.91	0.91	0.91	0.91
saturation degree	S =	0.0%	29.2%	58.5%	78.0%	87.7%	97.5%
Summary of measured power from the two types of tests (average values)							
all values are in [W]							
test series:		Pds	Pws	Pws	Pws	Pws	Pws
water-sand		115.2	124.3	130.3	-	125.2	-
foam-water-sand (Pws)		115.9	-	-	128	126.2	125.5
Average values		115.55	124.3	130.3	128	125.7	125.5
				Pf	Pf	Pf	
foam-water-sand (Pf)			-	-	112.0	113.4	114.5

 Relative Power increase: $Dp = (P - Pair) / (Pds - Pair)$ with respect to Pds

in air	0.00					
dry sand	1.00					
water - sand	1.000	2.577	3.658	3.243	2.828	2.793
foam - water - sand	-	-	0.360	0.360	0.608	0.811

				$Pair =$	110
				$Pds - Pair =$	5.55

Table 3.1: Compression tests (Rowe cell)								
n	name	date	Materials					Remarks
			sand	water content	foamer type	quantity	ER	
1	f01	01 08 1999	fine_1500g	27%	-	-	-	not fully saturated sand
2	f02	01 08 1999	fine_1500g	45%	-	-	-	sand was poured into the cell
3	f03	02 08 1999	fine_1500g	33%	-	-	-	
4	f04	10 08 1999	fine_1500g	35%	-	-	-	
5	f05	03 08 1999	fine_1500g	30%	P90	400 ml	10% ER-12	drained -stable foam
6	f06	04 08 1999	fine_1500g	30%	P90	500 ml	10% ER-9	drained -stable foam
7	f07	05 08 1999	fine_1500g	30%	P90	750 ml	10% ER-14.8	drained -stable foam
8	f08	07 08 1999	fine_1500g	30%	PP90	500 ml	5% ER-22.4	undrained/drained
9	f09	09 08 1999	fine_1500g	30%	PP90	500 ml	5% ER-10	undrained/drained
10	f10	10 08 1999	fine_1500g	30%	PP90	750 ml	5% ER-27.1	drained
11	f11	11 08 1999	fine_1500g	32%	PP90	1000 ml	5% ER-12.4	drained
12	f12	12 08 1999	fine_1500g	30%	SC200	500 ml	5% ER-16.9	drained (PHPA IP425 added, 0.03%)
13	f13	13 08 1999	fine_1500g	30%	SC200	750 ml	5% ER-13	drained (PHPA IP425 added, 0.03%)
14	f14	14 08 1999	fine_1500g	30%	Versa	400 ml	5% ER-11.2	drained
15	f15	17 08 1999	fine_1500g	30%	Versa	600 ml	5% ER-11	drained
16	f16	18 08 1999	fine_1500g	27%	Versa	500 ml	7% ER-12	drained
17	f17	19 08 1999	fine_1500g	30%	Versa	800 ml	7% ER-40	drained- high ER
18	f18	20 08 1999	fine_1500g	30%	Versa	800 ml	7% ER-14	drained-low ER
19	f19	21 08 1999	fine_1500g	27%	Versa	800 ml	7% ER-15.7	undrained/drained
20	c20 *	24 08 1999	coarse_1500g	25%	PP60	250 ml	5% ER-12	Inconclusive no volume changes
21	c21 *	29 08 1999	coarse_1500g	25%	PP90	1000 ml	5% ER-11	Inconclusive (final sample too thin)
22	f22	01 09 1999	fine_1500g	30%	Versa	900 ml	7% ER-14.8	undrained/drained
23	c23	01 10 1999	coarse_1500g	26%	-	-	-	not fully saturated sand
24	c24	02 10 1999	coarse_1500g	30%	-	-	-	
25	f25	29 11 1999	fine_1500g	30%	Versa	600 ml	3% ER-15	reduced foam proportion
26	f26	30 11 1999	fine_2000g	32%	Versa	1000 ml	3% ER-15	Unexplained low volume changes
27	c27	28 11 1999	coarse_1500g	27%	Versa	400 ml	3% ER-15	small volume changes (friction)
28	c28	29 11 1999	coarse_2000g	27%	Versa	600 ml	3% ER-13	Inconclusive (not saturated after adding slurry)
29	c29 *	17 01 1999	coarse_2000g	25%	-	-	-	
30	f30	20 01 2000	fine_2000g	33%	-	-	-	80g@400ml
31	f31	21 01 2000	fine_2000g	32%	-	-	-	40g@300ml
32	f32 *	22 01 2000	fine_2000g	35%	Versa	500ml	3% ER-15	80g@400ml
33	c33	23 01 2000	coarse_2000g	29%	-	-	-	60g@350ml
34	c34	24 01 2000	coarse_2000g	30%	-	-	-	Inconclusive, differences in voids ratio
35	c35	24 01 2000	coarse_2000g	30%	Versa	600ml	3% ER-20	60g@400ml
36	f36	01 02 2000	fine_2000g	30%	Versa	400 ml	3% ER-20	Inconclusive - height measurement
37	c37	02 02 2000	fine_2000g	31%	-	-	-	21.9
38	f38	15 02 2000	fine_2000g	32%	Versa	600 ml	3% ER-15	Low compressibility
39	f39	17 02 2000	fine_2000g	35%	-	-	-	Unexpected low compressibility
40	f40	21 02 2000	fine_2000g	35%	Versa	1000ml	3% ER-21	Intermediate compression stages incomplete
41	f41	22 02 2000	fine_2000g	35%	Versa	1000ml	3% ER-20	creep in last stages?
42	c42	25 02 2000	coarse_2000g	32%	-	-	-	final consolidation stages incomplete
43	f43	28 02 2000	fine_2000g	35%	Versa	700ml	3% ER-20	low water drainage
44	c44	29 02 2000	coarse_2000g	30%	Versa	900ml	3% ER-15	duration 50h - 3stages (compression only)
45	f45	10 03 2000	fine_2000g	35%	Versa	1000ml	3% ER-18	duration 1h - (compression only)
46	f46	16 03 2000	fine_2000g	35%	Versa	1100 ml	3% ER-20	duration 10h - (compression only)
47	f47	17 03 2000	fine_2000g	35%	Versa	1100 ml	3% ER-20	

*Tests c20,c21,c29 and f32 were characterised unsuccessful.

Table 3.2: COMPRESSION TEST f40 (Example)						
Oxford University - Engineering Science Department - Civil Engineering Laboratory				(21/02/2000)		1 of 2
Mixture proportions						

1. Sand mixture						
Materials	Proportion			Comments:		
	mass (g)	Gs	volume (ml)	1.00	mass (g)	volume (ml)
Air	0.0	0.001	0.0	1.00	0.0	0.0
Water	700.0	1.00	700.0		700.0	700.0
Sand	2000.0	2.65	754.7		2000.0	754.7
sum	2700.0		1454.7		2700.0	1454.7

2. Foam						
Materials	Proportion			Comments:		
	mass (g)	Gs	volume (ml)	0.95	mass (g)	volume (ml)
Air	0.95	0.001	950.00	0.95	0.90	902.50
Liquid	50.00	1.00	50.00		47.50	47.50
ER	20.00		20.00		19.00	19.00
sum	50.95		1000.00		48.40	950.00

3. Bentonite						
Materials	Proportion			Comments:		
	mass (g)	Gs	volume (ml)	0.90	mass (g)	volume (ml)
Air	0.00	0.00	0.00	0.90	0.00	0.00
Water	780.00	1.00	780.00		702.00	702.00
Bentonite	60.00	2.35	25.53		54.00	22.98
sum	840.00		805.53		756.00	724.98

4. Polymer mixture ('WOP')						
Materials	Proportion			Comments:		
	mass (g)	Gs	volume (ml)	0.667	mass (g)	volume (ml)
PHPA	11.50	1.15	10.00	0.667	7.67	6.67
OIL	36.00	0.90	40.00		24.01	26.68
WATER	10.00	1.00	10.00		6.67	6.67
Mix	57.50		60.00		38.35	40.02

Mixture							
Materials	Proportion			By mass		By volume	
	mass (g)	Spec. Grav.	volume (ml)	Volatile	"Volatile"	"Non-volatile"	"Volatile"
Air	0.90	0.001	902.50	1.00	0.90	0.00	902.50
Water	1456.17	1.000	1456.17	1.00	1456.17	0.00	1456.17
Sand	2000.00	2.650	754.72	0.00	0.00	2000.00	0.00
Bentonite	54.00	2.350	22.98	0.00	0.00	54.00	0.00
oil	24.01	0.900	26.68	0.02	0.53	23.48	0.59
PHPA	7.67	1.150	6.67	0.03	0.21	7.46	0.18
Total	3542.76	2.573	3169.72		1457.81	2084.95	2359.44
symbol	M	Gs	V		Mw	Ms	Vv
							Vs

$w_0 = M_w/M_s$	0.699	water content
$S_0 = V_w/V_v$	61.7%	degree of saturation
$e_0 = V_v/V_s$	2.912	theoretical voids ratio
$FIR = V_f/V$	30.0%	Foam Injection Ratio
$\rho = M/V$	1.12	bulk density

= Measured quantities

Table 3.2: COMPRESSION TEST f40 (Example)									
Oxford University - Engineering Science Department - Civil Engineering Laboratory				(21/02/2000)		2 of 2			
Sample measurements & Calculations									
Compression test measurements							comments:		
<i>End of test</i>	<i>Beginning of test</i>								
<i>Hf [mm]</i>	15.79	<i>Hi [mm]</i>	26.86	f = final	SAMPLE: H : height , Hs : solids height	MEASUREMENTS: P : vertical pressure			
<i>D [mm]</i>	74.6	<i>dH [mm]</i>	11.07	i = initial	D : diameter	dH : compression			
<i>A [mm²]</i>	4370.87	<i>dH/Hf</i>	0.701	w = water	A : area	dVw : expelled water			
		<i>dH//Hi</i>	0.412	q = gas	M : mass	m : sub-sample mass			
<i>Mf [g]</i>	108.8	<i>Mi [g]</i>	135.7		Gs : specific gravity	t : time			
<i>Gs</i>	2.573	<i>Gs</i>	2.573		w : water content				
Subsample-mass [g]	Subsample-mass [g]								
m wet+tin	98.89	m wet+tin	34.12		V : volume				
m dry+tin	76.89	m dry+tin	28.56		p : density				
m tin	9.36	m tin	20.11		e : voids ratio				
					S : saturation degree				
Computed values									
m wet	89.53	m wet	14.01	sample	final	initial	comments:		
m dry	67.53	m dry	8.45	<i>Ms</i>	82.06	81.85	These values have been computed based on the initial and final values of test measurements.		
<i>wf</i>	0.326	<i>wi</i>	0.658	<i>Mw</i>	26.74	53.85			
<i>Vf [mm³]</i>	69016	<i>Vi [mm³]</i>	117401	<i>eq</i>	0.331	0.998			
<i>pf [Mg/m³]</i>	1.576	<i>pi [Mg/m³]</i>	1.156	<i>ew</i>	0.832	1.693			
<i>pf_D</i>	1.189	<i>pi_D</i>	0.697	<i>eg/ew</i>	0.40	0.59			
<i>ef</i>	1.164	<i>ei</i>	2.691	<i>Hg</i>	2.41	7.26			
<i>Sf</i>	72.0%	<i>Si</i>	62.9%	<i>Hw</i>	6.10	12.32			
<i>Hs [mm]</i>	7.28	<i>Hs [mm]</i>	7.28	compressibility			permeability		
<i>P [kPa]</i>	<i>dH [mm]</i>	<i>de=dH/Hs</i>	<i>e=ei-de</i>	<i>mv [1/Mpa]</i>	<i>t₉₀^{0.5} [sec]</i>	<i>Cv [m²/y]</i>	<i>k [m/sec]</i>		
0.0	0.000	0.000	2.691						
20.0	-0.020	-0.003	2.688	0.04	n/a	n/a	n/a		
28.3	-0.081	-0.011	2.680	0.37	n/a	n/a	n/a		
40.0	-1.182	-0.162	2.528	3.94	n/a	n/a	n/a		
56.6	-2.512	-0.345	2.346	6.21	n/a	n/a	n/a		
80.0	-4.335	-0.596	2.095	8.22	n/a	n/a	n/a		
113.0	-5.923	-0.814	1.877	8.57	12	1.20E+04	3.18E-05		
160.0	-8.027	-1.103	1.588	9.07	17	6.76E+03	1.90E-05		
226.0	-12.349	-1.697	0.994	12.89	37	1.80E+03	7.21E-06		
160.0	-12.262	-1.685	1.006	<i>T₉₀</i> = 0.848 (vertical one way drainage square-root method) <i>Cv</i> = <i>T₉₀</i> <i>H²</i> / <i>t₉₀</i> <i>k</i> = <i>m_v</i> <i>Cv</i> <i>g_w</i>					
80.0	-11.955	-1.643	1.048						
40.0	-11.547	-1.587	1.104						
20.0	-11.067	-1.521	1.170						

Quality Control for compression tests

Discrepancies between the measured and the calculated values assumed in the analysis were due to a number of factors:
The minimum and the maximum losses in cc water were the limits which the measured values should be fell within.

Table 3.3	max loss		max gain		water losses [ml]		<i>Comments:</i>
	height [mm]	water [ml]	height [mm]	water [ml]	<i>initial</i>	<i>final</i>	
Errors							Calibration has been taken into account
1. caliper accuracy	0.50	2.19	0.50	2.19			
2. cell cap placing	1.14	5.00					
3. de-aired water			2.29	10.00			
4. sample weighting	1.14	5.00	1.14	5.00			
5. Mixture measurement	1.14	5.00					
<i>min</i>					-10.0	-17.2	
<i>max</i>					5.0	17.2	

Check type I

From the initial bulk weight of the sample M_i and the initial water content w_i the solids mass M_s was calculated:

$$M_s = M_i / (1 + w_i)$$

From the difference (dwo) between the water content of the mixture (w_o) and the measured one w_i the difference in water (cc) could be calculated as:

$$dM_w = (w_o - w_i) M_s$$

This was the amount of water needed to eliminate the discrepancy between w_o and w_i .

Check type II

For each test the initial (or the final) 'height' of water H_w was calculated from the initial (or final) degree of saturation S , voids ratio e and solids height H_s :

$$H_w = S e H_s$$

From the difference of the initial degree of saturation S_o in the mixture and the saturation degree measured from the sample S_i , the difference in water 'height' needed to eliminate the difference between S_o and S_i , was calculated as:

$$dH_w = (S_o - S_i) e i H_s$$

The difference in mass of water (g) would be:

$$dM_w = G_w p_w A dH_w \quad \text{where } A \text{ was the cross section area of the sample}$$

Table 3.4: Quality control for compression tests, comparing initial water contents.

Test	Water content			Differences			Mass Ms (g)	losses/gains [g]			QC
	foam	wo	wi	wie	dwoi	dwoie	dwie	dMw (oi)	dMw (oie)	dMw (ie)	
f5		0.321	0.315			0.006		148.2	0.89		A
f6		0.335	0.318			0.017		138.7	2.36		A
f7		0.346	0.403			-0.057		112.8	-6.43		A?
f8		0.314	0.304			0.010		120.0	1.20		A
f9		0.332	0.333			-0.001		123.2	-0.12		A
f10		0.319	0.321			-0.002		101.9	-0.20		A
f11		0.352	0.338			0.014		89.4	1.25		A
f12		0.319	0.295			0.024		116.6	2.80		A
f13		0.337	0.315			0.022		103	2.27		A
f14		0.323	0.375			-0.052		141.9	-7.38		A?
f15		0.333	0.335			-0.002		134.9	-0.27		A
f16		0.295	0.293			0.002		138.7	0.28		A
f17		0.332	0.327			0.005		103.3	0.52		A
f18		0.325	0.315			0.010		113.3	1.13		A
f19		0.295	0.245			0.050		103.5	5.18		A?
f22		0.339	0.322			0.017		92.3	1.57		A
f25		0.324	0.322			0.002		117.2	0.23		A
f26		0.33	0.309			0.021		111.6	2.34		A
c27		0.283	0.297			-0.014		147.0	-2.06		A
c28		0.284	0.265			0.019		159.2	3.02		A
c35		0.479	0.494			-0.015		129.1	-1.94		A
f36		0.313	0.329			-0.016		136.8	-2.19		A
f38		0.341	0.326			0.015		132.8	1.99		A
f40		0.699	0.658			0.041		81.5	3.34		A
f41		0.373	0.371			0.002		103.3	0.21		A
f43		0.373	0.353			0.020		104.3	2.09		A
c44		0.778	0.775			0.003		60.4	0.18		A
f45		0.371	0.393			-0.022		90.1	-1.98		A
f46		0.374	0.378			-0.004		75.5	-0.30		A
f47		0.376	0.384			-0.008		75.1	-0.60		A
non-foam	wo	wi	wie	dwoi	dwoie	dwie	Ms (g)	dMw (oi)	dMw (oie)	dMw (ie)	
f30		0.430	0.422	0.336	0.008	0.094	0.086	147.9	1.18	13.90	12.72
f31		0.449	0.476	0.424	-0.027	0.025	0.052	135.7	-3.66	3.39	7.06
c33		0.426	0.427	0.403	-0.001	0.023	0.024	177.5	-0.18	4.08	4.26
c34		0.465	0.407	0.320	0.058	0.145	0.087	179.7	10.42	26.05	15.63
c37		0.579	0.605	0.535	-0.026	0.044	0.07	94.4	-2.45	4.15	6.61
f39		0.680	0.661	0.639	0.019	0.041	0.022	103.3	1.96	4.23	2.27
c42		0.714	0.813	0.764	-0.099	-0.050	0.049	104.0	-10.29	-5.20	5.09

	dw (oi)	dw (oie)	dw (ie)
<i>non-foam tests</i>			
average	-	0.01	0.05
std deviation		0.05	0.06
<i>foam tests</i>			
average		0.006	
std deviation		0.018	

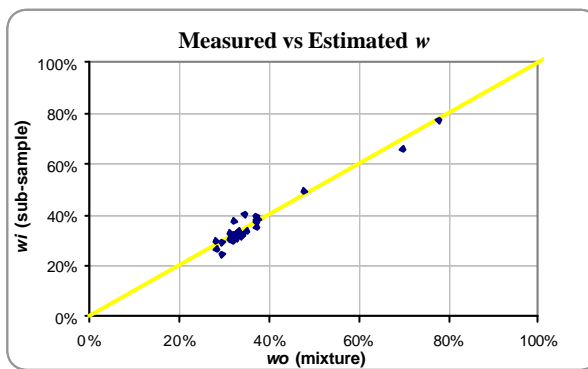


Table 3.5: Quality control for compression tests, comparing initial degrees of saturation

Test	Saturation degree			Differences		Height [mm]		Mass [g]	QC
	So	Si	Sf	dSi	ei	Hsi	dHw		
f5	0.580	0.544	0.463	0.036	1.54	12.80	0.71	3.10	A
f6	0.534	0.480	0.417	0.054	1.76	12.06	1.15	5.01	A?
f7	0.438	0.500	0.341	-0.062	2.16	9.74	-1.30	-5.70	A
f8	0.509	0.534	0.519	-0.025	1.51	10.36	-0.39	-1.71	A
f9	0.538	0.628	0.595	-0.090	1.41	10.36	-1.31	-5.75	A
f10	0.398	0.376	0.416	0.022	2.27	10.66	0.53	2.33	A
f11	0.376	0.379	0.589	-0.003	2.36	8.85	-0.06	-0.27	A
f12	0.517	0.490	0.397	0.027	1.60	7.70	0.33	1.45	A
f13	0.434	0.420	0.374	0.014	1.99	10.10	0.28	1.23	A
f14	0.583	0.678	0.589	-0.095	1.46	8.87	-1.23	-5.38	A?
f15	0.504	0.519	0.258	-0.015	1.71	11.65	-0.30	-1.31	A
f16	0.491	0.509	0.284	-0.018	1.53	11.98	-0.33	-1.44	A
f17	0.401	0.400	0.099	0.001	2.16	8.92	0.02	0.08	A
f18	0.396	0.393	0.125	0.003	2.13	9.78	0.06	0.27	A
f19	0.368	0.292	0.125	0.076	2.21	8.97	1.51	6.59	A?
f22	0.376	0.355	0.312	0.021	2.40	7.97	0.40	1.76	A
f25	0.491	0.496	0.420	-0.005	1.72	10.12	-0.09	-0.38	A
f26	0.440	0.460	0.407	0.020	1.80	9.7	-0.35	-1.53	A
c27	0.549	0.753	0.607	-0.204	1.01	13.15	-2.70	-11.82	R
c28	0.518	0.625	0.438	-0.107	1.10	14.03	-1.65	-7.23	A
c35	0.650	0.768	0.619	-0.118	1.67	11.41	-2.24	-9.80	R
c36	0.638	0.750	0.519	-0.112	1.14	11.81	-1.51	-6.60	A
c38	0.606	0.616	0.440	-0.010	1.40	11.46	-0.16	-0.70	A
f40	0.617	0.629	0.721	-0.012	2.71	7.25	-0.24	-1.03	A
f41	0.455	0.512	0.513	-0.057	1.88	9.1	-0.98	-4.27	A
f43	0.455	0.465	0.352	-0.010	1.97	9.19	-0.18	-0.79	A
c44	0.684	0.679	0.999	0.005	2.89	5.41	0.08	0.34	A
f45	0.453	0.489	0.720	-0.036	2.10	7.9	-0.60	-2.61	A
f46	0.419	0.360	0.727	-0.059	2.73	6.65	1.07	4.68	A
f47	0.421	0.359	0.903	-0.062	2.78	6.61	1.14	4.99	A
non-foam	So	Si	Sf	dSi	ei	Hsi	dHw	dMw	
f30	1.000	1.052	0.839	-0.052	1.06	12.79	-0.71	-3.08	A
f31	1.000	1.044	0.937	-0.044	1.18	11.98	-0.62	-2.72	A
c33	1.000	1.070	1.025	-0.070	1.05	15.37	-1.13	-4.94	A
c34	1.000	1.170	0.950	-0.170	0.90	15.87	-2.43	-10.63	R
c37	1.000	1.093	0.971	-0.093	1.41	8.5	-1.11	-4.86	A
f39	1.000	0.967	1.020	0.033	1.72	9.18	0.52	2.28	A
c42	1.000	1.120	1.085	0.120	1.84	9.37	-2.07	-9.06	A?

foam	dMw
average	- 1.72
st deviation	4.61
non foam	dMw
average	- 4.72
st deviation	4.27

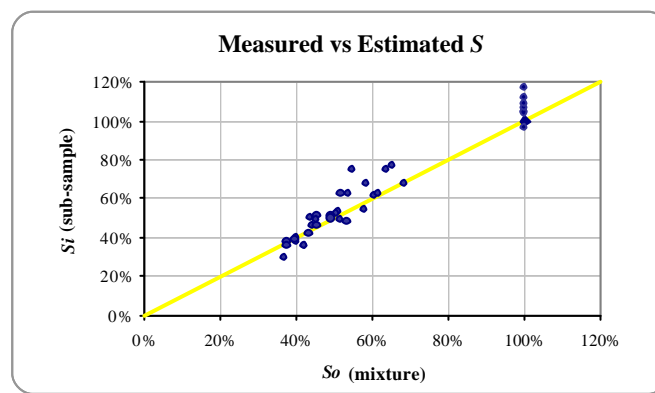


Table 3.6: Volume changes for 'Versa' foamed tests.

Test	voids ratios						difference (initial - final)		
	<i>ei</i>	<i>ewi</i>	<i>eai</i>	<i>ef</i>	<i>ewf</i>	<i>eaf</i>	<i>de</i>	<i>dew</i>	<i>deg</i>
f14	1.47	0.99	0.47	1.21	0.71	0.50	0.26	0.28	-0.02
f15	1.71	0.89	0.82	1.17	0.30	0.87	0.54	0.59	-0.05
f16	1.53	0.78	0.75	1.11	0.32	0.80	0.41	0.46	-0.05
f17	2.16	0.87	1.30	1.22	0.26	0.96	0.94	0.60	0.34
f18	2.13	0.84	1.29	1.19	0.15	1.04	0.93	0.69	0.25
f19	2.21	0.64	1.57	1.18	0.15	1.03	1.03	0.49	0.54
f22	2.40	0.85	1.55	1.13	0.35	0.78	1.27	0.50	0.77
f25	1.72	0.85	0.87	1.20	0.50	0.69	0.53	0.35	0.18
f26	1.78	0.82	0.96	1.31	0.53	0.78	0.47	0.29	0.19
c27	1.01	0.76	0.25	0.85	0.51	0.34	0.16	0.25	-0.09
c28	1.10	0.69	0.41	0.98	0.43	0.55	0.12	0.26	-0.14
c35	1.67	1.28	0.39	1.25	0.77	0.48	0.42	0.51	-0.09
f36	1.14	0.87	0.27	1.09	0.57	0.52	0.05	0.31	-0.25
f38	1.40	0.86	0.54	1.16	0.51	0.65	0.24	0.35	-0.11
f40	2.69	1.69	1.00	1.16	0.83	0.33	1.53	0.86	0.67
f41	1.88	0.96	0.92	0.83	0.43	0.41	1.05	0.54	0.51
f43	1.97	0.92	1.05	0.93	0.33	0.60	1.04	0.59	0.45
c44	2.90	1.98	0.92	1.86	1.86	0.00	1.04	0.12	0.92
f45	2.10	1.03	1.07	0.82	0.49	0.33	1.27	0.53	0.74
f46	2.73	0.98	1.74	0.86	0.61	0.25	1.87	0.37	1.50
f47	2.78	1.00	1.78	0.74	0.66	0.07	2.04	0.33	1.71
aver.							0.82	0.44	0.38
st. dev.							0.57	0.17	0.53

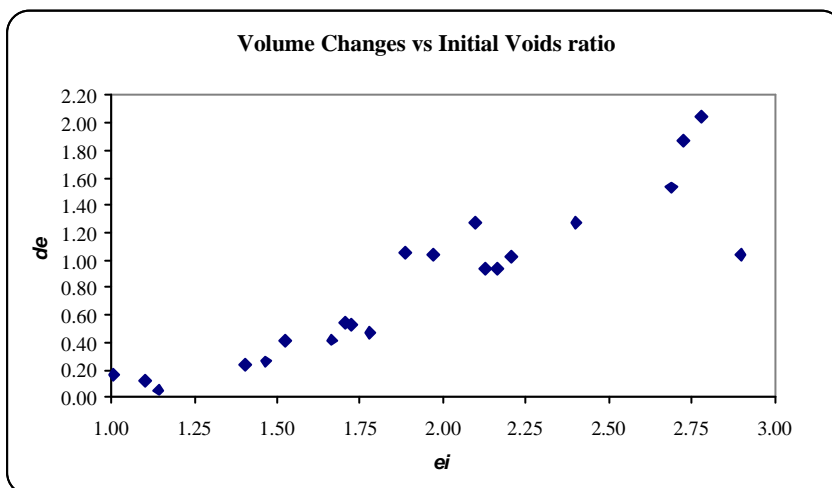


Table 3.7: Evaluation of sand permeability using empirical formulae

Permeability (m/s)						k
<u>Hazen's formula</u>						
particle size D_{10}						
fine sand	0.13					
coarse sand	0.65					
<u>Kozeny -Carman formula</u>						
	particle size range	passing	s	f	$pas. f s^2$	e
fine sand	0.6	0.425	0.00			
	0.425	0.355	33.72	15.45	1.25	10058.66
	0.355	0.212	58.55	21.87	1.25	35008.14
	0.212	0.125	7.62	36.86	1.25	12946.67
	0.125	0.0636	0.10	67.29	1.1	509.2686
			100.0		58522.73	0.91
coarse sand	1.18	0.6	0.0			
	0.6	0.355	94.0	13.00	1.25	19859.15
	0.355	0.212	3.2	21.87	1.25	1913.367
	0.212	0.125	2.5	36.86	1.25	4245.283
	0.125	0.063	0.0			
			99.7		26017.80	0.79
						2.12E-05

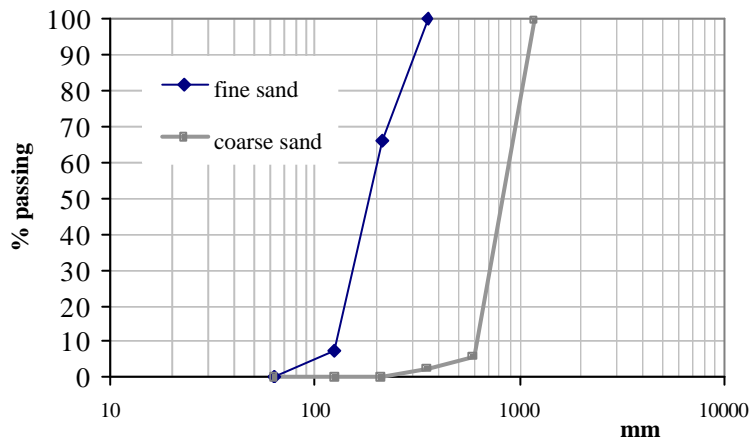
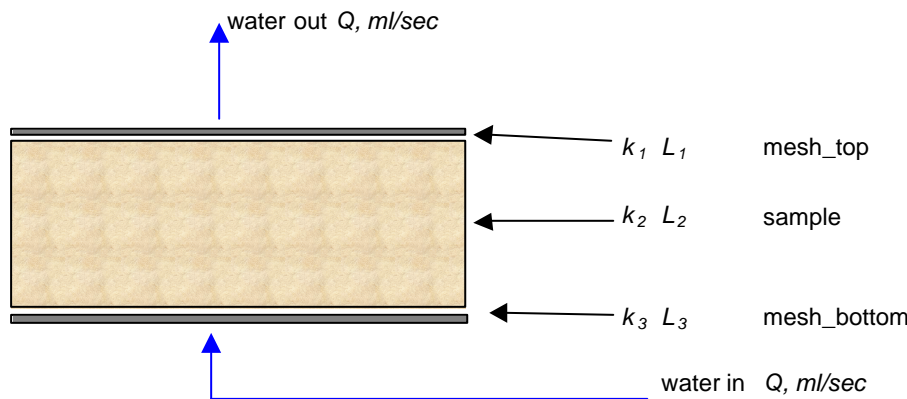
Particle size distribution for fine and coarse silica sands

Table 3.8: Summary of permeability results. All permeability (k_2) values are in m/sec

Material to test	Formula calculation:		Calculation via Cv, for different pressures - kPa					Permeability tests @ 20 kPa
	Hazen's	K-C's	<20	28-40	56-80	113-160	>226	
coarse sand	4.2E-03	2.1E-05						1.21E-05
coarse sand + foam + polymer			IN/VE	2.0E-05	IN/VE	IN/VE	IN/VE	1.80E-06
coarse sand + bentonite + polymer			IN/VE	IN/VE	9.1E-06	5.8E-07	8.2E-07	NOT TESTED
coarse sand + foam + bentonite + polymer			IN/VE	IN/VE	IN/VE	7.5E-05	1.3E-05	NOT TESTED
fine sand	1.7E-04	1.3E-05						2.70E-06
fine sand + foam			2.1E-05	IN/VE	1.7E-05	IN/VE	IN/VE	1.97E-07
fine sand + foam + polymer			5.1E-07	IN/VE	8.2E-05	1.0E-05	9.3E-05	2.30E-07
fine sand + polymer + bentonite			IN/VE	IN/VE	IN/VE	5.3E-06	6.7E-05	NOT TESTED
fine sand + foam + bentonite + polymer			IN/VE	IN/VE	IN/VE	2.6E-05	7.2E-06	NOT TESTED

* Permeability tests were carried out in Rowe cell. These values (bold) are the calculated permeability of the medium (sample), which was deduced from the measured combined permeability (k_c i.e. sample+meshes)- see section 3.4.

IN/VE: inconclusive



Calculation:

$$k_c = (L_2 + 2L_1) / (2L_1/k_1 + L_2/k_2)$$

$$L_1 = L_3 \text{ and } k_1 = k_3$$

$$k_2 = k_c k_1 L_2 / \{ k_1 (2L_1 + L_2) - 2k_c L_1 \}$$

solution for k_2 unstable when:

$$k_1 (2L_1 + L_2) = < 2 k_c L_1$$

Table 4.1: Shear-box tests

n	name	date	Materials				Final conditions $s_n [kPa]$, e_{final}	Shear strength m coefficient [$^\circ$]	Remarks
			Sand	FIR	foamer, quantity, ER	Polymer			
1	f50	26 10 1999	fine, 1500g	-	-	-	28.3 , 0.93	26.08	saturated fine sand
2	f51	26 10 1999	fine, 1500g	-	-	-	56.6 , 0.93	28.46	saturated fine sand
3	f52	12 11 1999	fine, 1500g	-	-	-	56.6 , 0.76	32.37	saturated fine sand, dilation
4	f53	27 10 1999	fine, 1500g	-	-	-	113 , 0.92	26.09	saturated fine sand
5	f54	27 10 1999	fine, 1500g	-	-	-	226 , 0.90	27.47	saturated fine sand
6	c60	22 10 1999	coarse, 1000g	-	-	-	28.3 , 0.85	31.87	saturated coarse sand, dilation
7	c61	23 10 1999	coarse, 1000g	-	-	-	56.6 , 0.87	32.62	saturated coarse sand, dilation
8	c62	12 11 1999	coarse, 1000g	-	-	-	56.6 , 0.77	33.23	saturated coarse sand, dilation
9	c63	24 10 1999	coarse, 1000g	-	-	-	113 , 0.82	32.64	saturated coarse sand, dilation
10	c64	25 10 1999	coarse, 1000g	-	-	-	226 , 0.78	31.43	saturated coarse sand
11	f70	29 10 1999	fine, 1500g	30.8%	Versa, 500ml-3%, ER:17	-	28.3 , 1.80	6.76	low friction coef., increase FIR
12	f71	09 11 1999	fine, 1500g	30.8%	Versa, 500ml-3%, ER:15	-	28.3 , 1.43	8.42	low friction coef.
13	f72	23 11 1999	fine, 1500g	30.8%	Versa, 500ml-3%, ER:15	-	40 , 1.16	15.16	
14	f73	29 10 1999	fine, 1500g	30.8%	Versa, 500ml-3%, ER:15	-	56.6 , 1.08	22.95	
15	f74	11 11 1999	fine, 1500g	30.8%	Versa, 500ml-3%, ER:15	-	56.6 , 1.09	20.45	
16	f75	23 11 1999	fine, 1500g	34.8%	Versa, 600ml-3%, ER:16	-	80 , 1.18	11.83	
17	f76	28 10 1999	fine, 1500g	30.8%	Versa, 500ml-3%, ER:15	-	113 , 1.14	22.44	
18	f77	29 11 1999	fine, 1500g	41.2%	Versa, 750ml-3%, ER:15	-	160 , 1.40	7.65	unexpected low friction coef.
19	f78	30 10 1999	fine, 1500g	30.8%	Versa, 500ml-3%, ER:18	-	226 , 0.96	20.74	large compression before shearing
20	c80	30 10 1999	coarse, 1000g	39.8%	Versa, 500ml-3%, ER:17	wop 40ml (141)	28.3 , 1.53	6.72	low friction coef.
21	c81	17 11 1999	coarse, 1000g	28.4%	Versa, 300ml-3%, ER:15	wop 40ml (141)	28.3 , 0.90	31.78	
22	c82	22 11 1999	coarse, 1000g	28.4%	Versa, 300ml-3%, ER:15	wop 40ml (141)	40 , 0.96	17.00	
23	c83	01 11 1999	coarse, 1000g	28.4%	Versa, 300ml-3%, ER:15	wop 40ml (141)	56.6 , 1.06	27.23	
24	c84	05 11 1999	coarse, 1000g	39.8%	Versa, 500ml-3%, ER:16	wop 40ml (141)	56.6 , 1.26	7.28	low friction coef
25	c85	22 11 1999	coarse, 1000g	28.4%	Versa, 300ml-3%, ER:15	wop 40ml (141)	80 , 0.94	7.05	low friction coef, dilation.
26	c86	02 11 1999	coarse, 1000g	28.4%	Versa, 300ml-3%, ER:15	wop 40ml (141)	113 , 0.98	26.88	
27	c87	30 11 1999	coarse, 1000g	28.4%	Versa, 300ml-3%, ER:15	wop 40ml (141)	160 , 0.74	25.41	large compression before shearing
28	c88	01 11 1999	coarse, 1000g	28.4%	Versa, 300ml-3%, ER:15	wop 40ml (141)	226 , 0.90	25.37	

Table 4.2: SHEAR-BOX TEST f74 (Example)						
Oxford University - Engineering Science Department - Civil Engineering Laboratory				(11/11/1999)		1 of 2
Mixture proportions						

1. Sand mixture							
Materials	Proportion						Comments:
	mass [g]	Spec. grav.	volume [ml]	1.00	mass [g]	volume [ml]	
Air	0.0	0.001	0.0	0.95	0.0	0.0	fine silica sand
Water	500.0	1.00	500.0		500.0	500.0	
Sand	1500.0	2.65	566.0		1500.0	566.0	
sum	2000.0		1066.0		2000.0	1066.0	

2. Foam							
Materials	Proportion						Comments:
	mass [g]	Spec. grav.	volume [ml]	0.95	mass [g]	volume [ml]	
Air	0.47	0.001	466.67	0.95	0.44	443.33	Versa foam, 3% per weight
Liquid	33.33	1.00	33.33		31.67	31.67	
ER	15.00		15.00		14.25	14.25	
sum	33.80		500.00		32.11	475.00	

3. Polymer mixture							
Materials	Proportion						Comments:
	mass [g]	Spec. grav.	volume [ml]	0.5	mass [g]	volume [ml]	
PHPA	0.00	1.15	0.00	0.5	0.00	0.00	n/a
OIL	0.00	0.90	0.00		0.00	0.00	
WATER	0.00	1.00	0.00		0.00	0.00	
Mix	0.00		0.00		0.00	0.00	

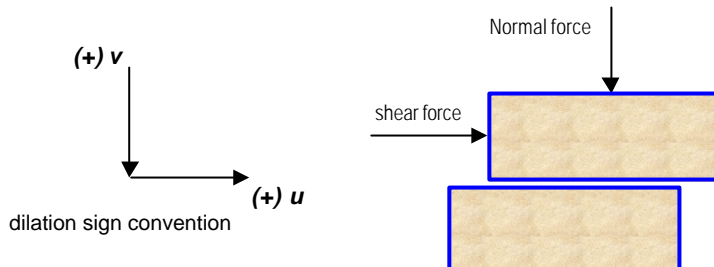
Mixture							
Materials	Proportion			By mass		By volume	
	mass [g]	Spec. grav.	volume [ml]	Volatile	"Volatile"	"Non-volatile"	"Volatile"
Air	0.44	0.001	443.33	1.00	0.44	0.00	443.33
Water	531.67	1.000	531.67	1.00	531.67	0.00	531.67
Sand	1500.00	2.650	566.04	0.00	0.00	1500.00	0.00
oil	0.00	0.900	0.00	0.02	0.00	0.00	0.00
PHPA	0.00	1.150	0.00	0.03	0.00	0.00	0.00
Total	2032.11	2.650	1541.04		532.11	1500.00	975.00
symbol	M	Gs	V		Mw	Ms	Vv
							Vs

$wo = Mw/Ms$	0.355	water content
$So = Vw/Vv$	54.5%	degree of saturation
$eo = Vv/Vs$	1.723	mixture voids ratio
$FIR = Vf/V$	30.8%	Foam Injection Ratio
$p = MV$	1.32	bulk density

= Measured quantities

Table 4.2: SHEAR-BOX TEST f74 (Example)		
Oxford University - Engineering Science Department - Civil Engineering Laboratory		(11/11/1999) 2 of 2
Shear-box test results		

calculations (at critical state)	symbol	value
shear stress = shear force / sample area	t	13.563 kPa
normalized shear strength = shear stress/normal stress	t/s	0.240 -
dilation angle psi = atan(dv/du)	γ	7.59 °
coefficient m = shear strength + dilation	m	0.373 -
friction angle = tan(shear strength)	f	13.48 °
NORMAL STRESS	s	56.6 kPa



Sample measurements & calculations				Shear-box parameters		
parameters	initial	consolidation	final	dead load :	5.83	kg
length mm	60.00	60.00	60.00	calibration factor :	3.21	N/division
breadth mm	60.00	60.00	60.00	stress factor :	0.89	kN/m ² /div
height mm	34.60	30.05	28.51	rate of displacement :	0.3	mm/min
area A mm ²	3600.00	3600.00	3600.00	horizontal strain rate :	0.5	%
volume V mm ³	124560	108180	102636	Normal force coefficient :	0.367	kg/kPa
mass bulk g	3252.5	n/a	3237.0	Normal stress [kPa]		
mass net M g	179.50	n/a	164.00	Required load [kg]		
bulk density Ma/m ³	1.44	n/a	1.60	Added load [kg]		
sub-sample wet g	29.41	n/a	15.01	40.0	14.68	8.8
sub-sample dry g	23.57	n/a	13.03	56.6	20.77	14.9
water content w	0.32	n/a	0.26	80.0	29.36	23.5
dry density Ma/m ³	1.09	n/a	1.27	113.1	41.50	35.7
voids ratio e	1.43	n/a	1.09	160.0	58.72	52.9
specific gravity Gs	2.65	2.65	2.65	226.2	83.01	77.2
saturation degree S	0.596	n/a	0.633			
initial compression dH mm			4.55			
height of solids Hs mm	14.23	14.23				
voids ratio change de			0.32			
Volumes				= Measured quantities		
solids Vs ml			51.233	= Measured quantities		
water Vw ml			35.371	= Measured quantities		
gas Vg ml			16.032	= Measured quantities		
total V ml		108.180	102.636	= Measured quantities		
Voids ratios				= Measured quantities		
water ew			0.69	= Measured quantities		
gas eg			0.40	= Measured quantities		
total e		1.11	1.09	= Measured quantities		
matrix e_m			0.49	= Measured quantities		

sand tests	e	m [°]	y	I_D	f [°]	s
<i>f50</i>	0.90	26.08	2.30	0.03	24.5	0.97
<i>f51</i>	0.88	28.46	1.46	0.10	27.33	0.99
<i>f52</i>	0.76	32.37	-2.38	0.50	33.9	0.96
<i>f53</i>	0.88	26.09	1.03	0.10	25.26	1.00
<i>f54</i>	0.87	27.47	2.07	0.13	25.82	1.00
<i>c60</i>	0.80	31.87	-2.40	-0.03	31.2	0.96
<i>c61</i>	0.81	32.62	-0.94	-0.07	33.28	0.98
<i>c62</i>	0.78	33.23	-0.87	0.03	33.83	1.00
<i>c63</i>	0.76	32.64	-0.26	0.10	32.82	0.99
<i>c64</i>	0.75	31.43	0.17	0.13	31.31	0.98

foamed tests	e	m [°]	y	I_D	f [°]	s
<i>f70</i>	1.80	6.76	1.20	-2.92	5.57	0.37
<i>f71</i>	1.31	8.42	0.40	-1.33	8.03	0.43
<i>f72</i>	1.16	15.16	0.81	-0.83	14.36	0.62
<i>f73</i>	1.08	22.95	6.12	-0.57	17.55	0.61
<i>f74</i>	1.09	20.45	7.59	-0.60	13.5	0.63
<i>f75</i>	1.16	11.83	0.36	-0.83	11.42	0.57
<i>f76</i>	1.14	22.44	4.00	-0.77	18.93	0.54
<i>f77</i>	1.35	7.65	0.24	-1.47	7.42	0.45
<i>f78</i>	0.96	20.74	4.26	-0.17	16.91	0.77
<i>c80</i>	1.56	6.72	0.52	-2.57	6.21	0.21
<i>c81</i>	0.90	31.78	0.92	-0.37	31.2	0.44
<i>c82</i>	0.99	17.00	1.44	-0.67	15.67	0.46
<i>c83</i>	1.07	27.23	4.03	-0.93	23.94	0.39
<i>c84</i>	1.28	7.28	0.46	-1.63	6.46	0.26
<i>c85</i>	0.94	7.05	-0.71	-0.50	7.75	0.47
<i>c86</i>	1.00	26.88	3.60	-0.70	24.49	0.43
<i>c87</i>	0.84	25.41	1.71	-0.17	23.89	0.65
<i>c88</i>	0.90	25.37	4.10	-0.37	22.43	0.45

Bolton's values (1986)	I_D	0.8y	f_{crit}	f_{max}
A	0.159	1.47	32.6	34.1
A	0.253	2.84	32.6	35.4
D	0.281	2.92	36.9	39.8
H	0.295	2.58	35.0	37.6
A	0.494	5.76	32.6	38.4
D	0.629	9.22	36.9	46.1
H	0.678	9.59	35.0	44.6
A	0.699	10.88	32.6	43.5
G	0.864	11.85	35.0	46.9
A	0.856	12.21	32.6	44.8
D	0.936	14.50	36.9	51.4

FIGURES & PHOTOS

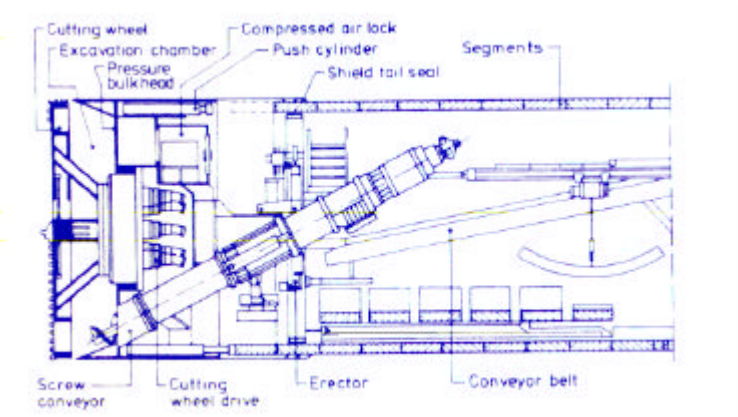


Figure 1.1: Typical EPB machine (Maidl *et al*, 1996).

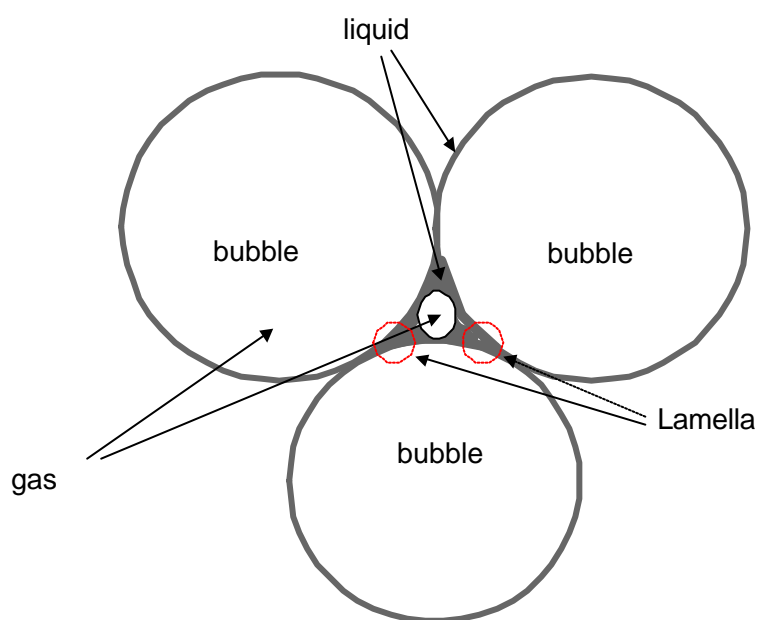


Figure 1.2: Lamella and the liquid-gas interface.

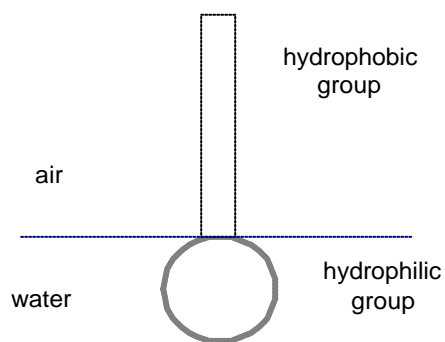


Figure 1.3: Surfactant molecule.

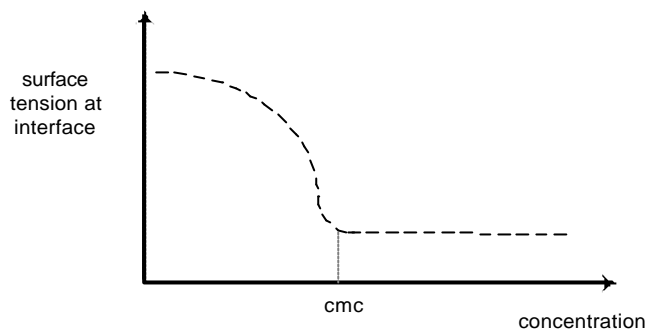


Figure 1.4: Critical micelle concentration.

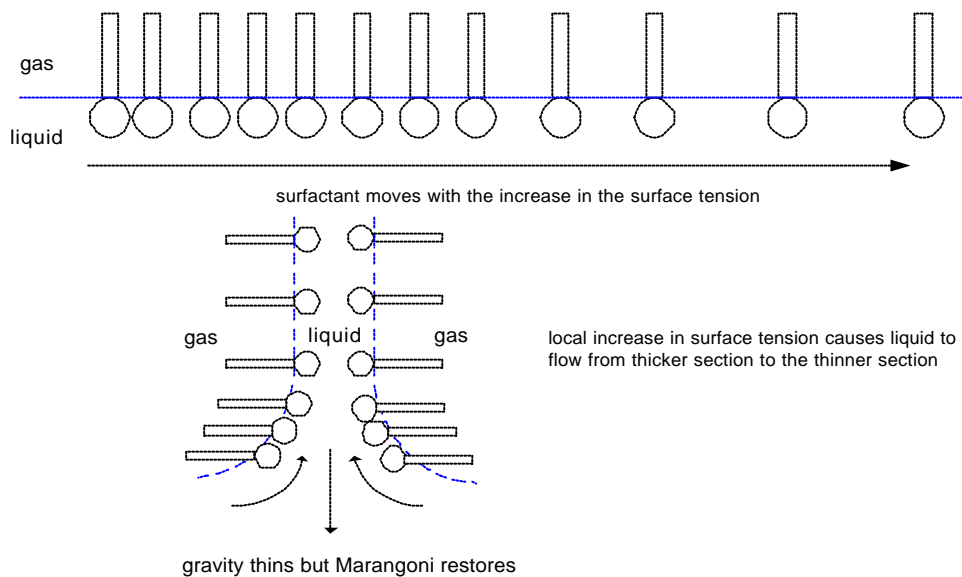


Figure 1.5: Gibbs -Marangoni effect.

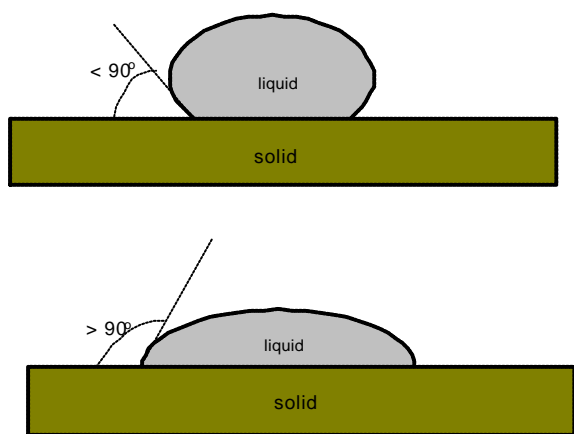


Figure1.6: Contact angle of a fluid on a solid surface.



Figure 2.1 Soil mixer

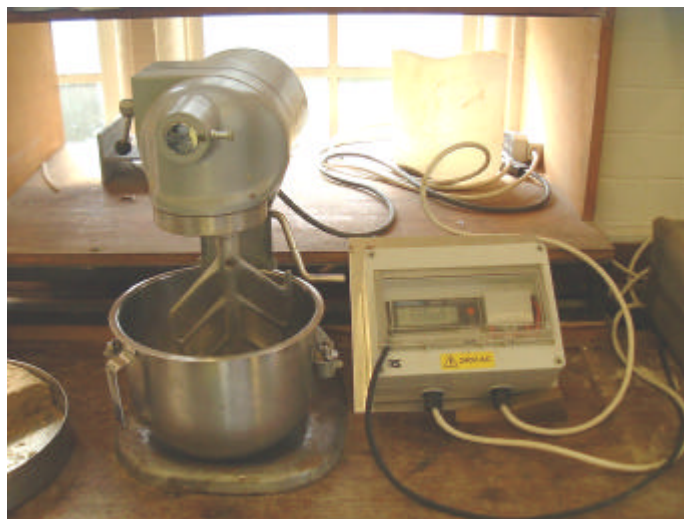


Photo 2.1 Soil mixer and the power measurement set-up.

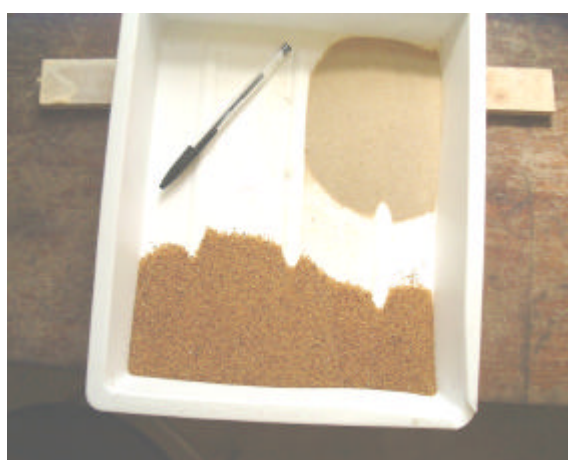


Photo 2.5 Fine and coarse sand.

Figure 2.2: The Oxford University Foam - Generator.

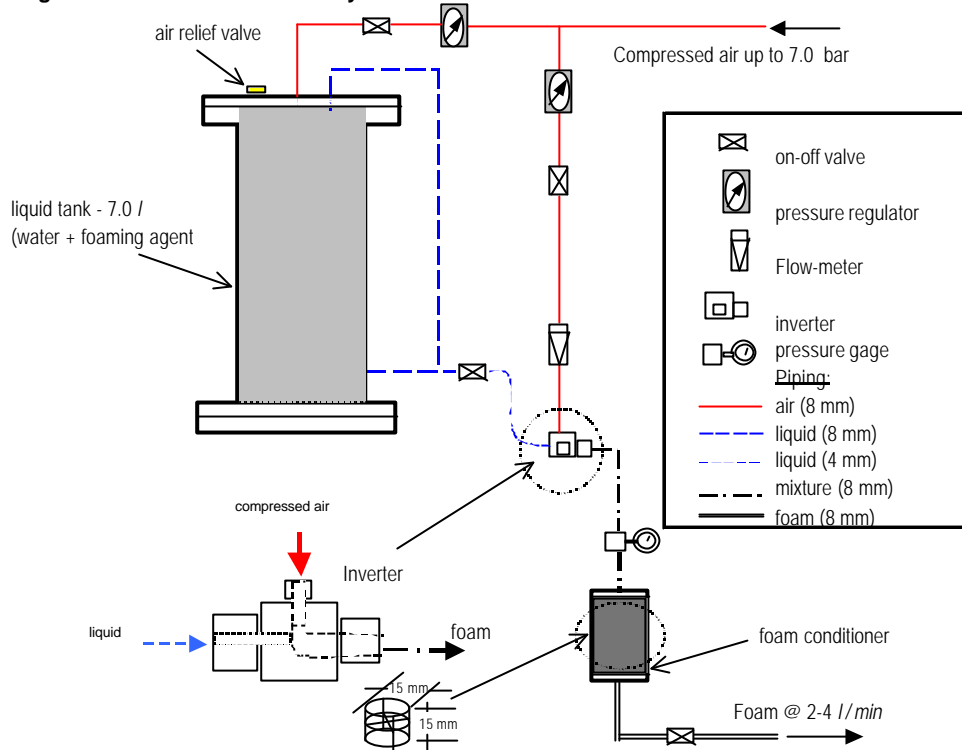


Photo 2.3 The perforated tubes

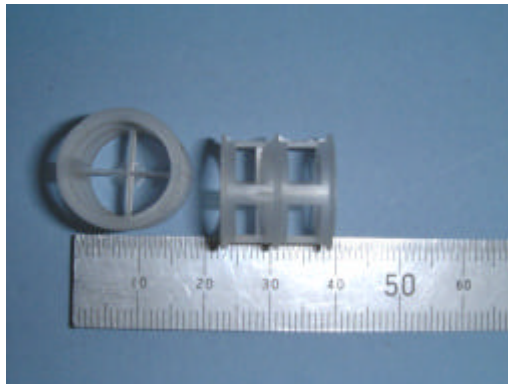


Photo 2.2 The Foam-Generator.



Photo 2.4 The 'Ventouri' Inverter

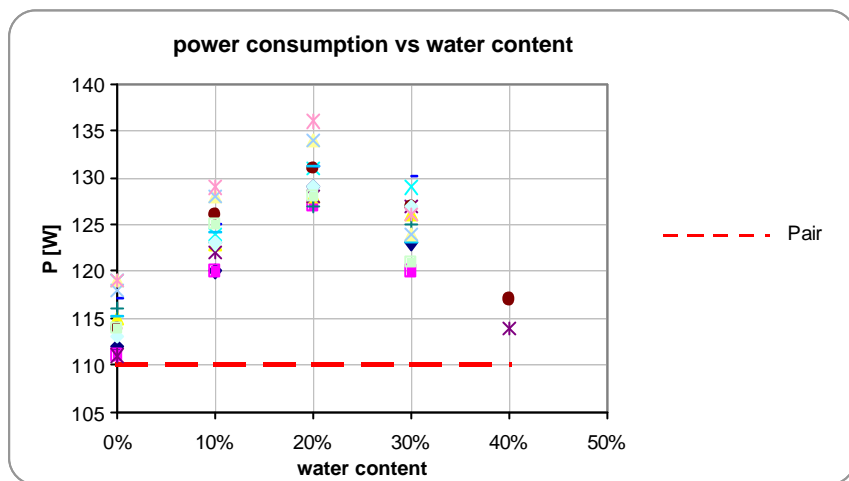


Figure 2.3: Power consumption for different water content for fine sand tests

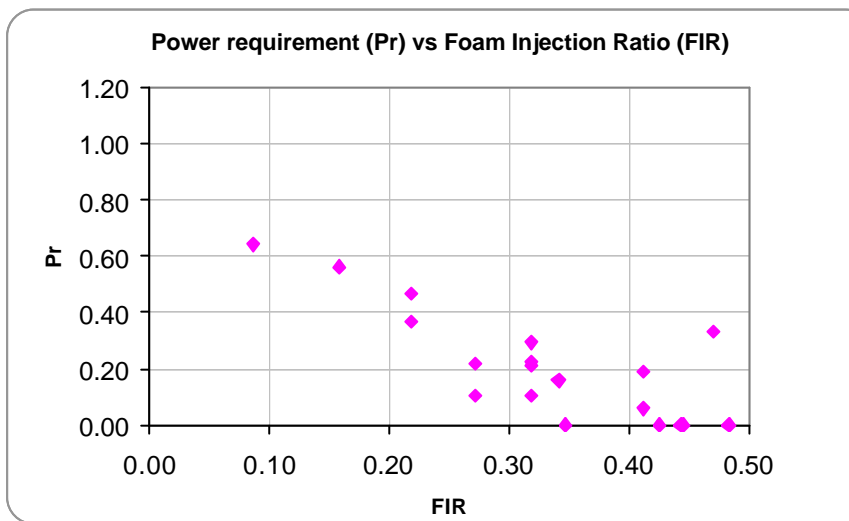


Figure 2.4: Relative power reduction due to foam for foamed fine sand tests

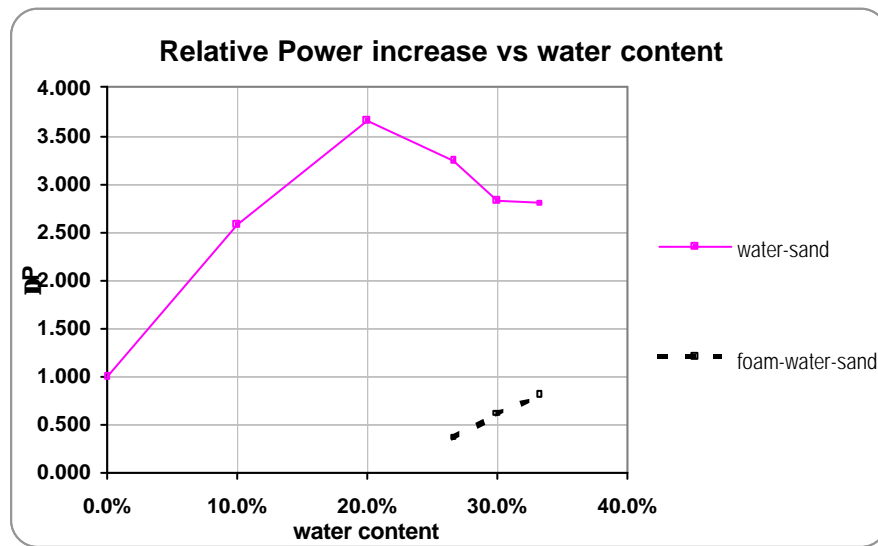


Figure 2.5: Relative power increase with respect to Pair for different water content

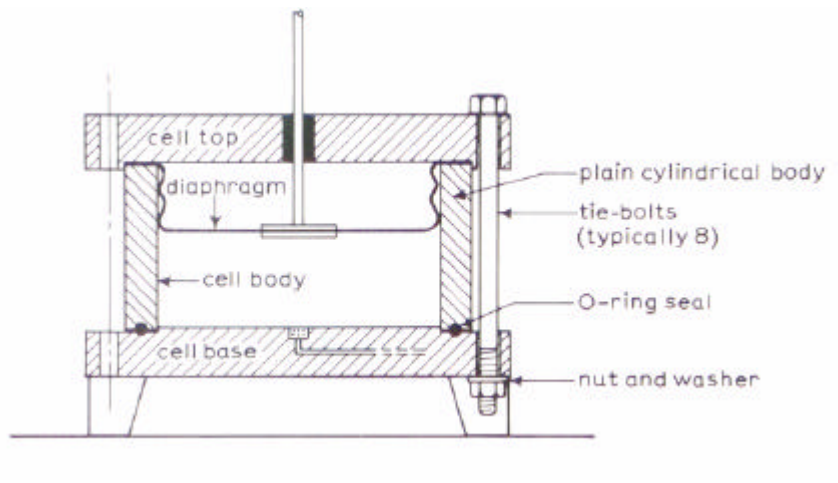


Figure 3.1: Rowe cell 75 mm (Head, 1986).

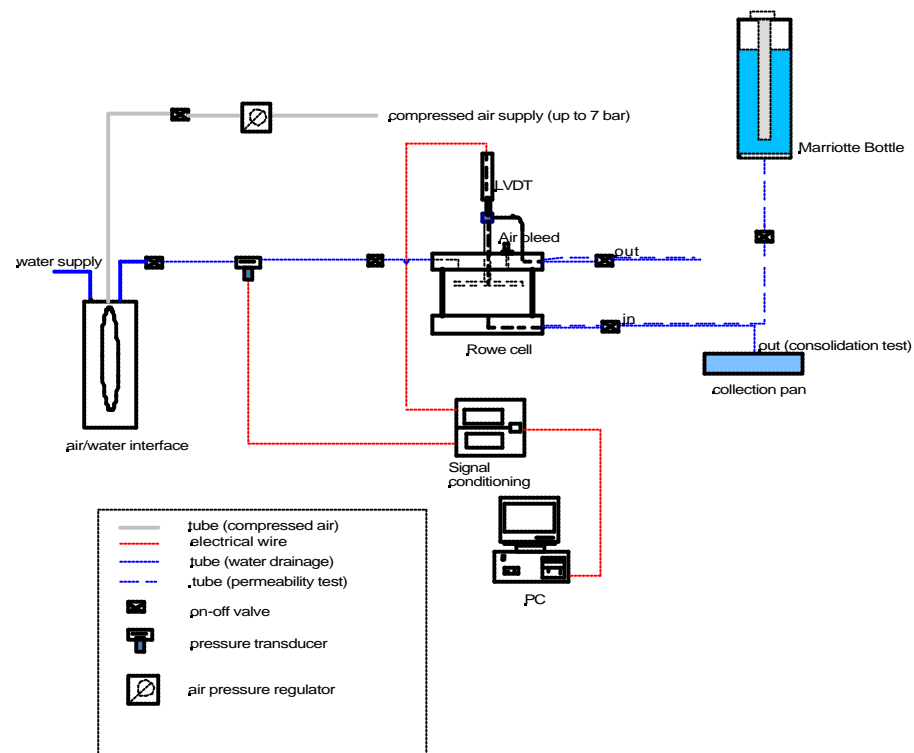


Figure 3.2: Experimental set for compressibility permeability tests.



Photo 3.1: Experimental set up for compressibility/permeability.

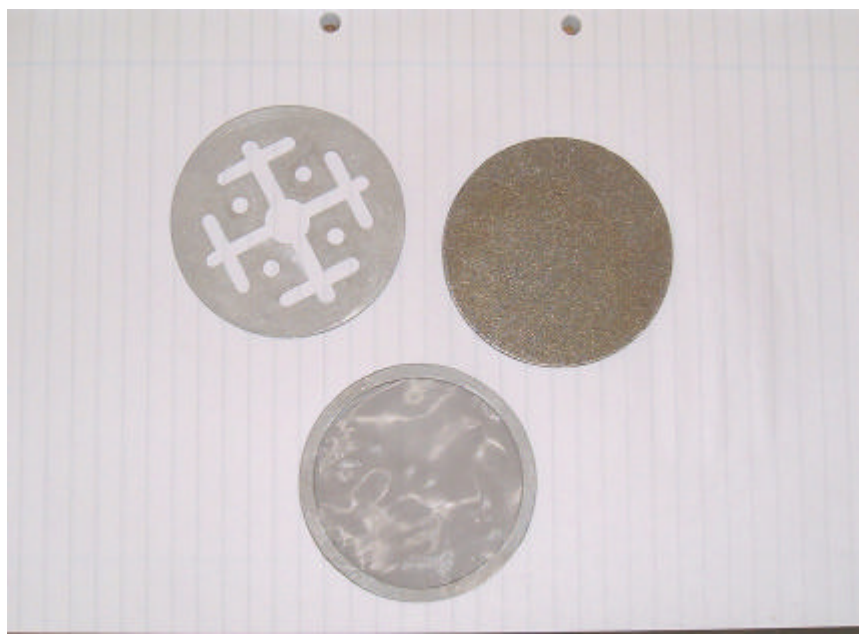


Photo 3.2: Permeability mesh (bottom), the plate (top left) and the cintered disc (top right).

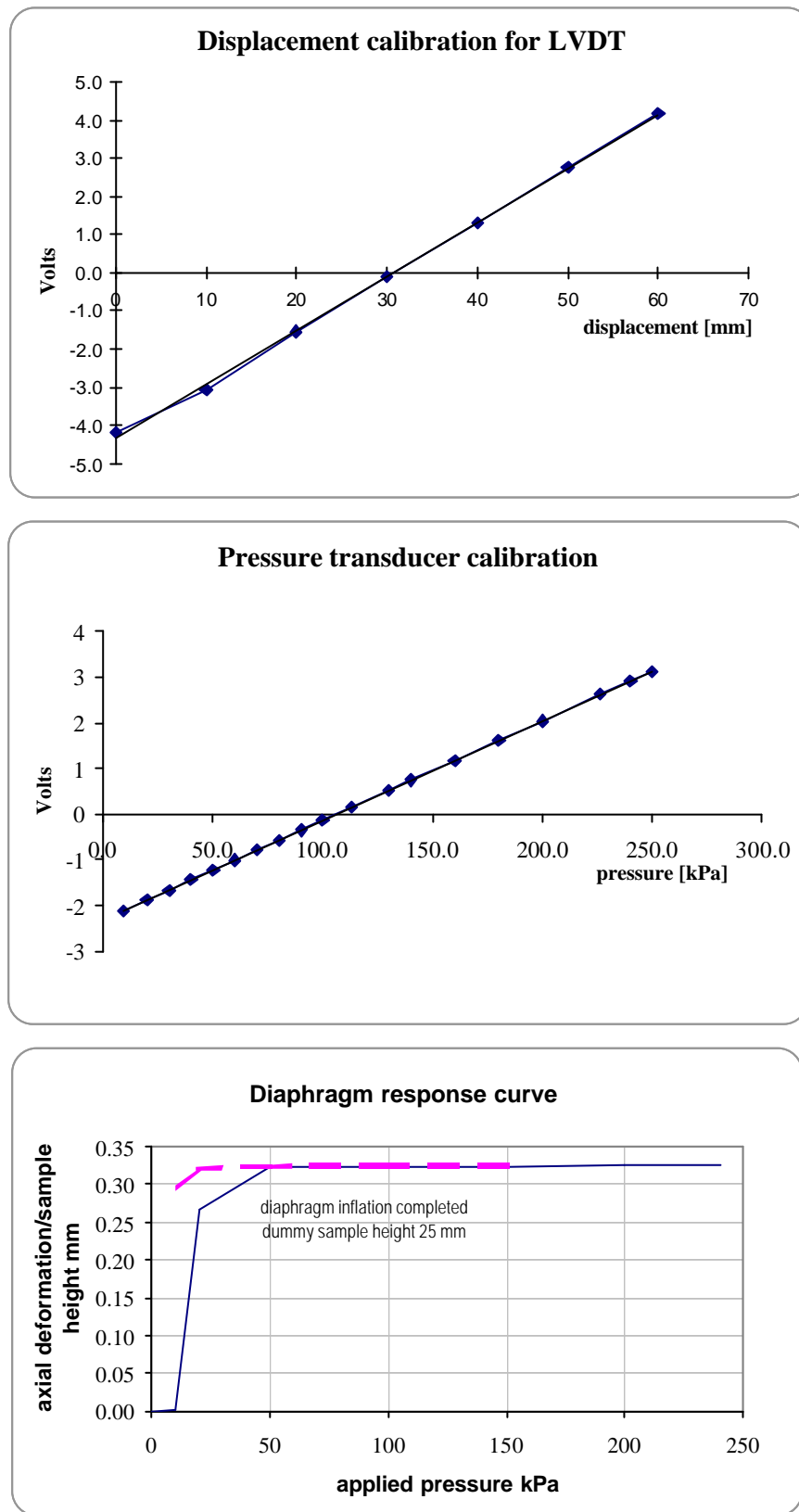
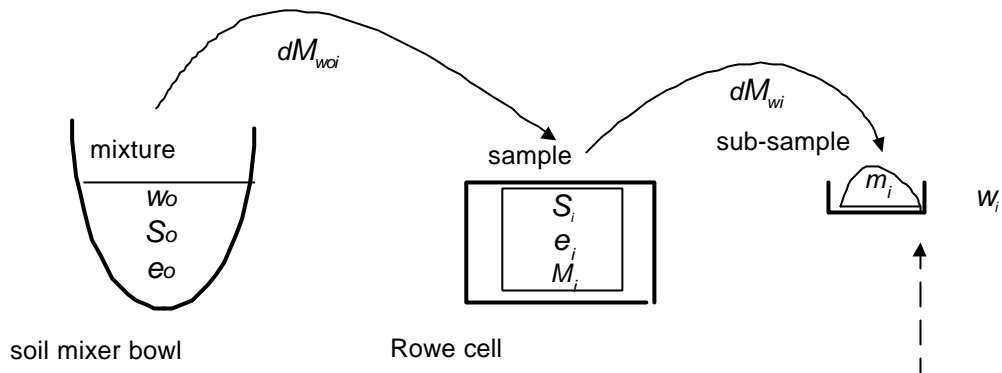
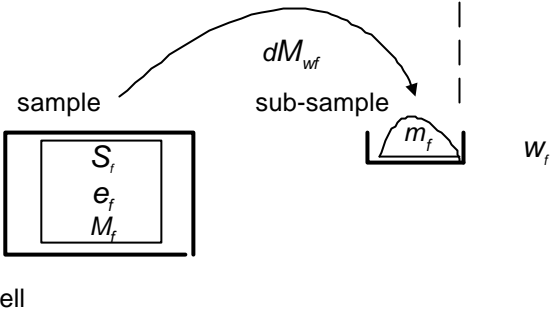


Figure 3.3: Calibration curves

1. Initial conditions



2. Final conditions



dM_{wk} : possible routes of losses or gains expressed in water mass(g)(

S : degree of saturation

w : water content

e : initial or final voids ratio

o : mixture conditions

i : initial conditions

f : final conditions

	<u>Measured</u>	<u>Calculated</u>
Mixture	mass M_o	w_o, S_o, e_o
sub-sample	mass m_i, m_f	w_p, W_p, W_{if} (from quality control)
Sample	compression DH , masses M_i, M_f	S_i, S_f, e_i, e_f

Figure 3.4: Compression test procedure and quality control

Figure 3.5a: Consolidation test f22 (foamed fine sand)

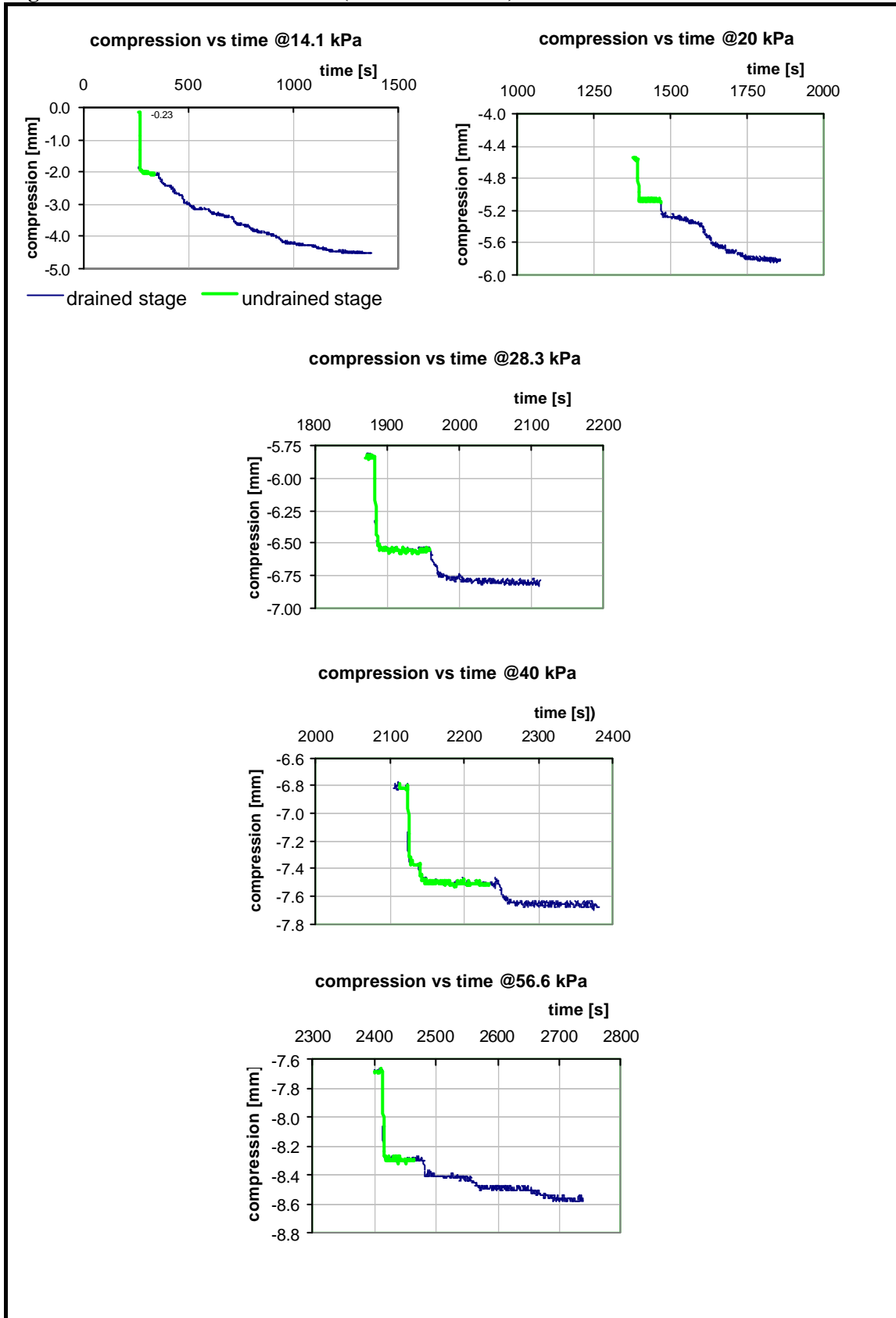


Figure 3.5b: Consolidation test f22 (foamed fine sand)

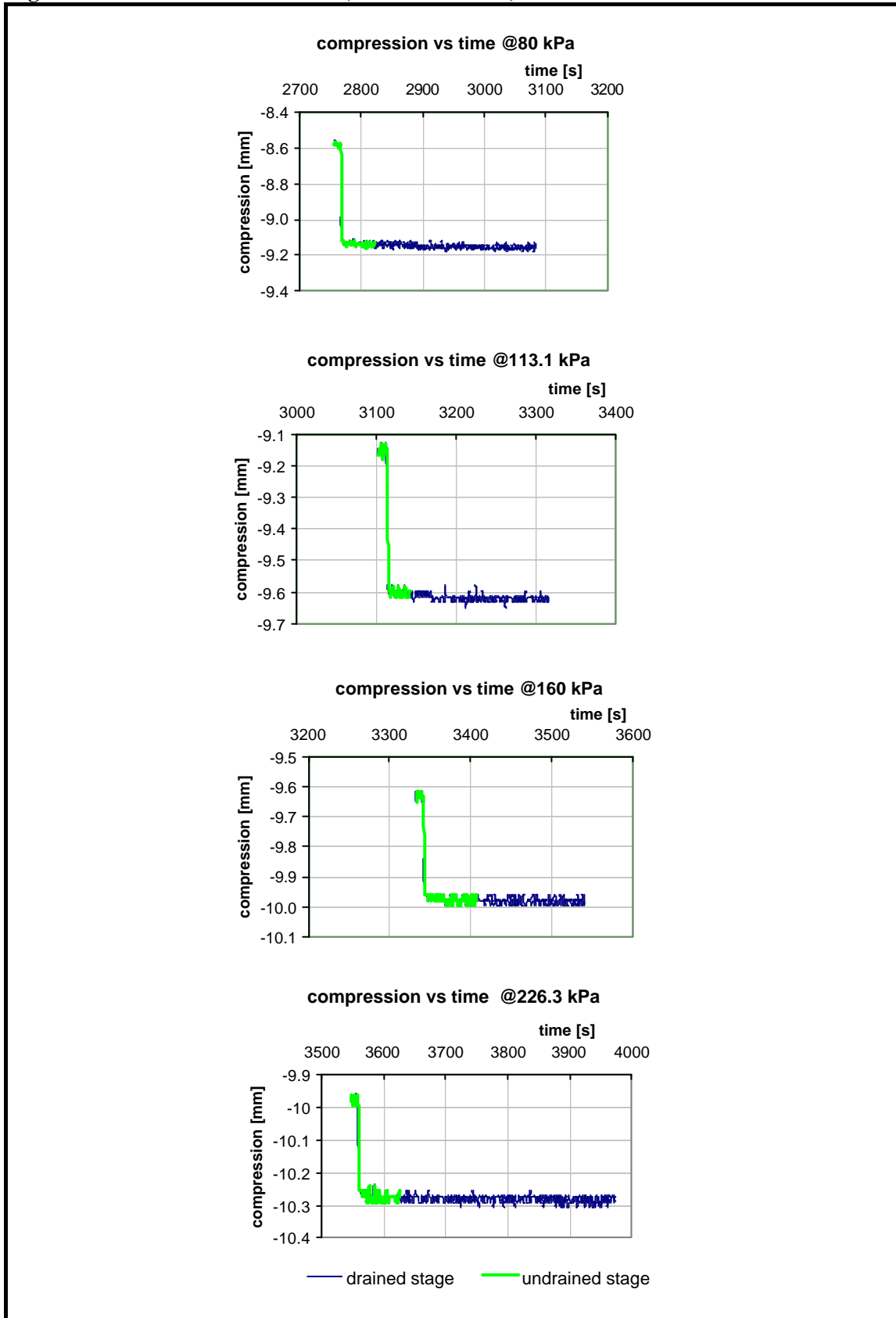


Figure 3.6a: Consolidation test f39 (fine sand with bentonite and polymer)

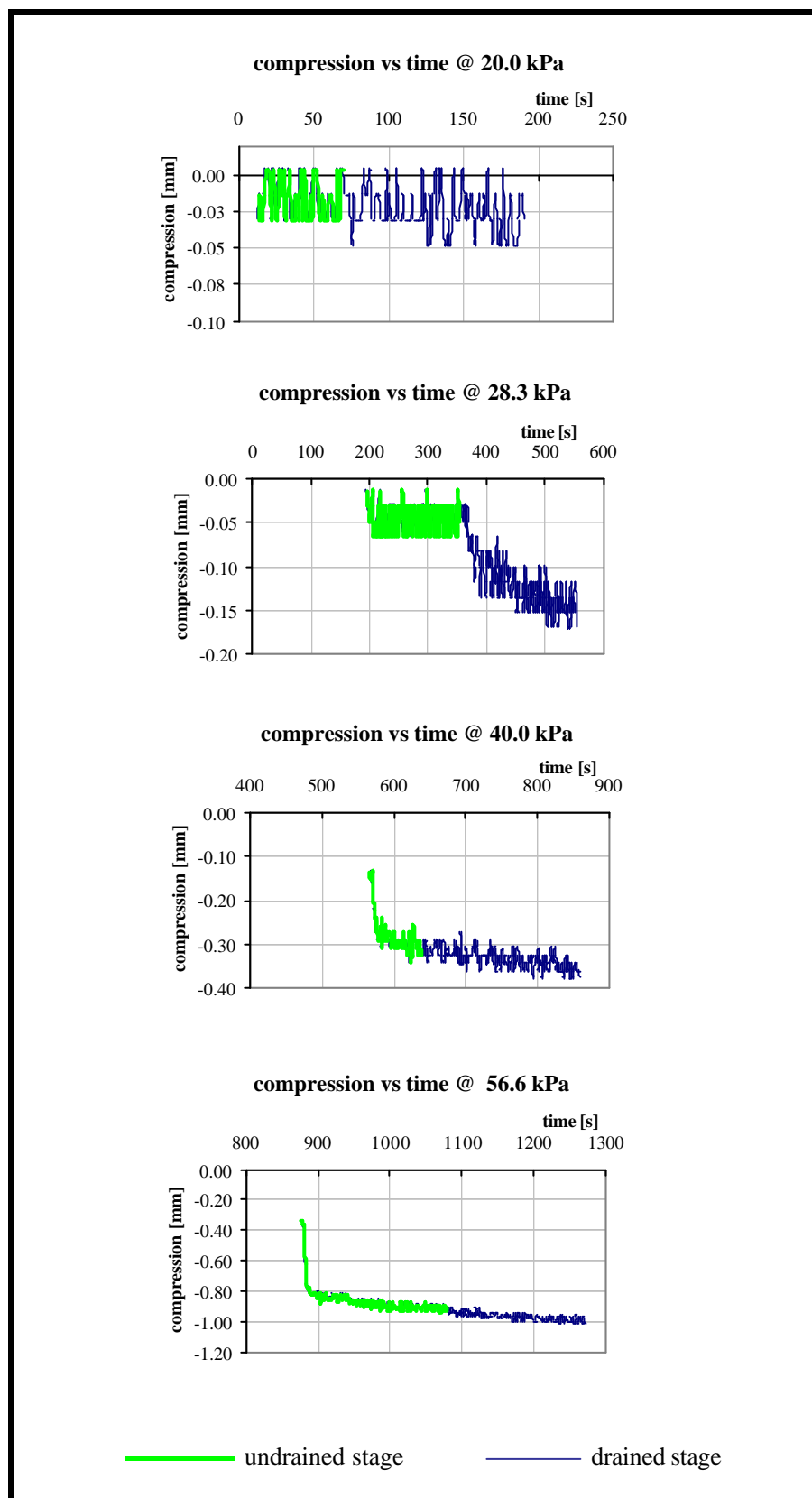


Figure 3.6b: Consolidation test f39 (fine sand with bentonite and polymer)

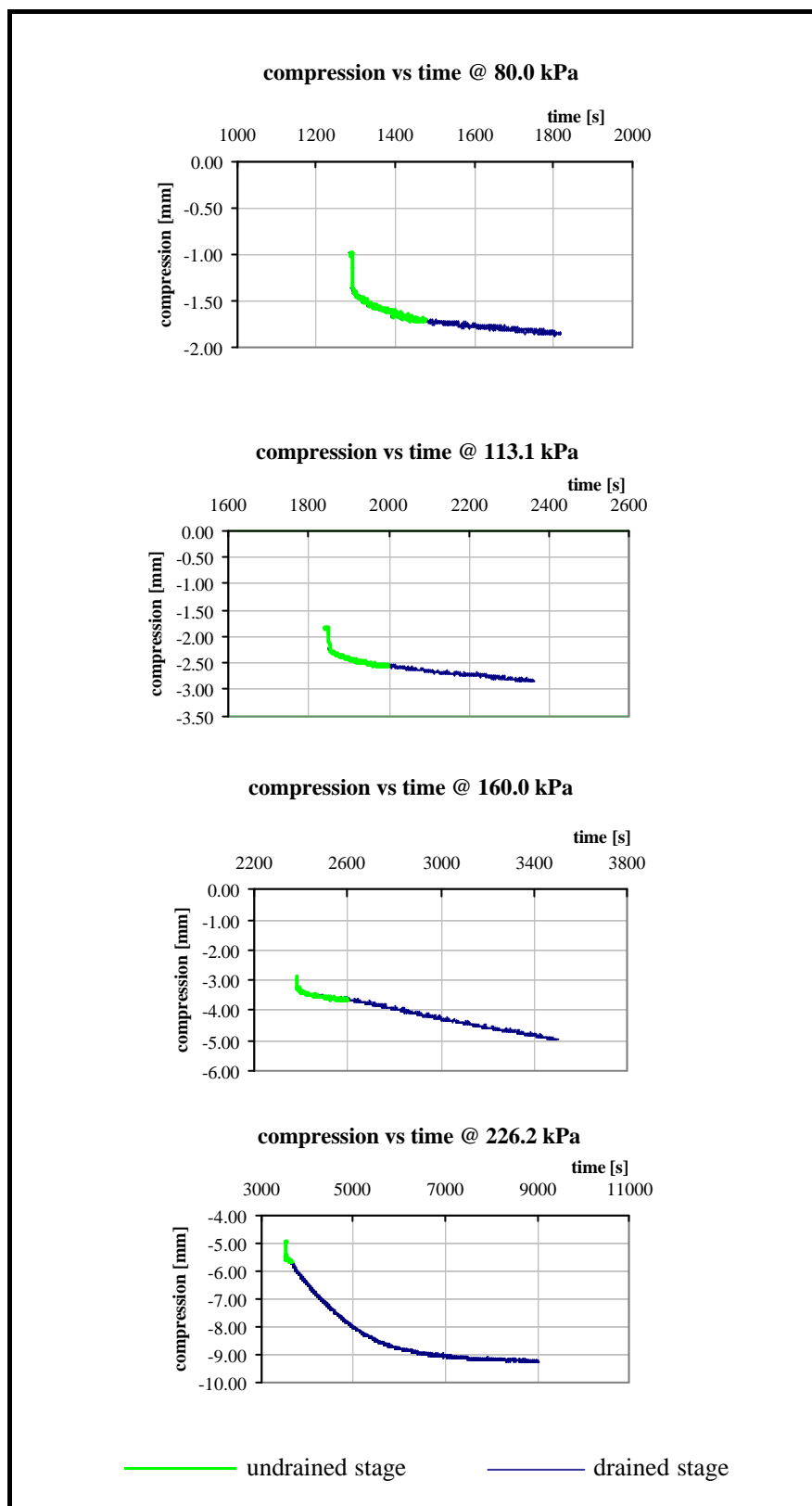


Figure 3.7a: Consolidation test f40 (foamed fine sand with bentonite and polymer)

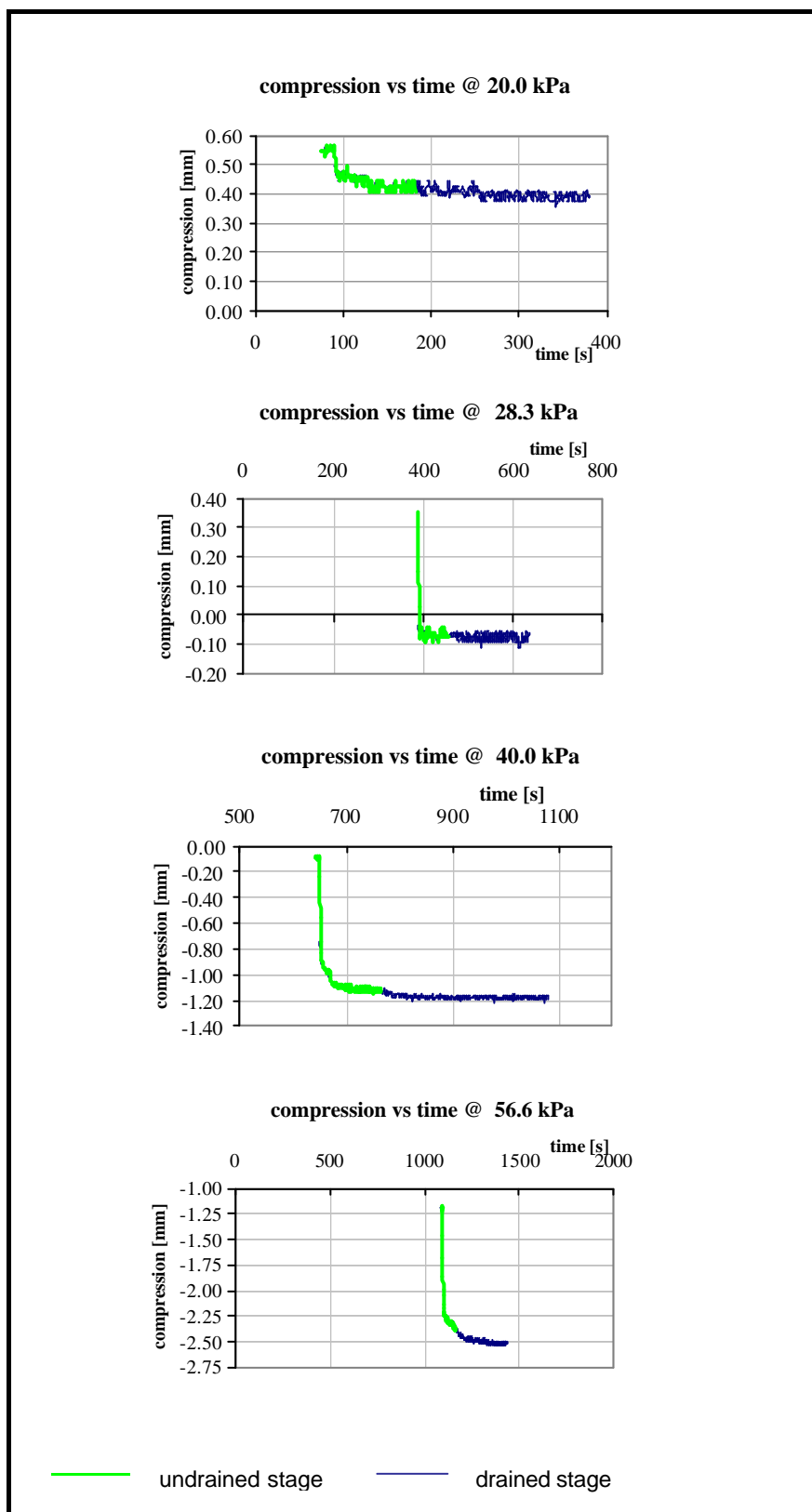


Figure 3.7b: Consolidation test f40 (foamed fine sand with bentonite and polymer)

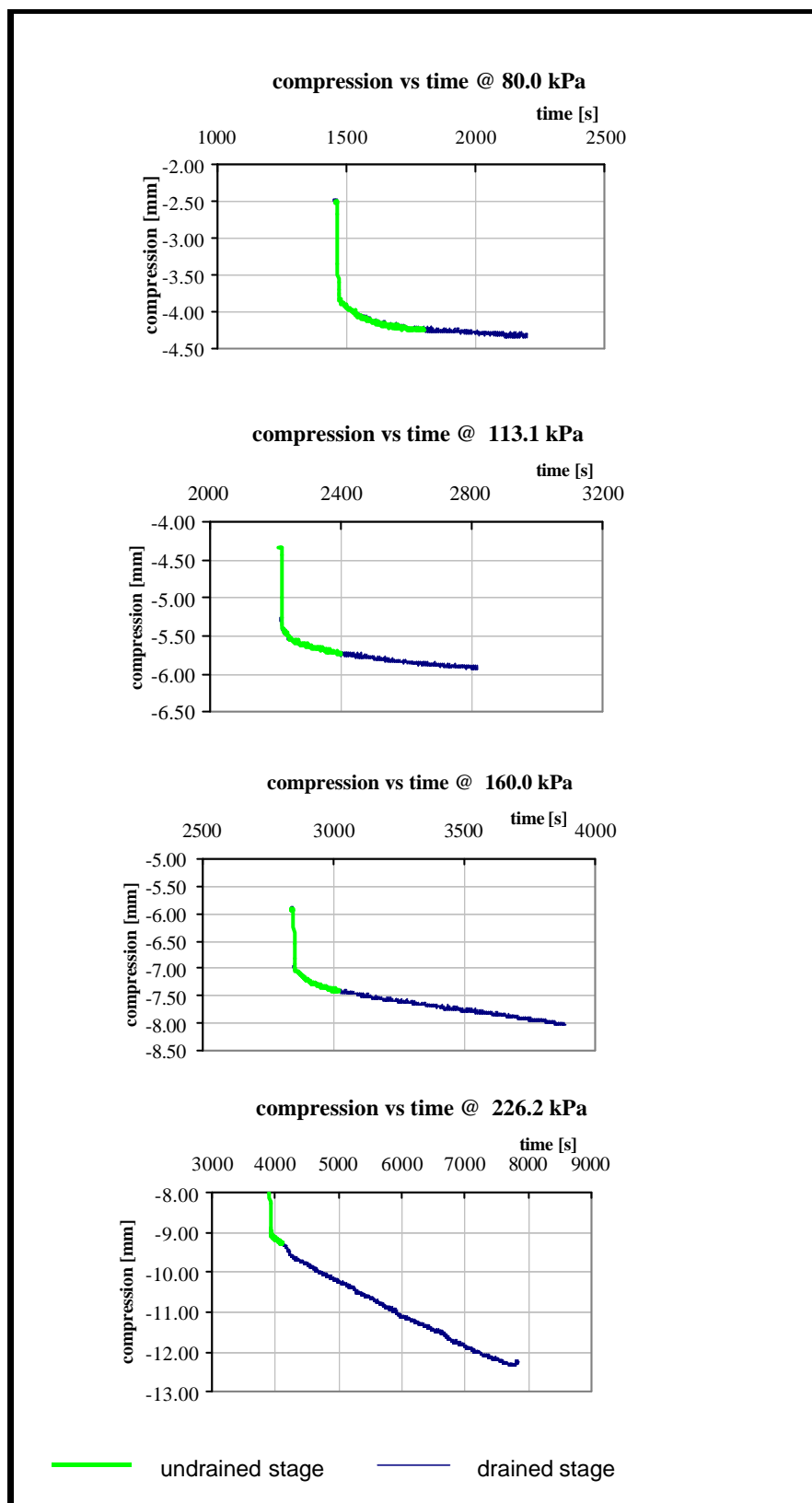


Figure 3.8a: Compression test f46 (foamed fine sand with polymer)

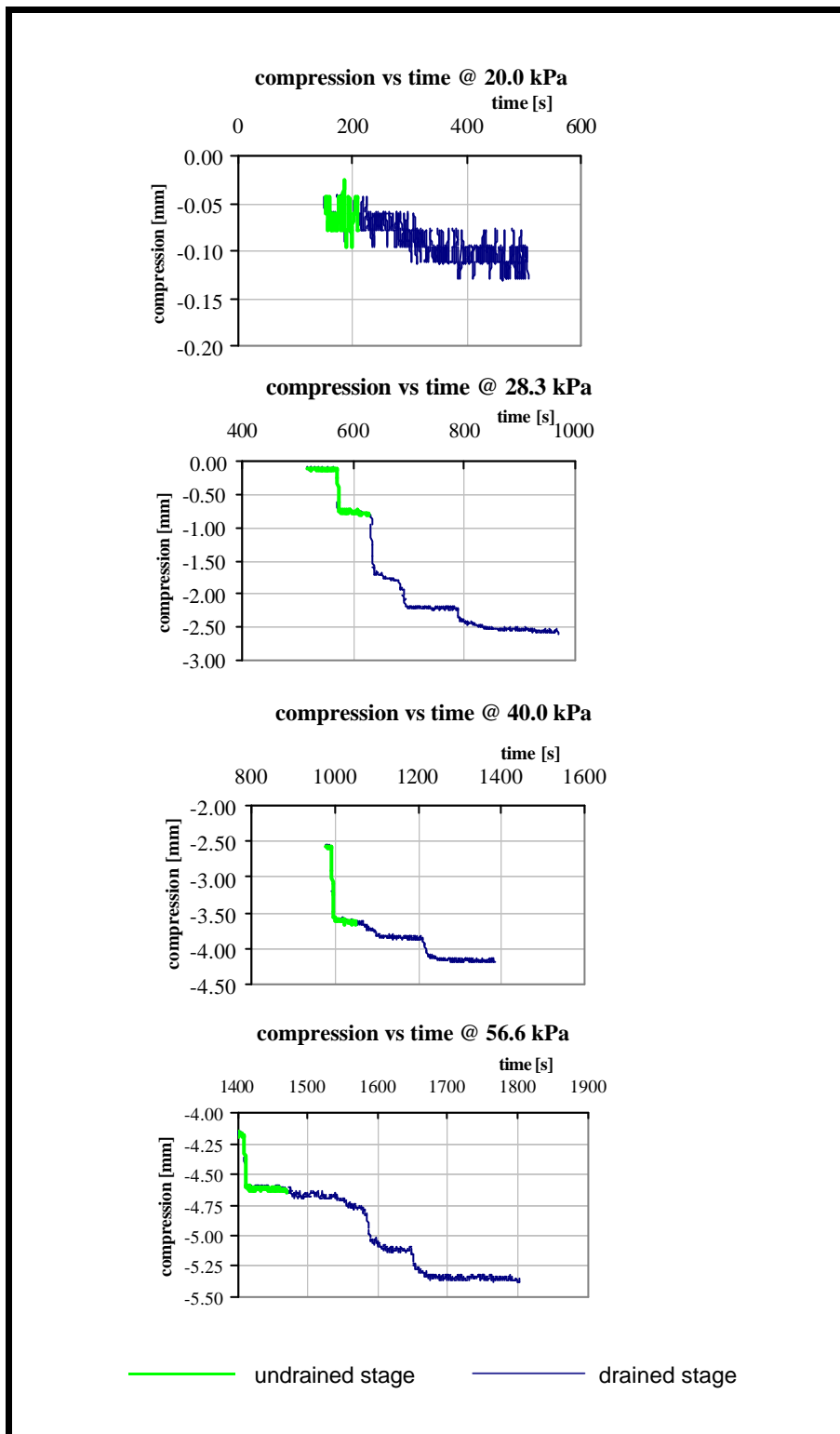
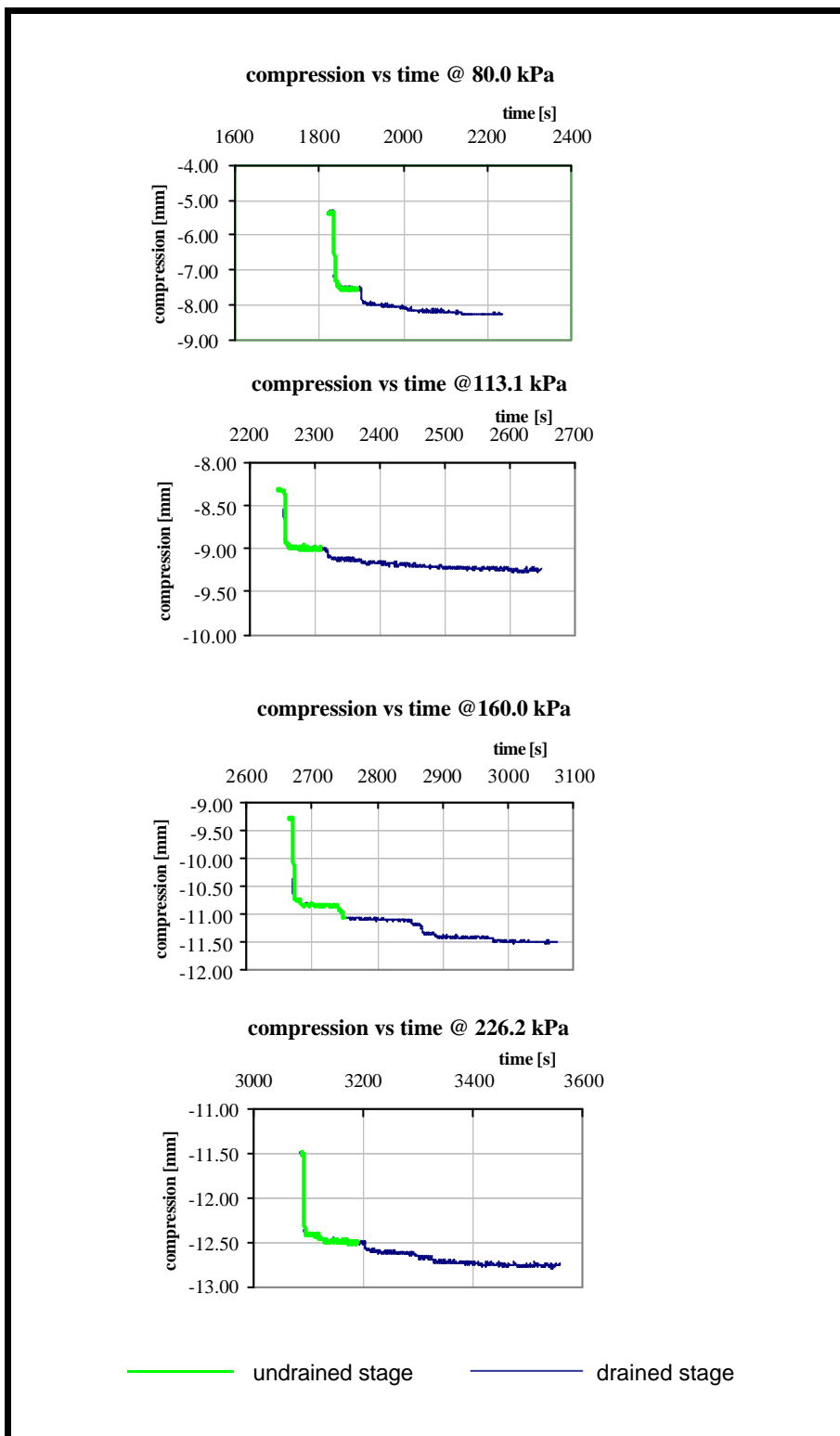
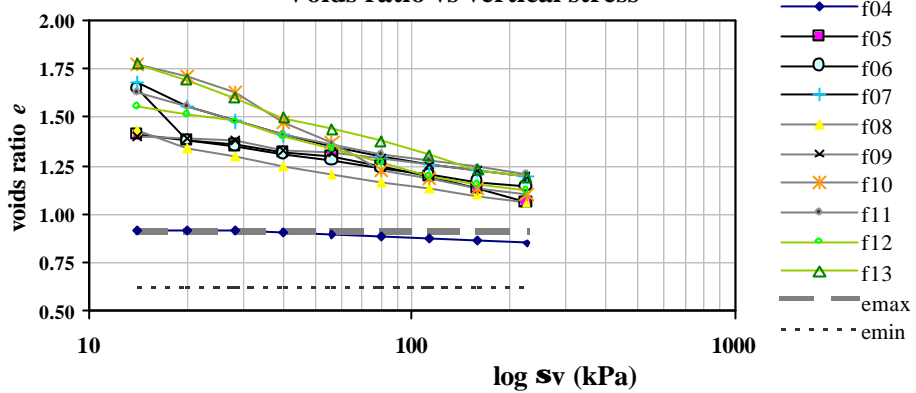


Figure 3.8b: Compression test f46 (foamed fine sand with polymer)



**Figure 3.9: Foamed fine sand (Series I) -
Voids ratio vs vertical stress**



**Figure 3.10: Foamed fine sand (Series II) -
Voids ratio variation with vertical stress (low FIR)**

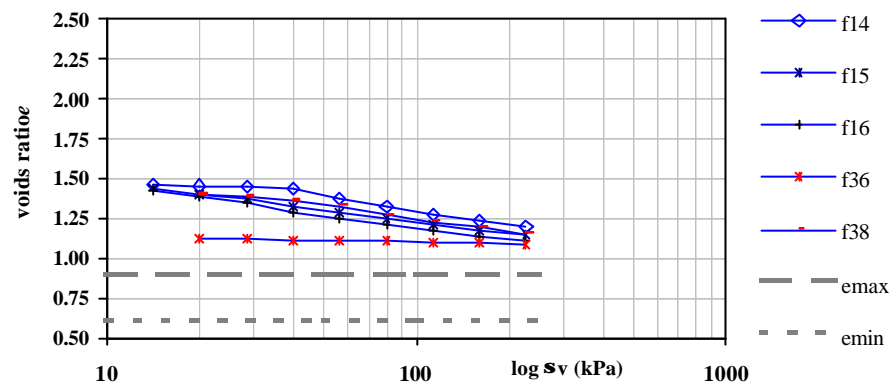


**Figure 3.11: Foamed fine sand (Series II) -
Voids ratio variation with vertical stress (high FIR)**

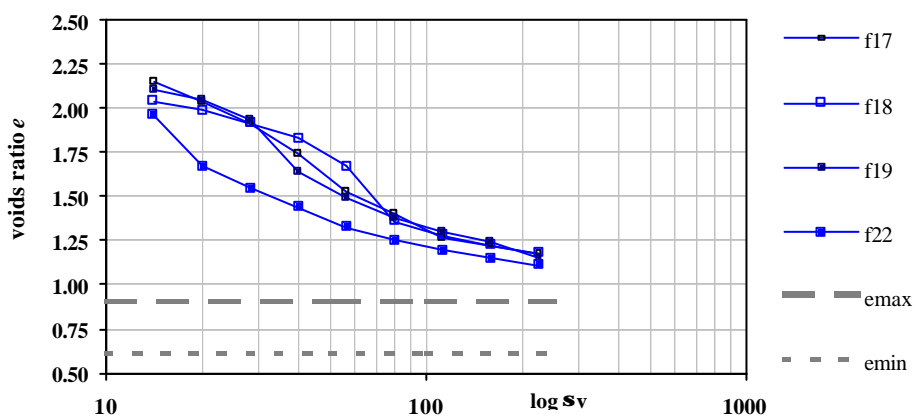


Figure 3.12: Foamed fine sand (Series II) - FIR effect on volume change variation with vertical stress

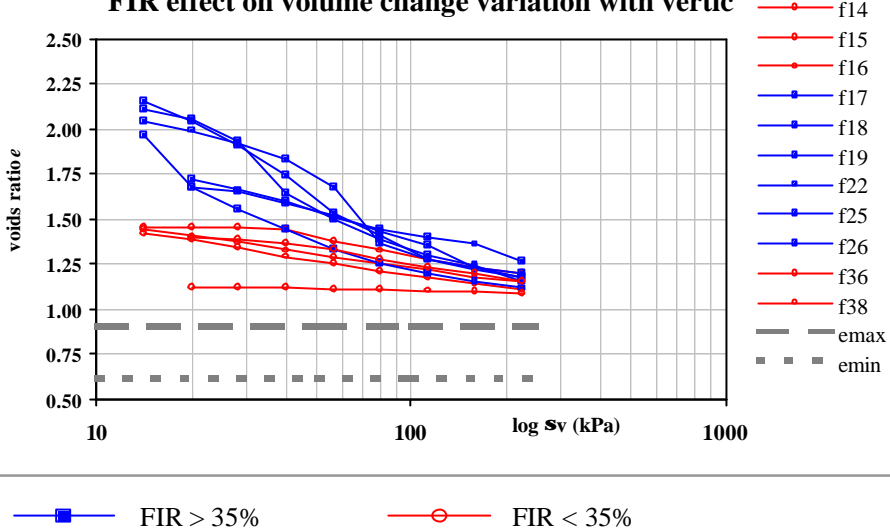


Figure 3.13: Foamed fine sand (average values) - Voids ratio vs vertical stress

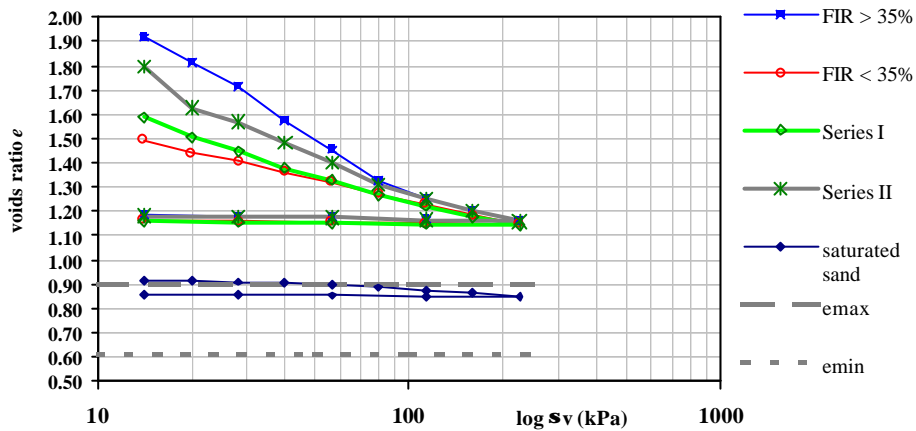
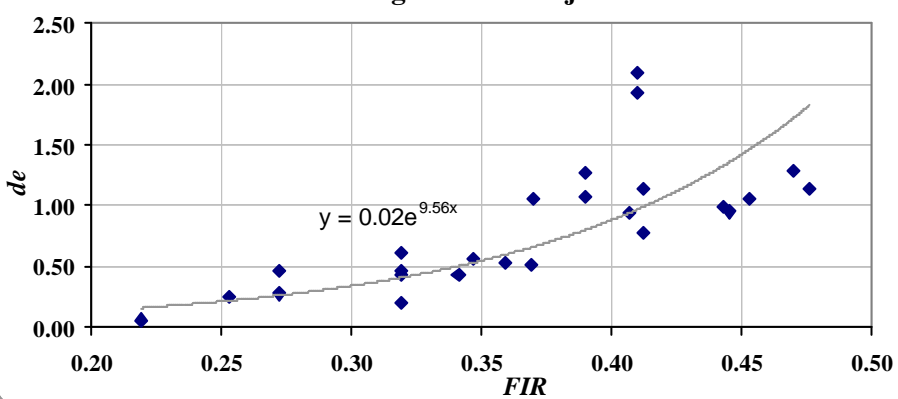
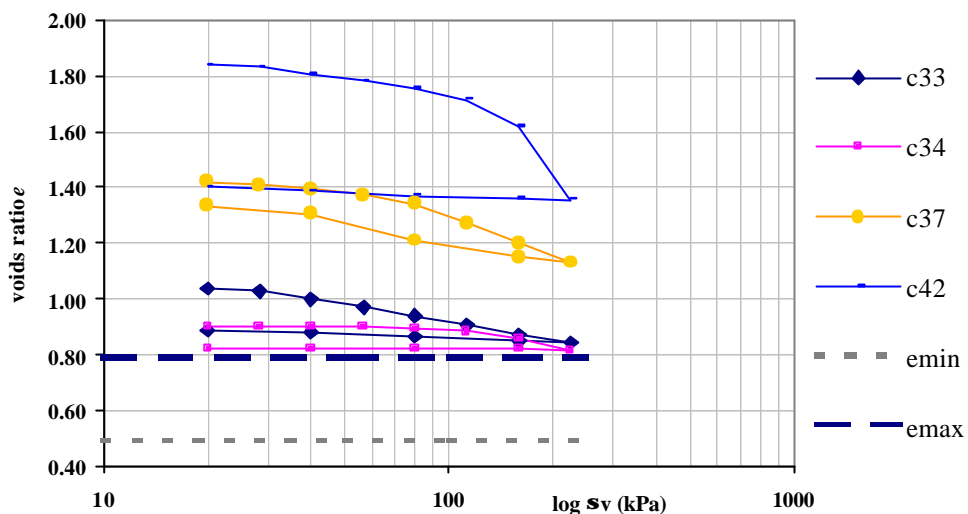


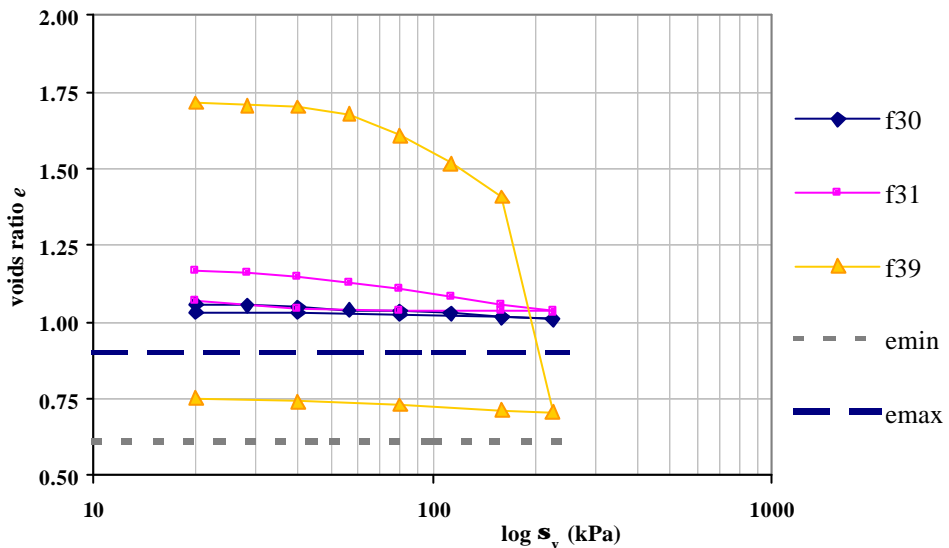
Figure 3.14: Fine foamed sand - Volume change vs Foam Injection Ratio



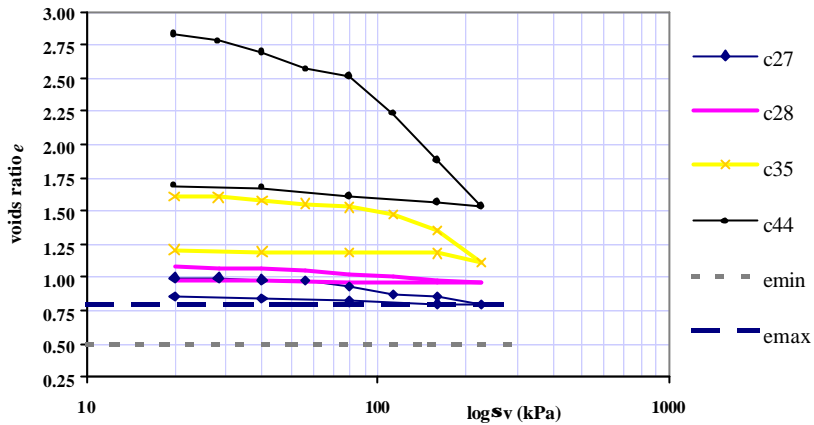
**Figure 3.15: Non-foam coarse sand -
Voids ratio vs vertical stress**



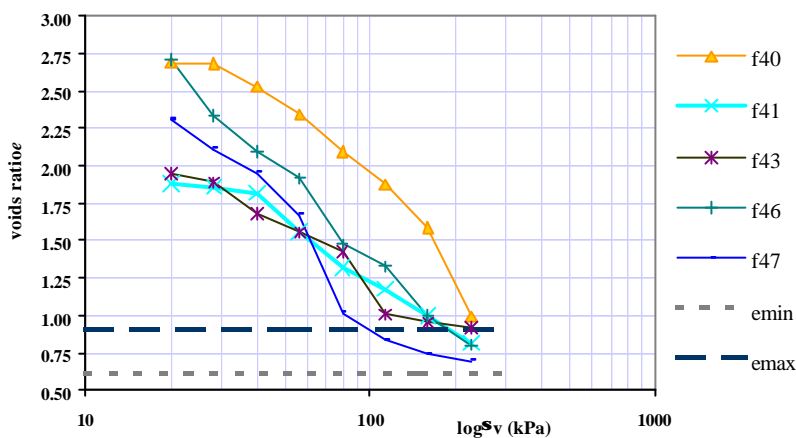
**Figure 3.16: Non-foam fine sand -
Voids ratio vs vertical stress**



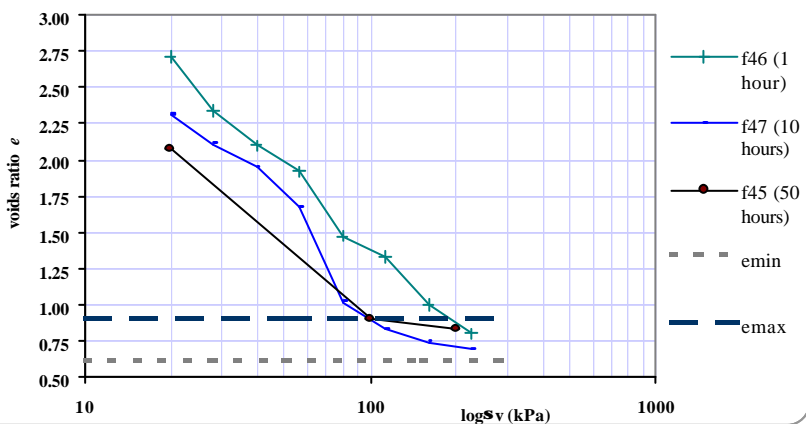
**Figure 3.17: Foamed coarse sand (with polymer) -
Voids ratio vs vertical stress**



**Figure 3.18: Foamed fine sand (with polymer) -
voids ratio vs vertical stress**



**Figure 3.19: Foamed fine sand (with polymer) -
Time effects on volume change behaviour**



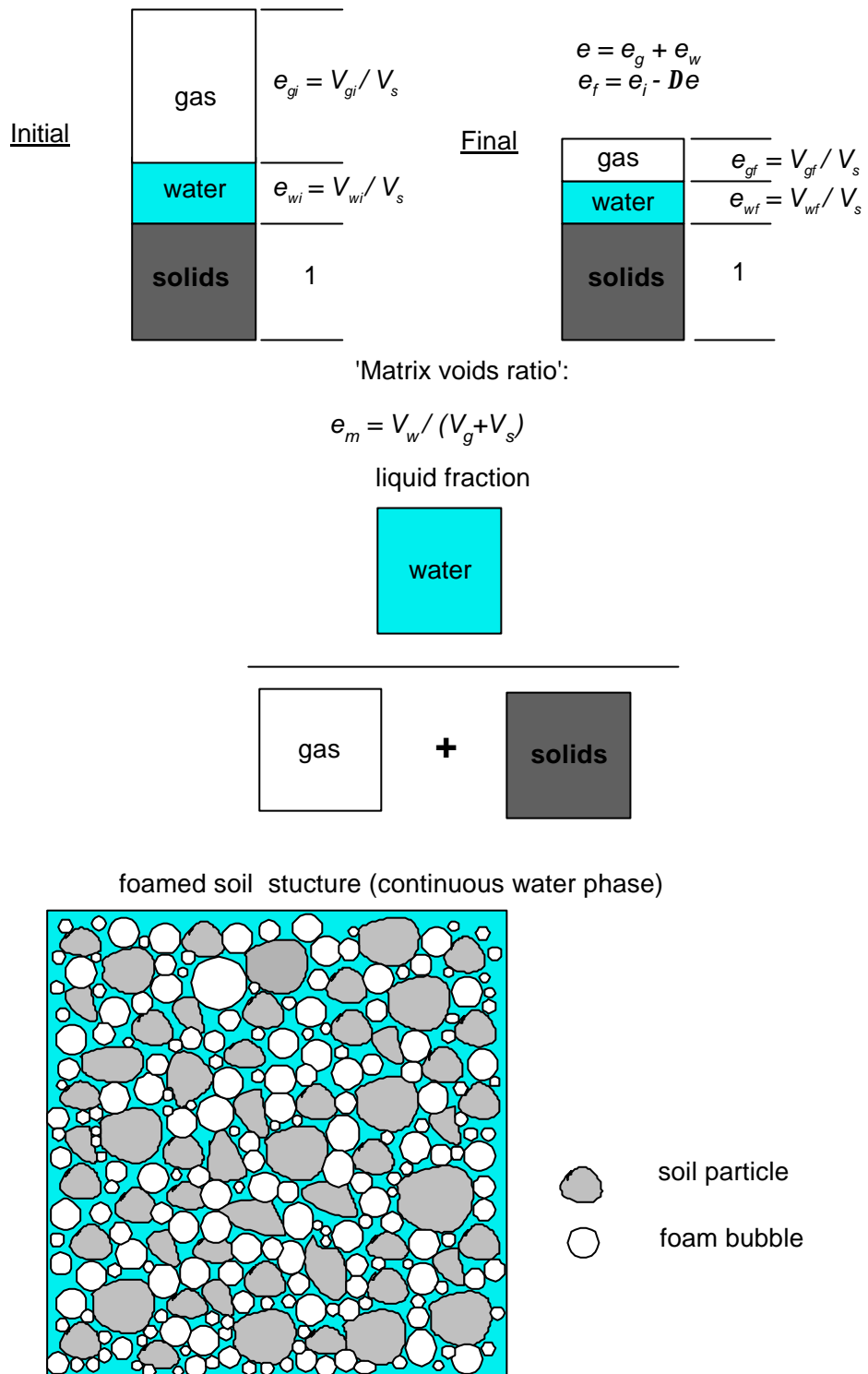
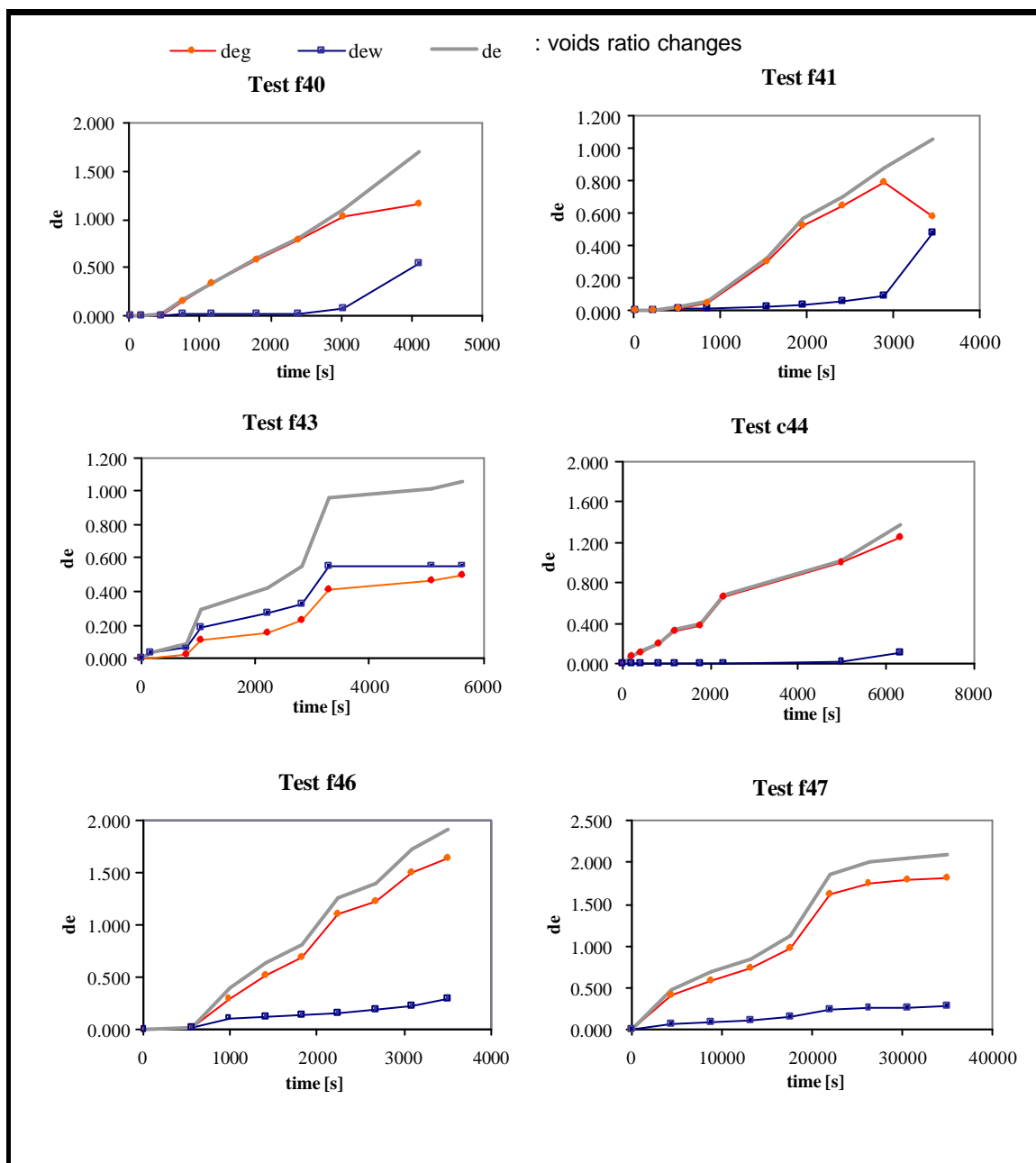
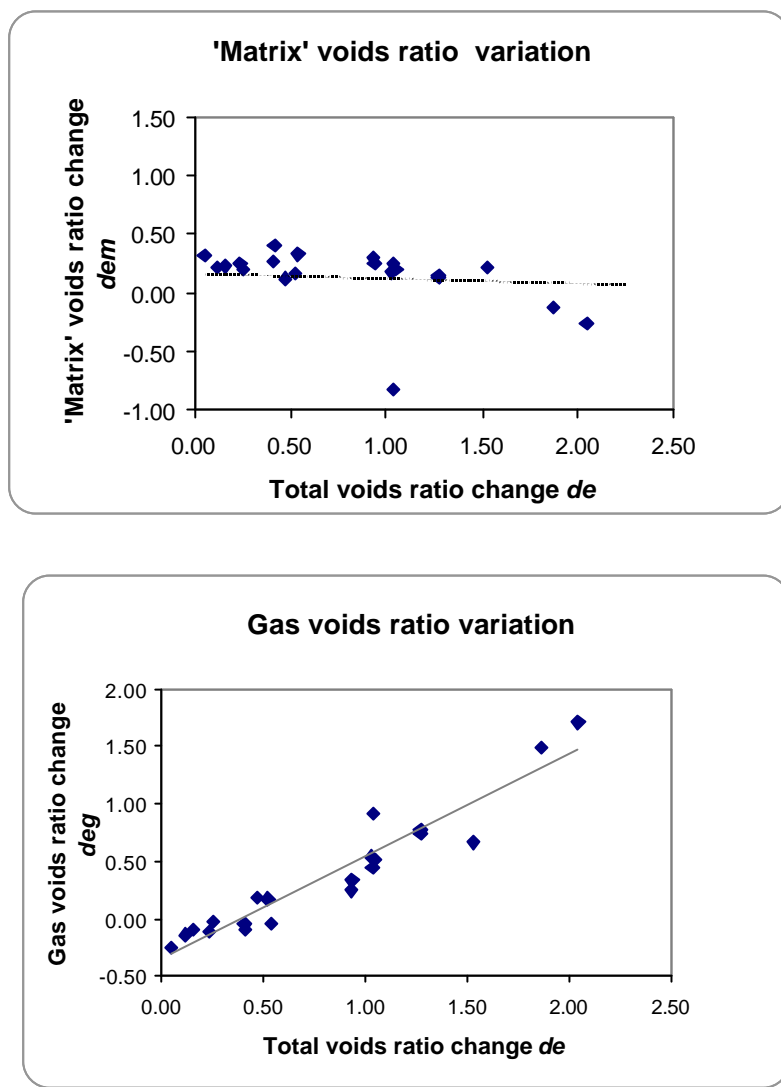


Figure 3.20: Matrix voids ratios and illustration of foamed soil structure.

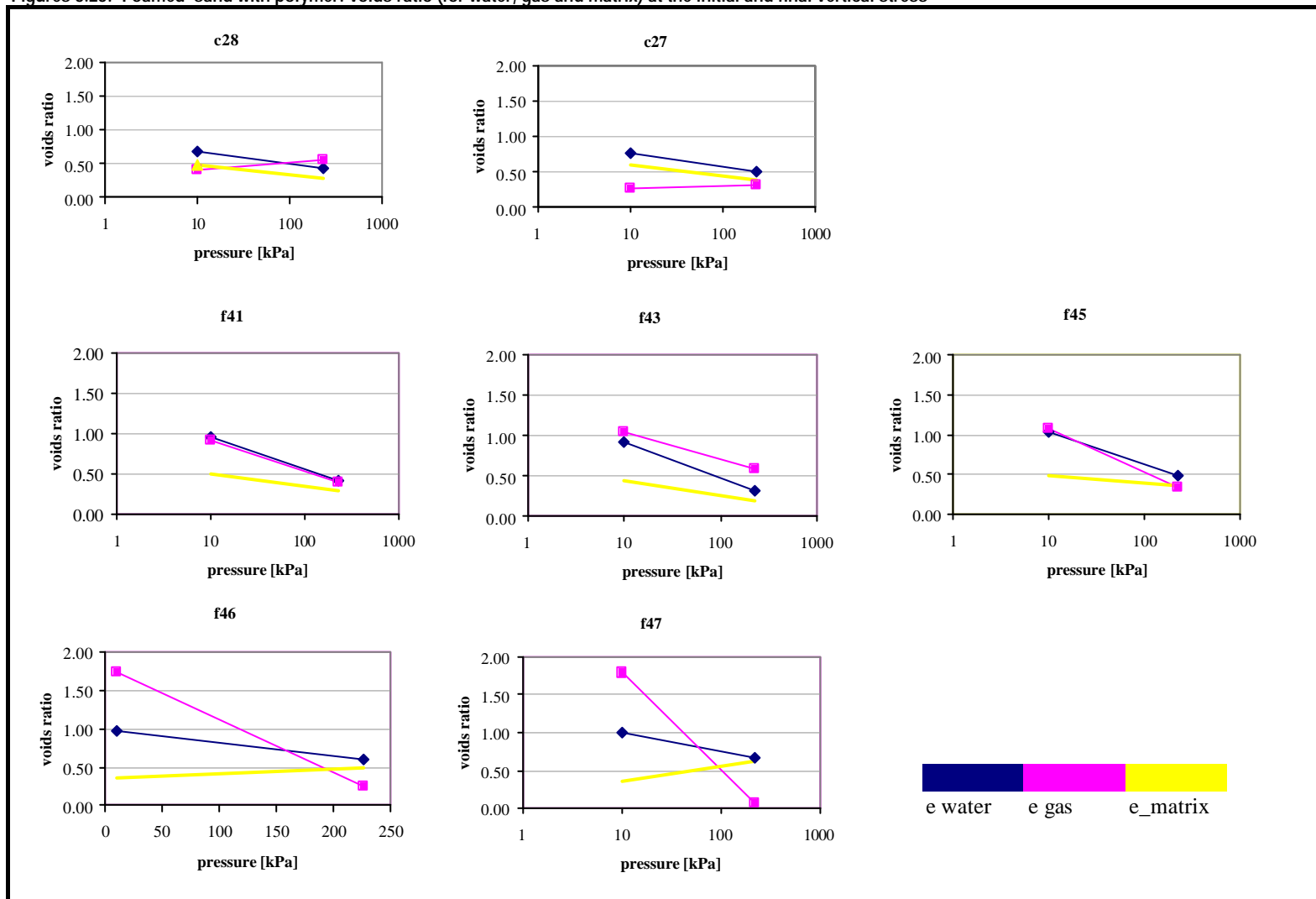
Figures 3.21: Volume changes variation with time



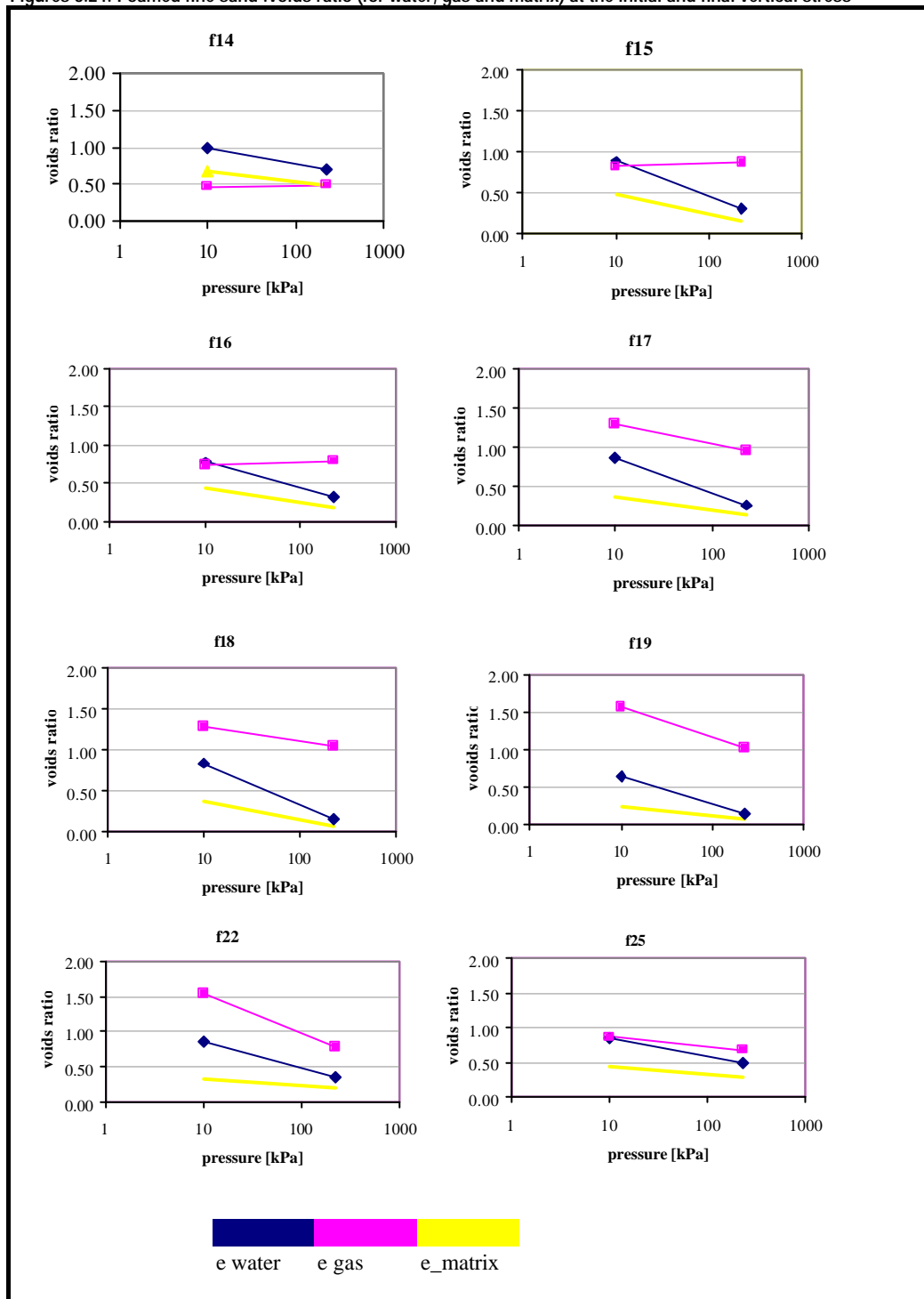


Figures 3.22: Change in 'matrix ' and gas voids ratio for 'versa' foam/sand tests.

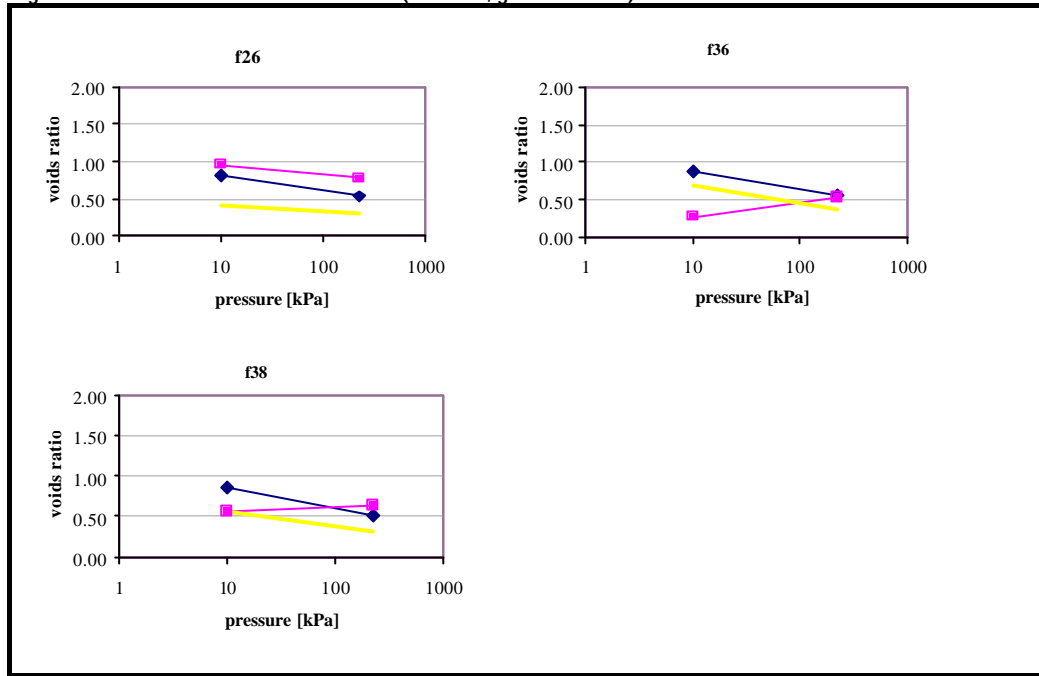
Figures 3.23: Foamed sand with polymer: voids ratio (for water, gas and matrix) at the initial and final vertical stress



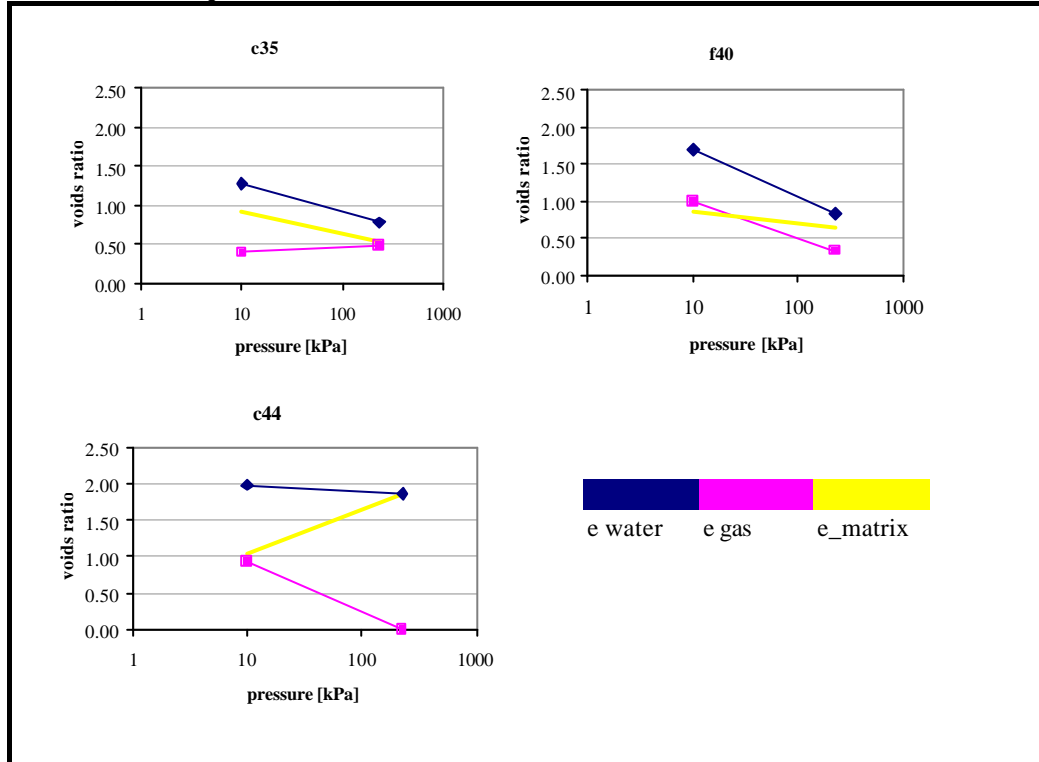
Figures 3.24: Foamed fine sand :voids ratio (for water, gas and matrix) at the initial and final vertical stress

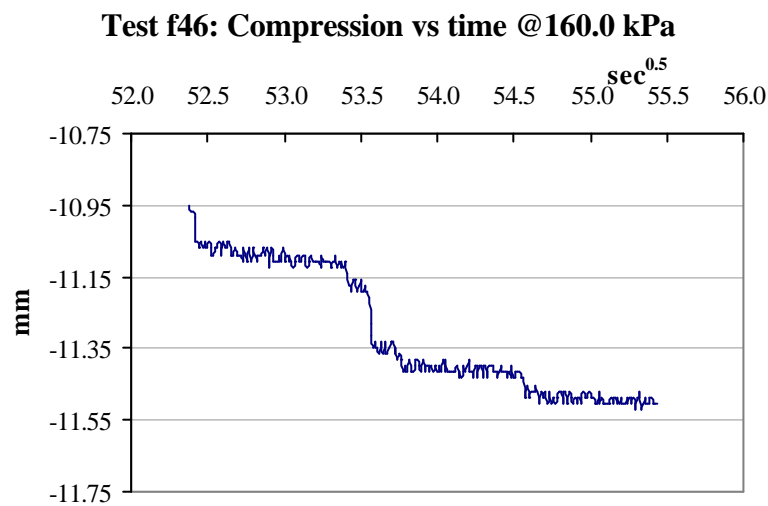
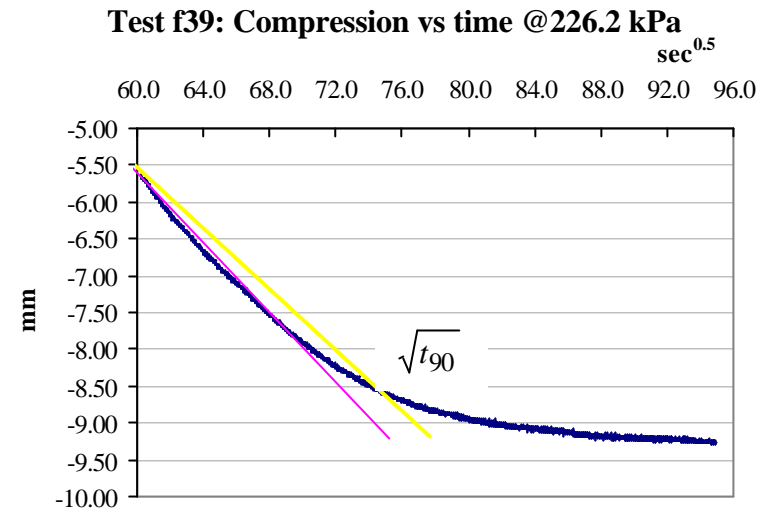


Figures 3.25: Foamed fine sand :voids ratio (for water, gas and matrix) at the initial and final vertical stress



Figures 3.26: Foamed sand with bentonite : voids ratio (for water, gas and matrix) at the initial and final vertical stress





Figures 3.27: Different curve shape for compression test *f39* (fine sand with bentonite and polymer) and compression test *f46* (foamed fine sand with polymer).

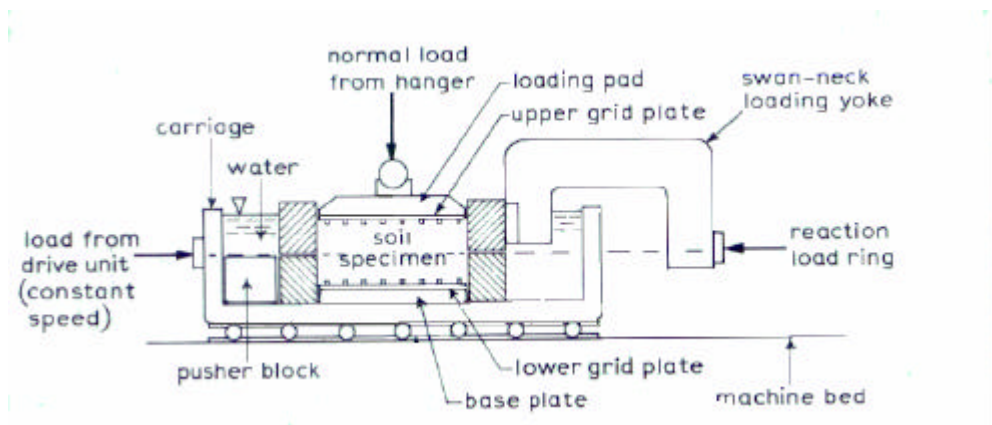


Figure 4.1: Direct small shear-box (Head, 1994).



Photo 4.1: Shear-box apparatus at Civil Engineering laboratory.

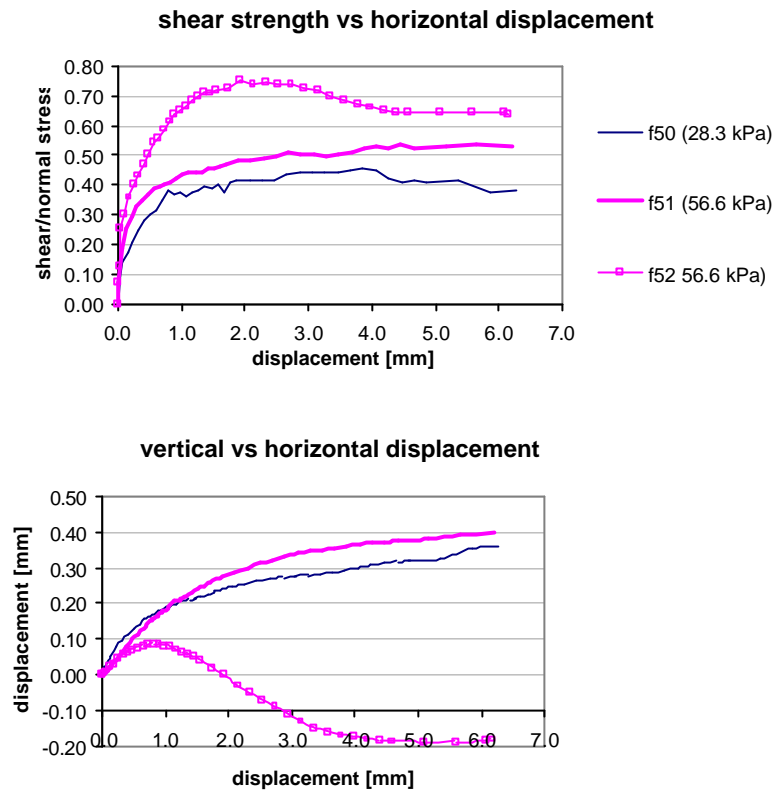


Figure 4.2a: Shear strength and vertical displacement against horizontal deformation.

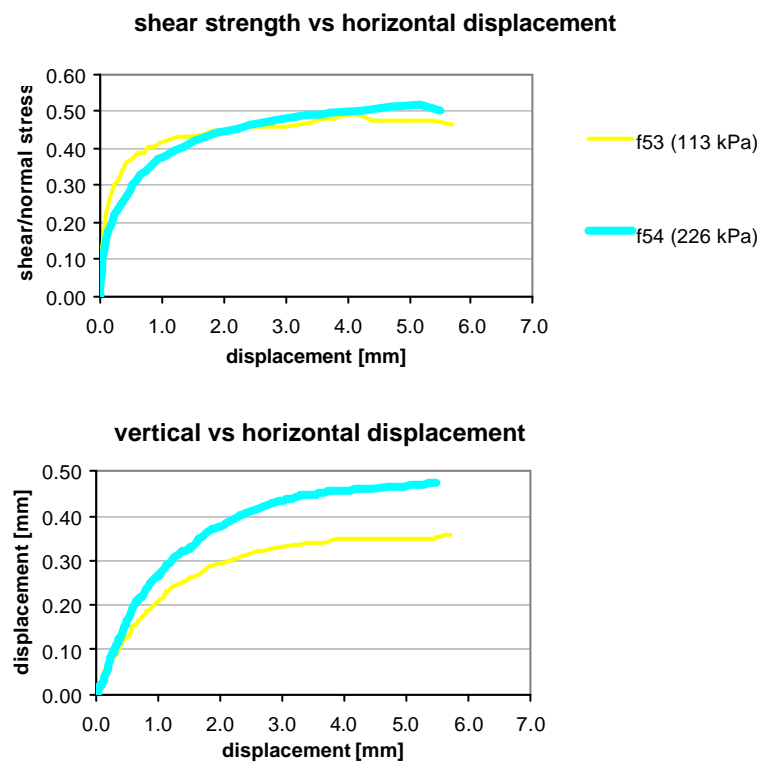


Figure 4.2b: Shear strength and vertical displacement against horizontal deformation.

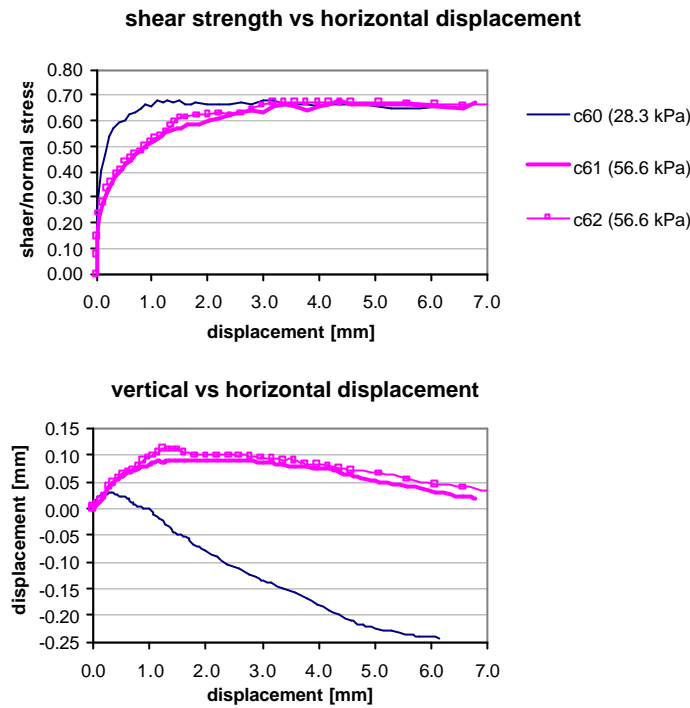


Figure 4.3a: Shear strength and vertical displacement against horizontal deformation.

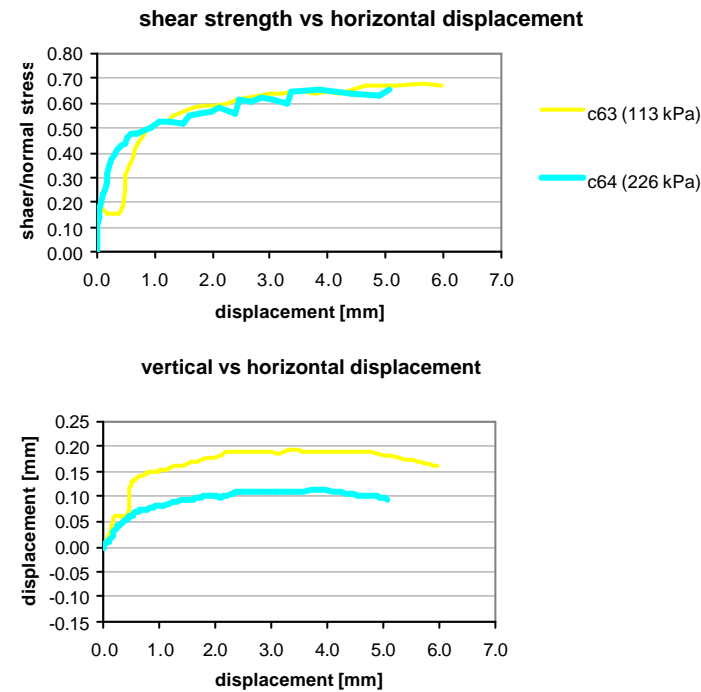


Figure 4.3b: Shear strength and vertical displacement against horizontal deformation.

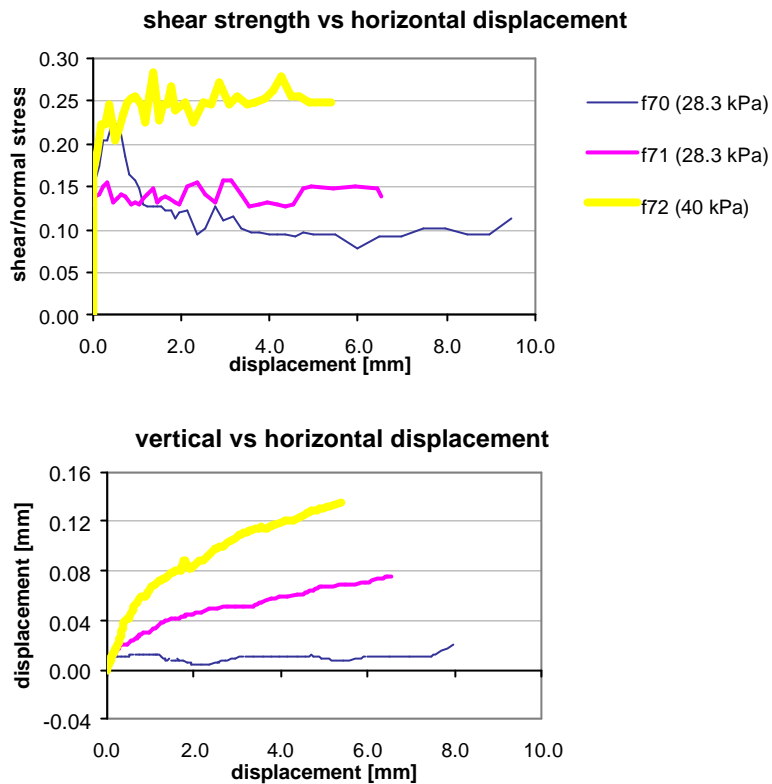


Figure 4.4: Shear strength and vertical displacement against horizontal deformation.

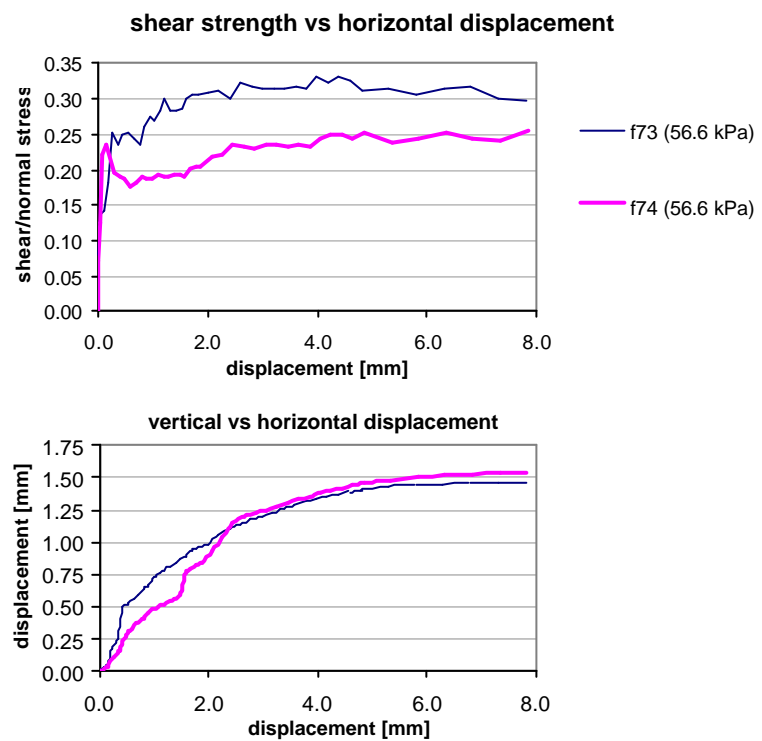


Figure 4.5: Shear strength and vertical displacement against horizontal deformation.

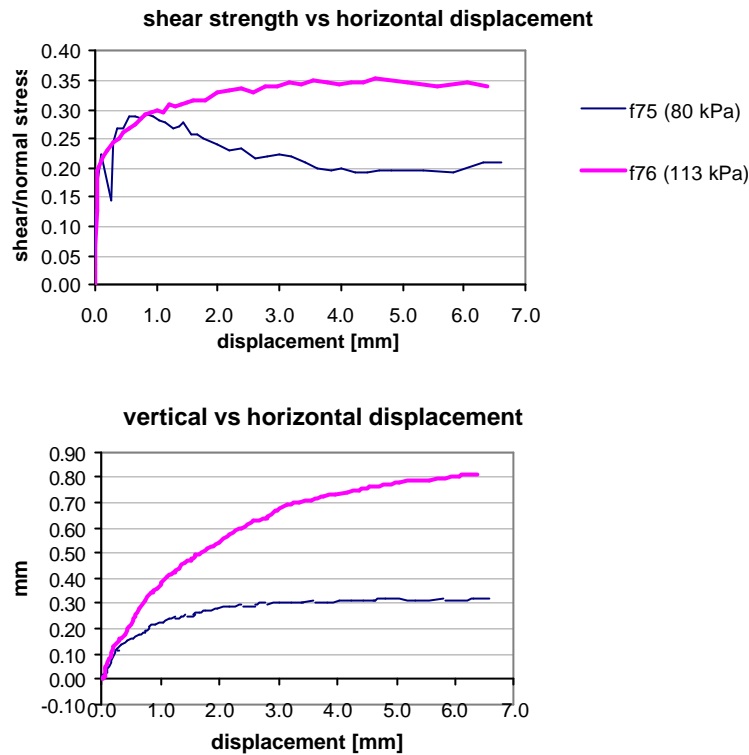


Figure 4.6: Shear strength and vertical displacement against horizontal deformation.

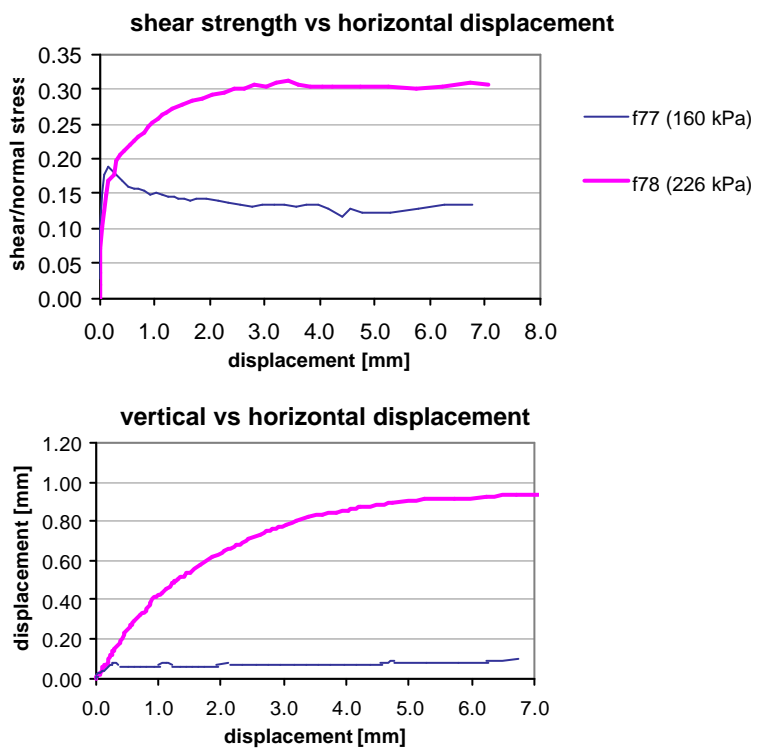


Figure 4.7: Shear strength and vertical displacement against horizontal deformation.

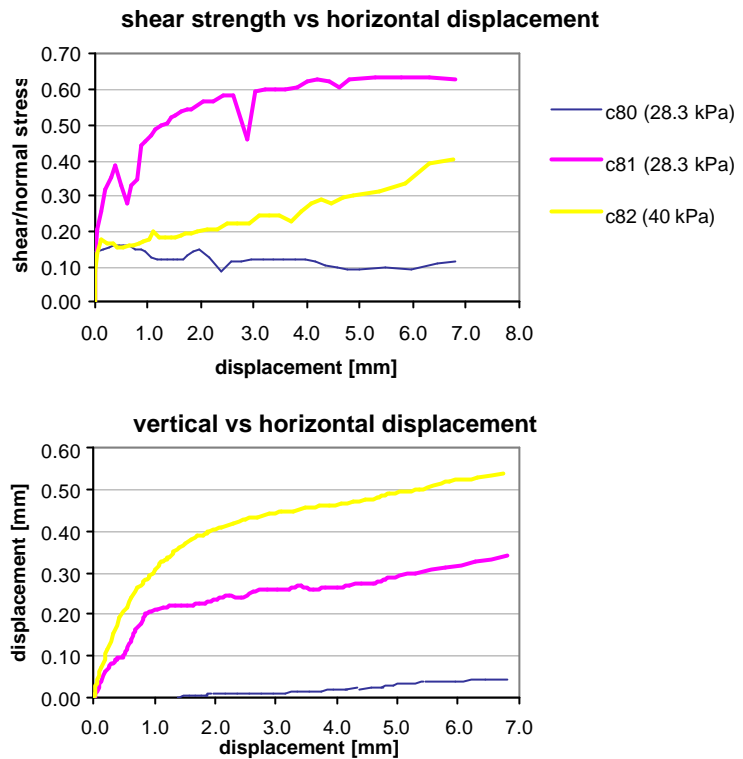


Figure 4.8: Shear strength and vertical displacement against horizontal deformation.

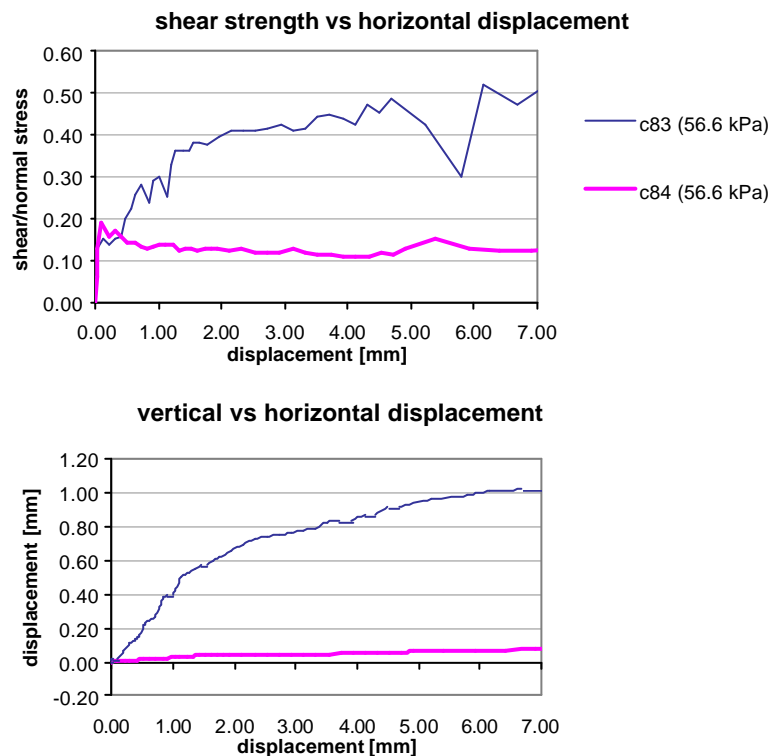


Figure 4.9: Shear strength and vertical displacement against horizontal deformation.

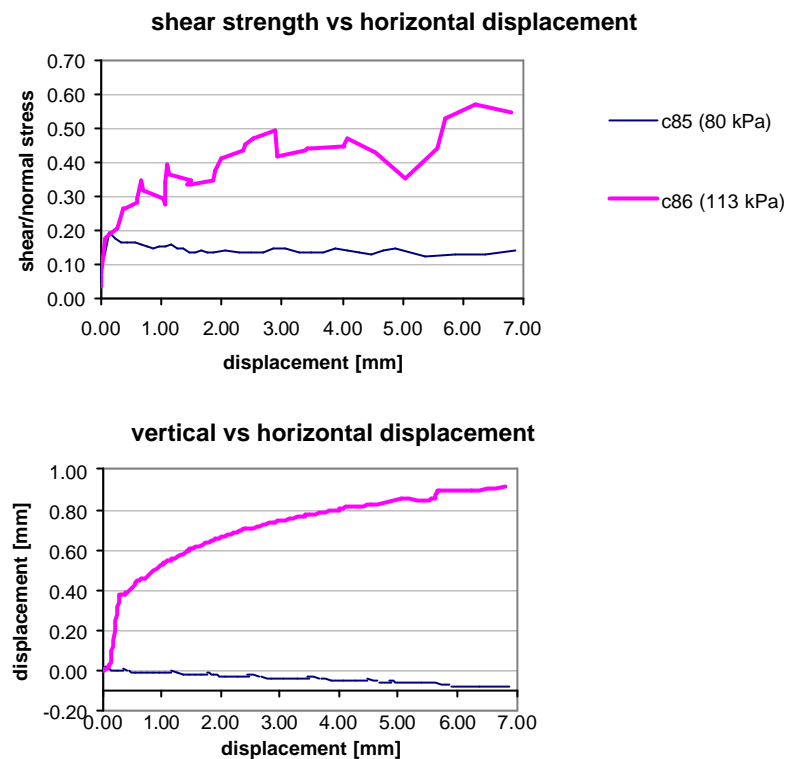


Figure 4.10: Shear strength and vertical displacement against horizontal deformation.

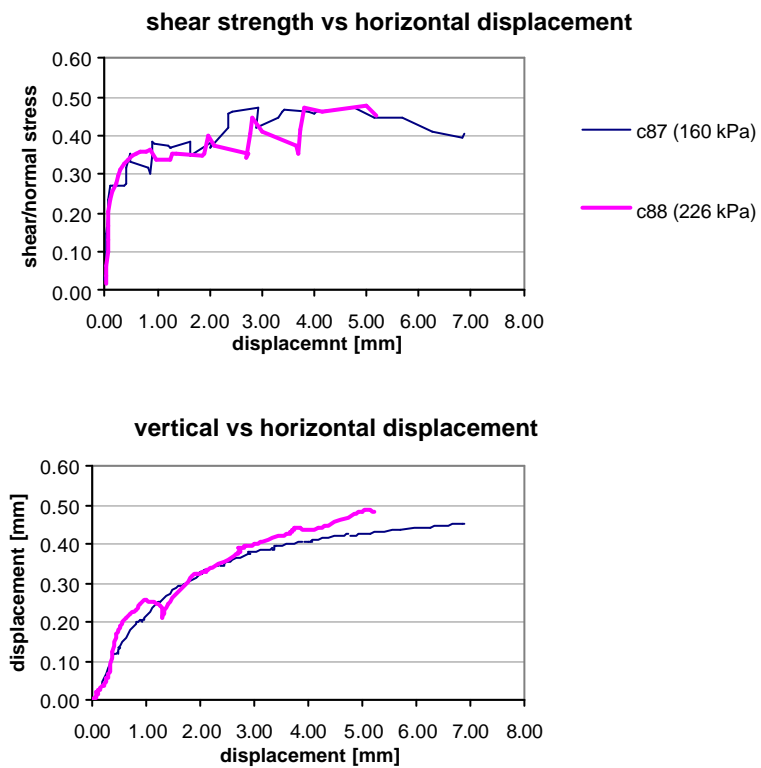
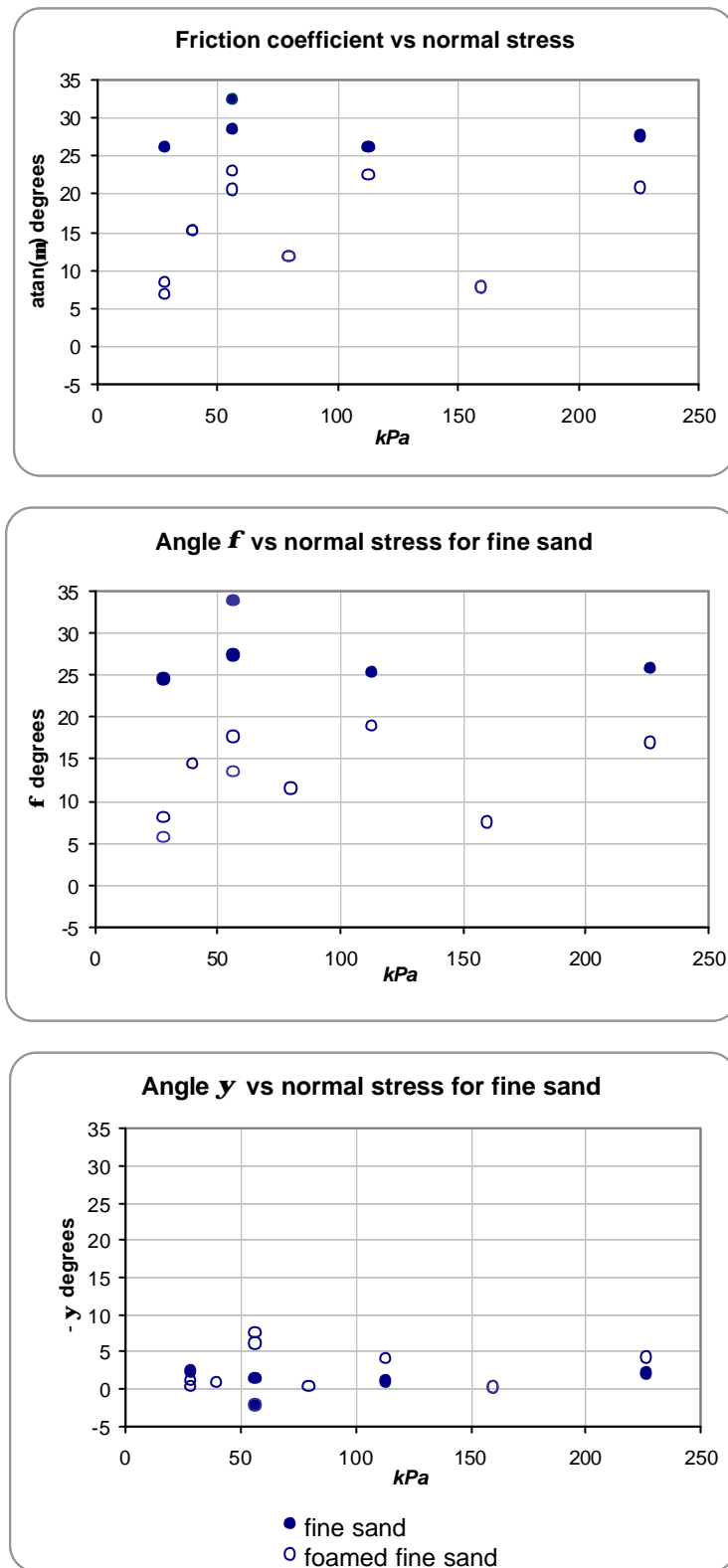
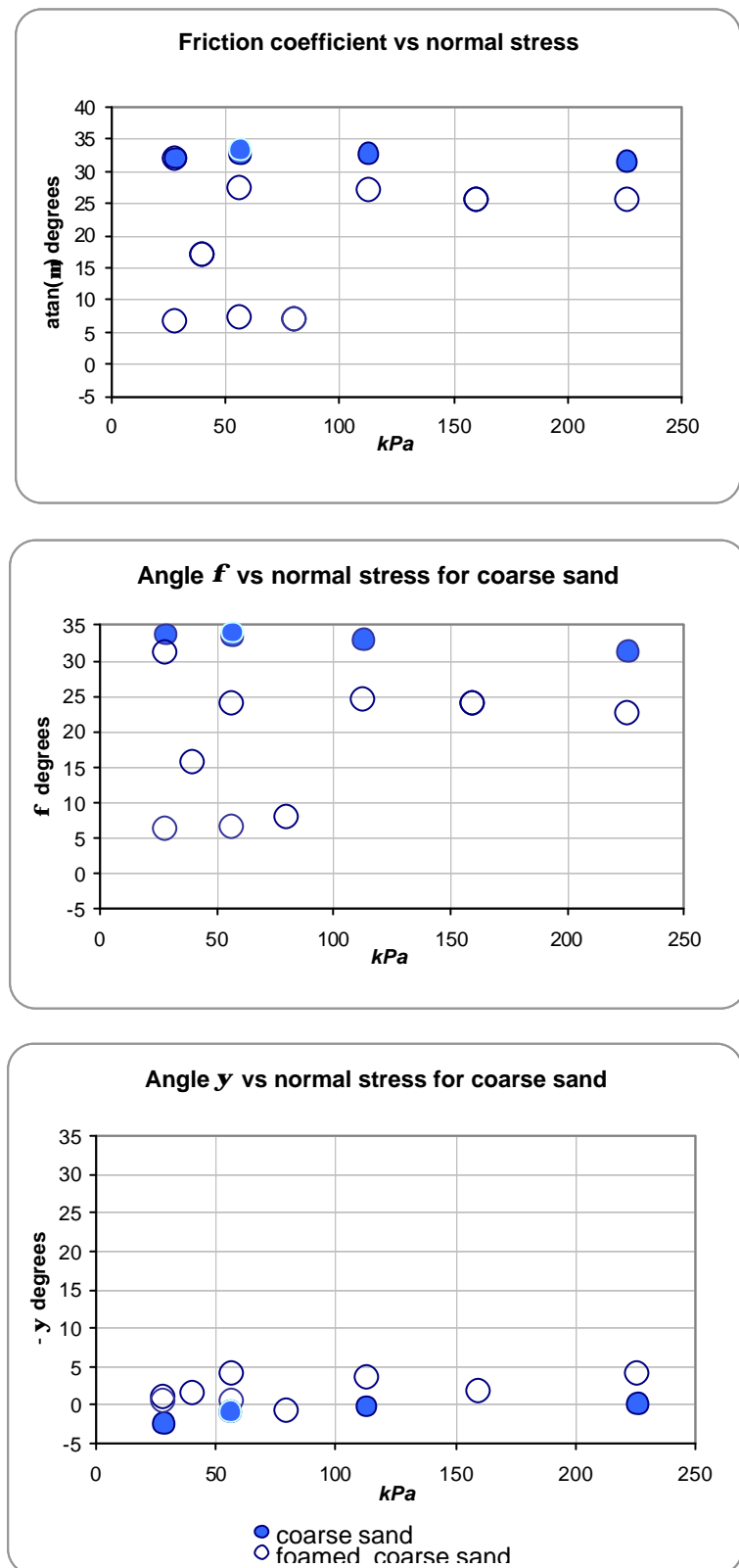


Figure 4.11: Shear strength and vertical displacement against horizontal deformation.



Figures 4.12: Shear-box test results for fine sand.



Figures 4.13: Shear-box test results for coarse sand.

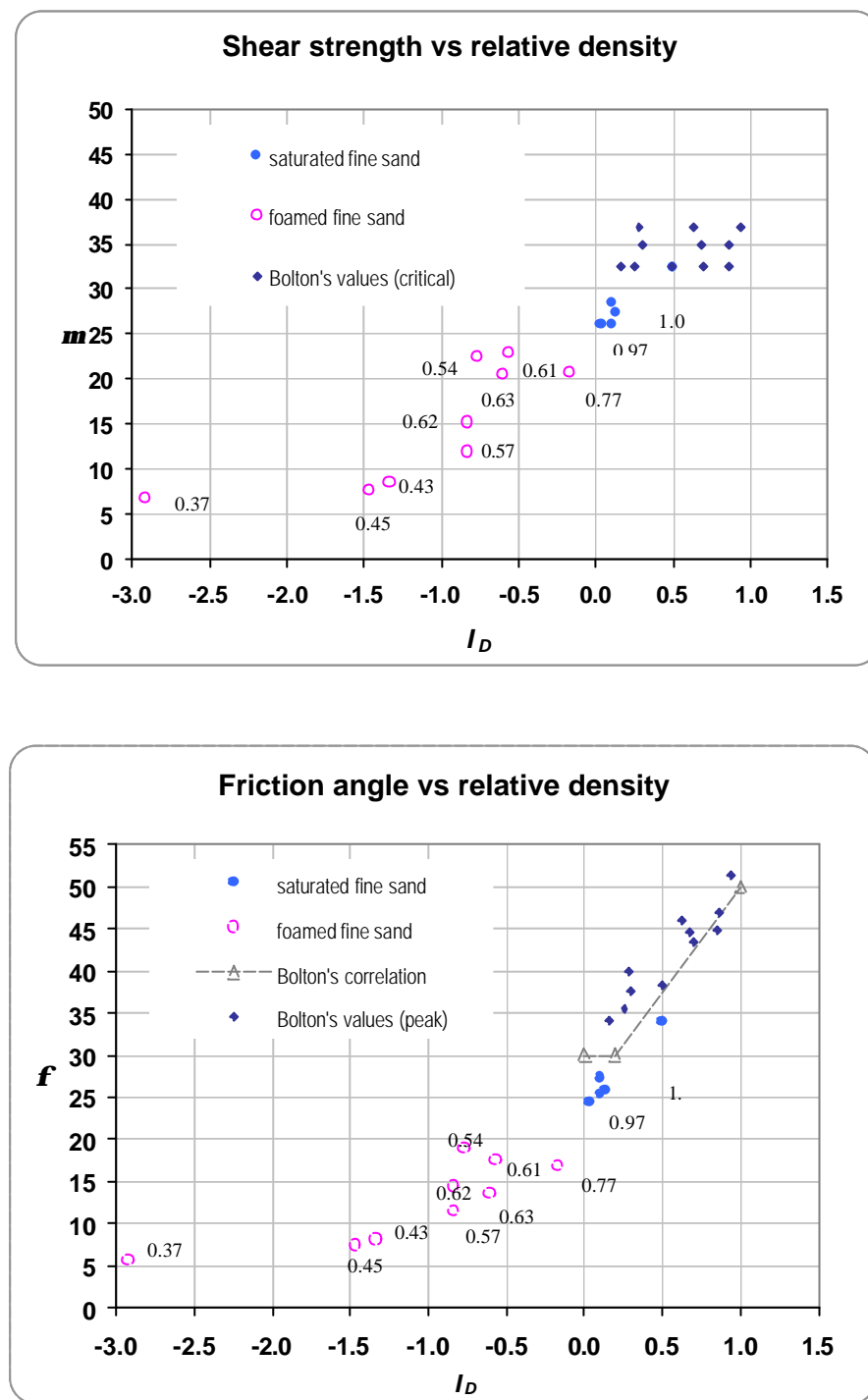


Figure 4.14: Friction angle variation with relative density for fine sand tests

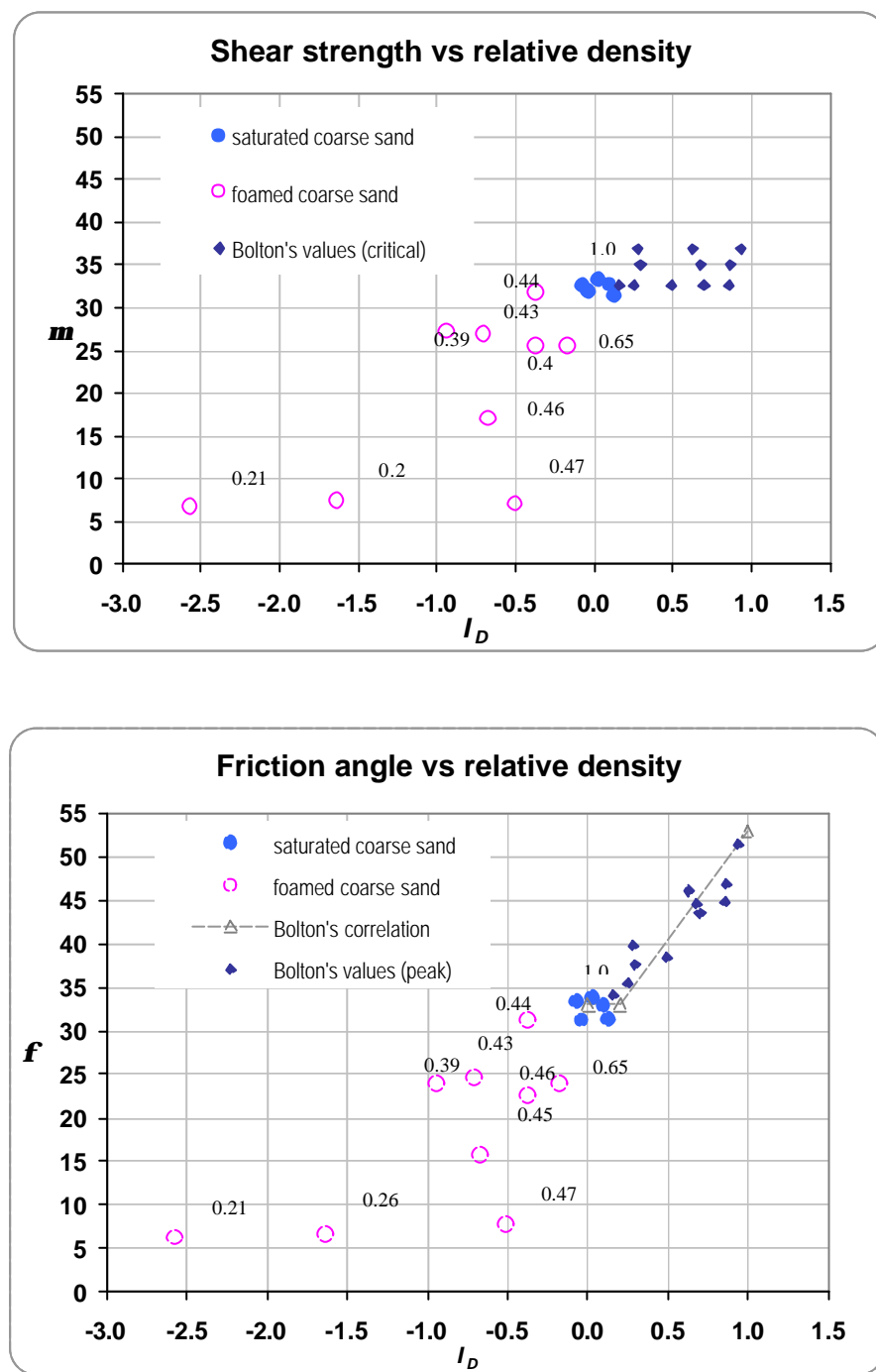


Figure 4.15: Friction angle variation with relative density for coarse sand tests

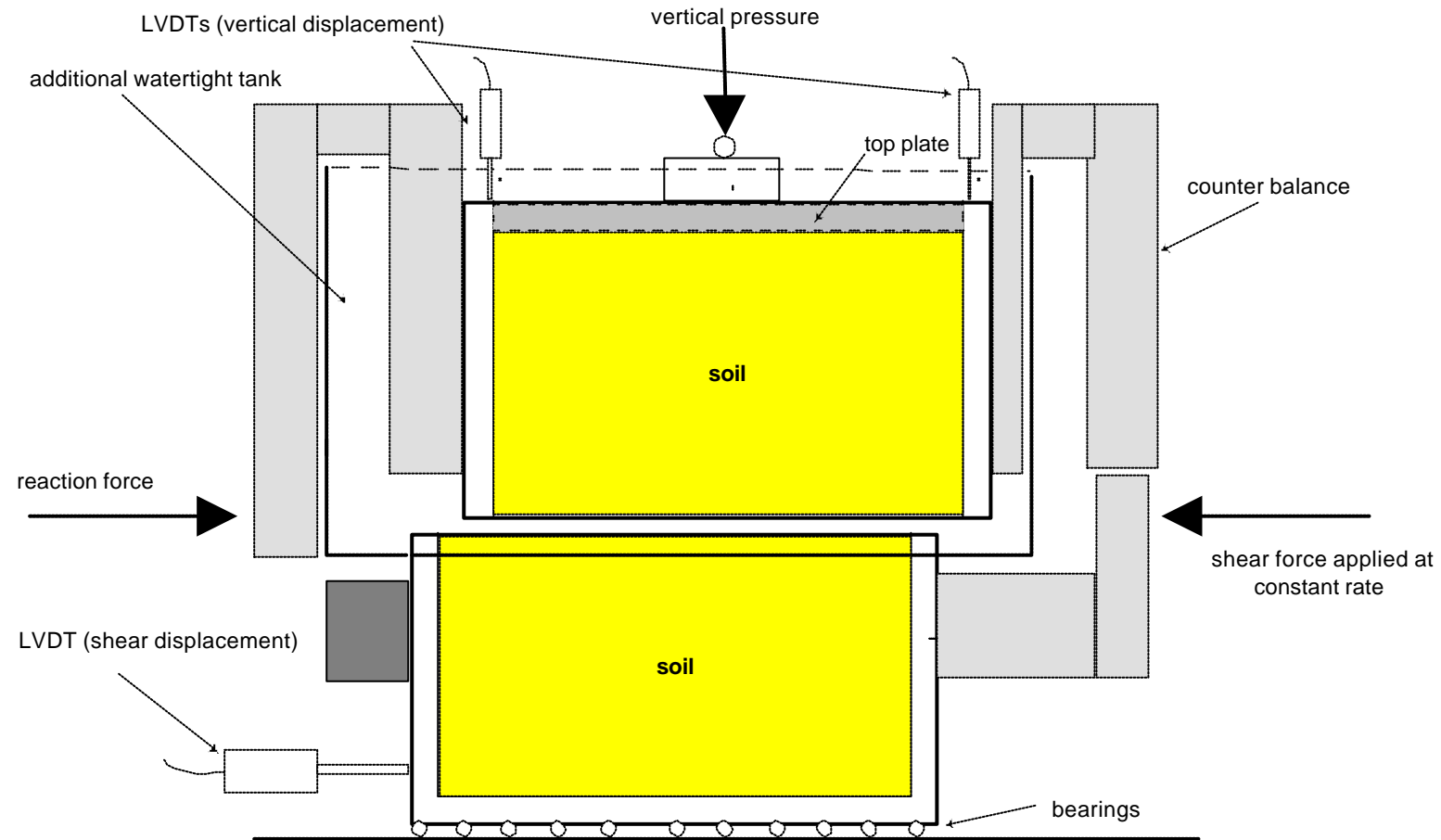


Figure 5.1: Outline of the modified large shear-box for testing foam/sand mixtures.